FOULING AND ACCUMULATION OF DISSOLVED ORGANIC MATTER IN MEMBRANE BIOREACTORS

LIANG SHUANG

NATIONAL UNIVERSITY OF SINGAPORE

2007

FOULING AND ACCUMULATION OF DISSOLVED ORGANIC MATTER IN MEMBRANE BIOREACTORS

LIANG SHUANG

(B. Eng., Qingdao Technological University)

A THESIS SUBMITTED

FOR THE DEGREE OF DOCTOR OF PHILOSOPHY

DEPARTMENT OF CIVIL ENGINEERING

NATIONAL UNIVERSITY OF SINGAPORE

2007

ACKNOWLEDGEMENTS

I would like to take this opportunity to acknowledge and thank all those who have helped me along the way.

First and foremost, I would like to express the utmost appreciation from the bottom of my heart to my academic supervisor, Associate Professor Lianfa SONG, for sticking with me through these many years. Without his expert guidance, constructive advice, unbelievable support, and constant encouragement, this work could not have been completed. His foresight, erudition, and kindness have impressed me deeply. He has taught me a great deal about both science and engineering, and most of what I know about how to conduct research. My sincerest thanks also go to my co-supervisor Professor Say Leong ONG for his invaluable comments and pertinent suggestions on this work.

Special thanks are extended to the other members of my Thesis Committee, Associate Professor Wen-Tso LIU and Associate Professor Jiangyong HU for their critical and constructive feedback, which greatly improved my thesis.

Acknowledgements are made to all former and current staff at Environmental Laboratory in Centre for Water Research, especially Mr. Michael TAN, Mr. S. G. CHANDRASEGARAN, Ms. Leng Leng LEE, Ms. Xiaolan TAN, Ms. Hwee Bee TAN, and Dr. Lai Yoke LEE for their kind support and cooperation in various ways. The assistance of the staff at the Bedok Water Reclamation Plant is greatly appreciated. Heartfelt thanks are also conveyed to my former Final Year Project students who have made contributions to this work in whatever aspects.

I owe eternal gratitude to my parents, Mr. Xiliang LIANG and Ms. Fangying YANG. It is my parents who introduce me to environmental engineering, and encourage me to pursue it as a career. I am also most grateful to my wife Ms. Cui LIU. Only with her understanding, encouragement, and above all, her love have I been able to finish this work.

The research scholarship provided by the National University of Singapore throughout the whole period of candidature is greatly appreciated.

TABLE OF CONTENTS

ACKNOWLEDGEMENTS ..... **i**

TABLE OF CONTENTS ..... **iii**

SUMMARY ..... **viii**

LIST OF TABLES ..... **xi**

LIST OF FIGURES ..... **xii**

LIST OF SYMBOLS ..... **xvii**

CHAPTER 1 INTRODUCTION **1**

1.1 Background 1

1.2 Problem Statement 5

1.3 Research Objectives and Scope 7

1.4 Thesis Program 9

CHAPTER 2 LITERATURE REVIEW **11**

2.1 MBR Technology for Wastewater Treatment and Reclamation 11

2.1.1 Limitations of Conventional Treatment Processes 11

2.1.2 Overview of Membrane Processes 12

2.1.3 Development of MBR Technology 15

2.1.4 Advantages of MBR Technology 18

2.2 Membrane Fouling in MBR Systems 20

2.2.1 Characteristics of Mixed Liquor 20

2.2.2 Operating Conditions 24

2.2.3 Membrane Properties 26

2.3 Characterizing Dissolved Organic Matter 28

2.3.1 DOM Profiling by Resin Sorbents 28

2.3.2 Spectrophotometric Measurements 29

2.3.3 Size Analysis 30

2.3.4 Fractionation and Characterization 31

2.4 Organic Fouling during Membrane Filtration 33

2.4.1 Organic Foulants 33

2.4.2 Membrane Characteristics and Operating Conditions 34

2.4.3 Adsorption Fouling 37

2.4.4 Precipitation and Gel Formation 39

2.4.5 Pore and Surface Fouling 41

2.4.6 Fouling with Multivalent Cations 42

CHAPTER 3 MATERIALS AND METHODS 44

3.1 Experiments with DOM in Pilot MBR Systems 44

3.1.1 Sample Source and Collection 44

3.1.2 DOM Fractionation 46

3.1.3 Membranes 48

3.1.4 Stirred-cell Filtration System 49

3.1.5 Experimental Procedure 50

3.1.6 Calculation of Fouling Potential 51

3.2 Experiments with DOM in Lab-scale MBR System 52

3.2.1 MBR System Description 52

3.2.2 Synthetic Wastewater and Operating Conditions 54

3.2.3 DOM Fouling Experiment 56

3.3 Analytical Methods 56

CHAPTER 4 CHARACTERISTICS AND FOULING POTENTIAL OF DOM IN MBR SYSTEMS 59

4.1 Characteristics of DOM in MBR Systems 61

4.1.1 Hydrophobic/hydrophilic and Charge Properties 61

4.1.2 Molecular Size of DOM 63

4.2 DOM Fouling with Hydrophilic/Hydrophobic Membranes 64

4.3 Effect of Prefiltration on DOM fouling 68

4.4 Characteristics and Fouling Potential of Fractional Components 70

4.4.1 Characteristics of Fractional DOM Components 70

4.4.2 Fouling Potential of Fractional DOM Components 72

4.5 Concluding Remarks 75

CHAPTER 5 MODELING OF FOULING DEVELOPMENT IN MBR SYSTEMS 77

5.1 Theories and Models 78

5.1.1 Resistance-in-series Model 78

5.1.2 Reversible Fouling 80

5.1.3 Irreversible Fouling 82

5.1.4 Permeate Flux and Transmembrane Pressure 83

5.1.5 Biological Parameters X_T and C_{MBR} 85

5.2 Simulations and Discussions 85

5.2.1 Description of the pilot MBR System 85

5.2.2 Model Parameters 87

5.2.3 Performance Simulations and Model Verification 89

5.3 Concluding Remarks 92

CHAPTER 6 CHARACTERISTICS AND BEHAVIORS OF DOM AT DIFFERENT SRTS 94

6.1 Overall Performance of MBR System 95

6.2 Concentration of DOM at different SRTs 97

6.3 Composition of DOM at different SRTs 99

6.4 Molecular Size of DOM at different SRTs 102

6.5 Hydrophobic/hydrophilic and Charge Properties of DOM at different SRTs 104

6.6 Fouling Potential of DOM at different SRTs 107

6.7 Concluding Remarks 108

CHAPTER 7 RETARDED TRANSPORT AND ACCUMULATION OF DOM IN MBR SYSTEMS 110

7.1 Transport Experiment with Humic Acid 112

7.2 DOM Transport Mechanisms through Porous Membranes 114

7.2.1 Retarded Convection 114

7.2.2 Dispersion 115

7.2.3 DOM Transport Modeling 116

7.3 Modeling Study of DOM Transport through Porous Membranes ... 117

7.4. DOM Accumulation in MBR Systems 120

7.5 Concluding Remarks 125

CHAPTER 8 SUMMARY AND FUTURE PERSPECTIVE 127

8.1 Summary 127

8.2 Recommendations for Future Study 130

REFERENCE **133**

APPENDIX **153**

Appendix A: Photographs of the pilot MBR systems 153

Appendix B: Schematic Diagrams of the pilot MBR systems 155

Appendix C: Publications from This Research Work 156

SUMMARY

As an innovative technology, membrane bioreactor (MBR) systems have been increasingly utilized in wastewater treatment over the last decade to meet the progressively stringent discharge criteria. With the employment of membranes for more efficient solid-liquid separation, MBR systems possess numerous advantages over conventional activated sludge systems, e.g. excellent effluent quality, less sludge production, and smaller plant size. However, membrane fouling remains the principal obstacle constraining their more extensive and large-scale application.

Dissolved organic matter (DOM), mainly soluble microbial products, is a major concern in wastewater treatment because of its significant impacts on system performance. Along with the steadily growing application of MBR systems, the significance of DOM in MBR fouling is being increasingly noted. Moreover, DOM concentration is observed to be higher in the MBR than in the effluent, leading to severer membrane fouling and a significant increase in operating costs.

The primary objective of this thesis is to contribute towards a more fundamental understanding of DOM fouling and accumulation in submerged MBR systems. The

complex DOM mixture in MBR systems was fractionated into four homogeneous components, namely, hydrophobic aquatic humic substances (AHS), hydrophilic acids (HiA), hydrophilic bases (HiB), and hydrophilic neutrals (HiN). The hydrophobic AHS were found to be the most abundant component of DOM in MBR systems. Fouling experiments were carried out in the stirred-cell filtration system with either hydrophobic or hydrophilic microfiltration membranes. It was found that DOM fouling was much more serious on hydrophobic membranes and that the DOM fouling potential was dependent not only on DOM concentration but also on its characteristics. The order of fouling potential of the fractional DOM components, evaluated at comparable conditions, was observed to be AHS > HiN > HiB > HiA. In addition, it was noted that membrane fouling caused by HiN and AHS was mainly irreversible. It is thus suggested that DOM having larger AHS and HiN fractions would most likely cause more serious fouling in MBR systems.

The relative importance of DOM in MBR fouling was also theoretically investigated. The role of DOM was examined for membrane fouling in submerged MBR systems using a mathematical model, in which both reversible and irreversible fouling were quantified. While mixed liquor suspended solids are the major components of the reversible fouling layer, DOM is speculated as the key foulant responsible for the long-term irreversible fouling of the membrane module. The model was calibrated (parameter identification) with a set of operational data from the pilot MBR system and then verified with other independent operational data from the MBR system. The good agreement between theoretical predictions and operational data shows that the outlined modeling concept can be successfully applied to describe membrane fouling in submerged MBR systems.

The effect of sludge retention time (SRT) on DOM fouling and accumulation was investigated in the lab-scale submerged MBR system treating readily biodegradable synthetic wastewater. The concentrations of DOM in the MBR were found to be always higher than those in the effluent, indicating a certain degree of DOM accumulation in the MBR system. In addition, it was noted that DOM accumulation was more pronounced at short SRTs. Carbohydrates and proteins appeared to be the components of DOM prone to accumulate in the MBR compared with aromatic compounds. The fouling potential of DOM was observed to increase considerably as SRT shortened.

Size exclusion or sieving of the microfiltration membrane alone was experimentally demonstrated inadequate to explain DOM accumulation in the MBR system. The retarded transport of DOM through porous membranes was postulated as a new mechanism. Mathematical models were developed for DOM transport through porous membranes and for DOM concentrations both in the MBR and in the effluent. A good agreement between experimental data and model simulations indicates that the proposed transport mechanisms of retarded convection and dispersion of DOM through a porous membrane can be a better explanation for DOM accumulation in MBR systems.

***Keywords**:* Dissolved organic matter; Membrane bioreactor; Fractionation; Fouling potential; Accumulation; Sludge retention time

LIST OF TABLES

Table 3.1 Specifications of pilot MBR systems 45

Table 3.2 Recovery rate of fractional DOM components 48

Table 3.3 Characteristics of GVHP and GVWP membranes 49

Table 3.4 Composition and concentration of synthetic wastewater 54

Table 4.1 General characteristics of MBR supernatants 60

Table 4.2 Apparent molecular weight distributions of DOM in MBR systems 64

Table 4.3 Fouling potential of DOM for GVWP and GVHP membranes 66

Table 4.4 Fouling potential of fractional components of DOM in MBR3 at DOC concentration of 5 mg/L 74

Table 5.1 Typical characteristics of influent municipal wastewater 86

Table 5.2 Mean values of X_T and S_T in the three filtration intervals 87

Table 5.3 Values of σ during three filtration intervals 88

Table 5.4 Values of model parameters used in the simulation study 89

Table 6.1 Biomass concentration and metabolic activity at different SRTs[a] 97

Table 7.1 Values of kinetic and stoichiometric parameters 123

LIST OF FIGURES

Figure 2.1 **Overview of pressure-driven membrane processes commonly used in water and wastewater treatment and dimensions of various impurities found in waters** (Jacangelo et al., 1989). 13

Figure 2.2 **Configuration of membrane processes: Dead-end Filtration (left) and Cross-flow Filtration (right).** 15

Figure 2.3 **Configuration of MBR systems: (a) Side-stream MBR, (b) Suctioned-filtration submerged MBR, and (c) Gravitational-filtration submerged MBR.** 16

Figure 2.4 **Schematic of DOM classification.** 32

Figure 3.1 **Procedure for fractionation of DOM in MBR systems.** 47

Figure 3.2 **Schematic diagram of stirred-cell filtration system.** 50

Figure 3.3 **Schematic diagram of lab-scale MBR system.** 53

Figure 3.4 **DR/4000U Spectrophotometer (left) and 1010 TOC Analyzer (right).** 57

Figure 3.5 **DX500 ion chromatography system.** 58

Figure 4.1 **Fractionation results of DOM in pilot MBR systems.** 61

Figure 4.2 Apparent molecular weight distributions of DOM in MBR systems. 63

Figure 4.3 Normalized permeate flux for the filtration of MBR supernatants with (a) hydrophilic GVWP membranes and (b) hydrophobic GVHP membranes. 65

Figure 4.4 Characteristics of fouling resistance caused by DOM in the three pilot MBR systems during filtration with (a) hydrophilic GVWP membranes, and (b) hydrophobic GVHP membranes. R_m, membrane resistance; R_i, resistance of irreversible fouling; R_r, resistance of reversible fouling. 67

Figure 4.5 Normalized permeate flux for the filtration of three DOM samples, original, GVWP-prefiltered, GVHP-prefiltered with hydrophobic GVHP membranes. 68

Figure 4.6 Apparent molecular weight distributions of DOM in pilot MBR systems after GVHP membrane filtration. 69

Figure 4.7 SUVA values for different fractional DOM components in pilot MBR systems. 71

Figure 4.8 Apparent molecular weight distributions for the fractional DOM components in MBR3. 71

Figure 4.9 Normalized permeate flux for the filtration of the fractional components of DOM in MBR3 with hydrophobic GVHP membranes. 73

Figure 4.10 Normalized permeate flux for the filtration of the fractional components of DOM in MBR3 at the same level of Ca^{2+} with hydrophobic GVHP membranes. 74

Figure 4.11 **Characteristics of fouling resistance caused by the fractional components of DOM in MBR3 during filtration with hydrophobic GVHP membranes. R_m, membrane resistance; R_i, resistance of irreversible fouling; R_r, resistance of reversible fouling.**.....75

Figure 5.1 **The effect of detachment coefficients on the time and magnitude of reversible foulant accumulation on membrane surface (1. k_r = 1.5×10^{-5} s^{-1}, 2. k_r = 3.0×10^{-5} s^{-1}, 3. k_r = 5.0×10^{-5} s^{-1}, 4. k_r = 1.0×10^{-4} s^{-1}). Other parameters used in calculations: J = 3.0×10^{-6} m/s; X_T = 8.0 kg/ m^3.**.....82

Figure 5.2 **Evolution of TMP with operation time for different detachment coefficients (1. k_r = 1.5×10^{-5} s^{-1}, 2. k_r = 3.0×10^{-5} s^{-1}, 3. k_r = 5.0×10^{-5} s^{-1}, 4. k_r = 1.0×10^{-4} s^{-1}). Other parameters used in calculations: J = 3.0×10^{-6} m/s, X_T = 8.0 kg/m^3, σ= 1.0×10^{13} m/kg, R_m = 1.0×10^{12} m^{-1}, μ = 1.0×10^{-3} Pa s, S_T = 2.0×10^{-2} kg/m^3, k_i = 1.2×10^{13} m/kg.**.....84

Figure 5.3 **Operational data for TMP of the submerged MBR system (January 1 to August 1, 2004).**.....87

Figure 5.4 **Comparison of model simulations with TMP measurements (January 1 to February 24, 2004).**.....88

Figure 5.5 **Comparison of model simulations with TMP measurements (February 27 to June 27, 2004).**.....90

Figure 5.6 **Comparison of model simulations with TMP measurements (June 30 to August 1, 2004).**.....90

Figure 5.7 **Comparison of model simulations with TMP measurements (January 1 to August 1, 2004).**.....91

Figure 5.8 Comparison of model simulations with experimental data of filtration resistance resulted from membrane fouling (January 1 to August 1, 2004). 91

Figure 6.1 COD and NH_4^+-N removal efficiencies of MBR at different SRTs (number of measurements: n = 25). 96

Figure 6.2 Concentrations of DOM in the MBR and in the effluent at different sludge retention times (number of measurements: n = 26). 98

Figure 6.3 Relationship between C_e/C_{MBR} and SRT. 99

Figure 6.4 Concentrations of carbohydrate in the MBR and in the effluent at different sludge retention times (number of measurements: n = 25). 100

Figure 6.5 Concentrations of Protein in the MBR and in the effluent at different sludge retention times (number of measurements: n = 24). 100

Figure 6.6 SUVA values of DOM in the MBR and in the effluent at different sludge retention times (number of measurements: n = 26). 101

Figure 6.7 AMWD of DOM at different sludge retention times (a) AMWD of DOM in the MBR; (b) AMWD of DOM in the effluent (number of measurements: n = 15). 103

Figure 6.8 Hydrophobicity and charge property of DOM at different sludge retention times: (a) Hydrophobicity and charge property of DOM in the MBR; (b) Hydrophobicity and charge property of DOM in the effluent (number of measurements: n = 13). 105

Figure 6.9 **Relative proportion change of different fractional DOM components after passing through membrane at different sludge retention times (number of measurements: n = 13).** 106

Figure 6.10 **Fouling potential of DOM in the MBR and in the effluent at different sludge retention times.** 108

Figure 7.1 **Variation of humic acid concentrations in the MBR and in the effluent with operational time (a) DOC = 18 mg/L; and (b) DOC = 38 mg/L.** 113

Figure 7.2 **Transport of water and DOM through a porous membrane (The arrow length indicates the velocity.** 115

Figure 7.3 **Variation of C_e/C_{MBR} along membrane thickness with different dispersion factors. 1. $\beta = 1.0\times10^{-6}$, 2. $\beta = 3.0\times10^{-6}$, 3. $\beta = 1.0\times10^{-5}$, 4. $\beta = 3.0\times10^{-5}$, 5. $\beta = 1.0\times10^{-4}$; $\alpha = 0.1$, $v_w = 5.0\times10^{-6}$ m/s.** 119

Figure 7.4 **C_e/C_{MBR} as function of β with different retardation coefficients. 1. $\alpha = 0.001$; 2. $\alpha = 0.25$; 3. $\alpha = 0.50$; 4. $\alpha = 0.75$; 5. $\alpha = 1.0$; $v_w = 5.0\times10^{-6}$ m/s, L = 0.1mm.** 120

Figure 7.5 **Comparison of predicted DOM concentrations in the MBR (C_{MBR}) and in the effluent (C_e) with experimental observations.** 124

Figure 7.6 **Effect of membrane filtration factor on DOM concentration profiles in the MBR at a SRT of 10 days. 1. $f = 0.1$, 2. $f = 0.2$, 3. $f = 0.3$, 4. $f = 0.5$.** 125

Figure A.1 **Photographs of the three pilot MBR systems.** 154

Figure B.1 **Schematic diagram of MBR 1** 155

Figure B.2 **Schematic diagram of MBR 2** 155

Figure B.3 **Schematic diagram of MBR 3** 156

LIST OF SYMBOLS

b	endogenous decay rate coefficient, day^{-1}
C	concentration of DOM, mg/L
C_e	DOM concentration in effluent, mg/L
C_{MBR}	DOM concentration in MBR, mg/L
D	dispersion coefficient, m^2/s
f	filtration factor, dimensionless
J	permeate flux, m/s
J_0	pure water flux of a clean membrane, m/s
J_0'	pure water flux of the fouled-membrane after physical cleaning, m/s
J_D	DOM flux, m/s
J_f	quasi-steady state permeate flux with feed solutions, m/s
K_{max}	maximum specific substrate utilization rate, gCOD/gVSS·day
K_s	half-maximum rate concentration for substrate, g/m^3
k_{BAP}	formation rate coefficient for biomass associated products, gCOD/gVSS·day
k_{UAP}	formation rate coefficient for utilization associated products, dimensionless

k_d	decay rate constant of DOM, day^{-1}
k_f	fouling potential of DOM, Pa s/m^2
k_i	fouling strength factor, m/kg
k_r	detachment coefficient, s^{-1}
L	membrane thickness, m
m	accumulated mass of cake layer on membrane surface, kg/m^2
m_i	accumulated mass of irreversible foulant, kg/m^2
m_r	accumulated mass of reversible foulant, kg/m^2
$P_{Effluent}$	proportion of fractional DOM component in effluent, dimensionless
P_{MBR}	proportion of fractional DOM component in MBR, dimensionless
Q	flow rate, m^3/day
q	specific substrate utilization rate, gCOD/gVSS·day
R_f	resistance of membrane fouling, m^{-1}
R_i	resistance of irreversible fouling, m^{-1}
R_m	intrinsic membrane resistance, m^{-1}
R_r	resistance of reversible fouling, m^{-1}
R_t	total membrane resistance, m^{-1}
r_{SMP}	rate of SMP formation, mg/L·day
S	substrate concentration in MBR, mg/L
S_i	substrate concentration in influent, mg/L
V	volume of the bioreactor, m^3
v_D	velocity of DOM, m/s
v_w	velocity of water, m/s
X_T	total suspended solids in MBR, g/m^3
Y	true growth yield for substrate utilization, gVSS/gCOD

Greek symbols

ΔP	transmembrane pressure, Pa
α	DOM retardation coefficient, dimensionless
β	DOM dispersion factor, m
μ	permeate viscosity, Pa·s
θ	hydraulic retention time, day
θ_s	sludge retention time, day
σ	specific resistance of reversible fouling layer, m/kg

CHAPTER 1

INTRODUCTION

1.1 Background

Dissolved organic matter (DOM) is ubiquitous in surface water and sewage, and has been a major concern in water and wastewater treatment systems. In drinking water production, DOM is identified to be the main cause of fouling during microfiltration/ultrafiltration of surface water, resulting in severe loss of system productivity (Yuan and Zydney, 2000; Howe and Clark, 2002). DOM also reacts with chlorine, the most widely used disinfectant for water disinfection, to form undesirable disinfection by-products (DBP) (Kwon et al., 2005). In biological wastewater treatment, the amount and nature of DOM, of which the majority is soluble microbial products (SMP), affect both the kinetic activity and flocculating/settling properties of activated sludge (Barker and Stuckey, 1999). In recent years, along with the steadily growing application of membrane bioreactor (MBR) systems, the significance of

DOM in MBR fouling has been increasingly noted (Bouhabila et al., 2001; Lee et al., 2003; Kimura et al., 2005). Moreover, DOM has been observed to accumulate in MBR systems, which in turn augments the adverse effect of DOM on system performance.

Over the last decade, MBR systems have been increasingly implemented in advanced wastewater treatment and reclamation partly due to more stringent discharge regulations, and continuously improved performance and decreased cost of membranes. By employing microfiltration or ultrafiltration membranes for solid-liquid separation, a complete retention of biomass can be achieved in MBR systems. This enables MBR systems to be operated at much higher biomass concentration than that in conventional activated sludge processes. The advantages of MBR systems include highly enhanced treatment efficiency and significantly reduced sludge production and bioreactor volume (Bouhabila et al., 1998; Xing et al., 2001; Bai and Leow, 2002). Effluents from MBR systems are hallmarked by their superior quality (i.e., free of suspended solids and bacteria), which is especially desirable when the treatment purpose is reuse. At present, two MBR configurations are commercially available: (i) side-stream where membrane modules are placed outside bioreactors, and (ii) submerged where membrane modules are mounted directly within bioreactors. The latter is characterized by rather low energy consumption due to elimination of external circulation pumps and has thus become increasingly popular (Gander et al., 2000; Howell et al., 2004).

Despite many advantages of MBR systems, membrane fouling remains the principal obstacle constraining their more extensive application. Membrane fouling, commonly

indicated by permeate flux decline or transmembrane pressure increase with operation time, is essentially a consequence of the interactions between membranes and foulants in MBR mixed liquor. It leads to deteriorated membrane performance, severe loss of system productivity, more frequent membrane cleaning/replacement, and more intensive aeration for stable operation, all of which significantly increase operating and maintenance costs of MBR systems. Therefore, tremendous research efforts have been undertaken to mitigate and control membrane fouling in MBR systems (Defrance and Jaffrin, 1999; Chang et al., 2002; Ognier et al., 2002).

Fouling in MBR systems is a rather complicated phenomenon in terms of various types of foulants and different fouling mechanisms involved (Bouhabila et al., 2001; Chang et al., 2002). The composition of MBR mixed liquor is complex and heterogeneous comprising a wide range of components, such as suspended solids, colloids, SMP, and extracellular polymeric substances (EPS). Different components of MBR mixed liquor can contribute to membrane fouling in one way or another (Defrance et al., 2000; Lee et al., 2003). At the early stages of MBR research, most efforts have been made to elucidate the influence of mixed liquor suspended solids (MLSS) on membrane fouling (Fane et al., 1981; Yamamoto et al., 1989). Since the concentration of DOM is normally several orders of magnitude less than that of MLSS, its contribution to the total filtration resistance is often intuitively supposed to be insignificant and, therefore, does not attract much attention.

However, it has been clearly demonstrated in many recent studies that DOM in MBR mixed liquor does play an important role in membrane fouling. Several researchers have attempted to evaluate the significance of DOM fouling in MBR systems by

comparing the relative contribution of each different mixed liquor fraction to total filtration resistance. Wisniewski and Grasmick (1998) quantified the role in membrane fouling of three main fractions of MBR mixed liquor, i.e., MLSS, colloids, and DOM recovered after filtration through 0.05 μm membranes. They found that 52% of the filtration resistance was attributable to the DOM. It was then suggested that the interactions between DOM and membranes play a major role in MBR fouling. Shortly afterwards, Bouhabila et al. (2001) investigated the relative contribution of different mixed liquor fractions to membrane fouling in a submerged MBR system equipped with 0.1 μm hollow fiber membranes. Their results revealed that DOM contributed to 26% of the filtration resistance. More recently, Lee et al. (2003) examined the fouling potential of supernatant, where DOM resides, in submerged MBR systems equipped with 0.4 μm polypropylene membranes and reported that the contribution of DOM to the filtration resistance varied from 28% to 37% depending on sludge retention time (SRT).

In addition, the importance of DOM in membrane fouling has also been observed in practical MBR operation. Defrance et al. (2000) reported that the composition of the adsorbed material on/in the membrane was very close to that of the DOM in the MBR system, indicating that DOM was the dominant foulant. It was suggested that internal fouling caused by adsorption of DOM into membrane pores forms the major part of the irreversible fouling of membrane modules, which ultimately leads to MBR system failure (Chang et al., 2002). In another study, Kimura et al. (2005) found that the nature and amount of DOM in the MBR system had significant effect on membrane fouling. The higher the amount of carbohydrate presented, the more serious the fouling occurred.

On the other hand, it has been observed that the concentration of DOM in MBR mixed liquor was much higher than that in effluent. This indicates that membranes in MBR systems act as a selective barrier for some DOM components, resulting in DOM accumulation inside MBR systems (Huang et al., 2000; Shin and Kang, 2003). The accumulated DOM has been shown to be inhibitory to the metabolic activity of activated sludge and also exert a negative impact on membrane permeability due to organic fouling. Huang et al. (2000) investigated the behavior of DOM in the submerged MBR system during long-term operation and reported that the accumulated SMP in the MBR can result in up to 70% decrease in permeate flux.

1.2 Problem Statement

Although the significance of DOM fouling in MBR systems has been widely acknowledged, the understanding of the complicated DOM fouling phenomenon is far from complete. In most previous studies of membrane fouling in MBR systems, various dissolved organic compounds were simply treated as one foulant in parallel with suspended solids and colloids in MBR mixed liquor. Therefore, only the gross impact of the complex DOM mixture on MBR fouling can be evaluated. However, it is well known that DOM in MBR systems represents a large group of structurally complex organic compounds with distinctly different characteristics. It is reasonable to expect that various DOM components may play different roles in MBR fouling. Some may be able to cause serious membrane fouling through either the same or different mechanisms, while others may have little or no effect on membrane fouling due to the weak interactions with the membranes and therefore are not foulants. Apparently, a more fundamental research on the characteristics and fouling potentials

of various DOM components would provide more detailed insights into the DOM fouling phenomenon in MBR systems.

In addition, despite the great importance of DOM fouling, it has not been seriously taken into account in the models for fouling development in MBR systems. In most existing models, the particular role of dissolved organic compounds has not been sufficiently delineated or speculated, but commonly lumped together with other foulants. This severely impairs the utility of these MBR fouling models and leads to possible misinterpretations of simulation results. It is believed that an explicit presentation of the role of DOM in the fouling models would better describe fouling behaviors in MBR systems.

The accumulation of DOM is an important and interesting phenomenon observed in both laboratory and full-scale MBR systems. Although DOM accumulation is commonly attributed to the sieving effect (size exclusion) of the membranes, little or no experimental evidence has been reported in the literature. In particular, it is surprisingly found that the molecular size of DOM in the effluent was not measured and compared with that in the MBR. Moreover, it is noteworthy that the sieving effect alone appears insufficient to explain DOM accumulation in many cases, especially when microfiltration membranes with large pore size are employed in MBR systems. More research efforts, both experimental and theoretical, are therefore required for an in-depth understanding of the underlying mechanisms governing DOM accumulation in MBR systems.

Finally, it is worth noting that DOM fouling and accumulation in MBR systems are inherently interrelated with the coupled activated sludge process. As a key biological parameter in MBR operation, SRT is supposed to significantly affect the amount and nature of DOM, and consequently the extent of DOM fouling and accumulation in MBR systems. Nevertheless, at present, very little is known about the characteristics, fouling potential, and accumulation of DOM at different SRTs.

1.3 Research Objectives and Scope

Based on the aforementioned information, it is evident that DOM fouling and accumulation are of key importance in MBR operation. The primary objective of this thesis is, therefore, to contribute towards a better understanding of the characteristics, fouling behaviors, and accumulation of DOM in submerged MBR systems under various scenarios. The specific objectives are listed as follows:

i) To characterize DOM in MBR systems from membrane fouling and accumulation perspectives, with special emphasis on molecular size, hydrophobic/hydrophilic and charge properties.

ii) To identify the major foulants from the complex DOM mixture by evaluating and comparing the fouling potentials of different fractional DOM components.

iii) To develop a fouling model for submerged MBR systems based on the improved understanding of the role of DOM in both reversible and irreversible fouling.

iv) To investigate the composition, characteristics, and fouling potential of DOM both in the MBR and in the effluent during MBR operation at different SRTs.

v) To examine the fundamental mechanisms responsible for the high DOM concentration in MBR systems and propose a new theory for a better

explanation of DOM accumulation.

In order to fulfill the objectives of this study, the characteristics of DOM obtained from the pilot MBR systems were investigated using the classical dissolved organic carbon (DOC) preparative fractionation method. DOM was fractionated into four more homogeneous components for subsequent experiments on the basis of hydrophobic/hydrophilic and charge properties. Fouling experiments were then carried out with microfiltration membranes in a stirred-cell filtration system, where the rate and extent of flux reduction due to DOM fouling can be quantified under well-defined operating conditions. With the concept of DOM fouling, a mathematical model was proposed to describe fouling development in submerged MBR systems. The relative importance of DOM in MBR fouling can be theoretically quantified based on the model simulations. The validity of the model was evaluated with the operational data from the pilot MBR system.

It should be pointed out that DOM fouling in MBR systems is extremely complicated. There are a myriad of foulants present and a number of fouling mechanisms involved. Although it is recognized that various kinds of foulants are inherently interrelated as they exist in a single system, the focus of this thesis is mainly on DOM fouling in MBR systems. Therefore, it is not the task of this thesis to either investigate the roles of other components in MBR fouling, or analyze the extremely complex correlations between DOM and other foulants in MBR mixed liquor.

On the other hand, a lab-scale submerged MBR system was constructed and operated for readily biodegradable synthetic wastewater treatment. The composition,

accumulation, and fouling potential of DOM were investigated at SRT of 10, 20 and 40 days. At each SRT, a steady-state of four weeks was maintained, during which measurements were evenly conducted for parameters of interest. In particular, the effect of membrane sieving on DOM accumulation was experimentally evaluated by comparing the molecular size of DOM in the MBR and in the effluent. A new theory was subsequently proposed to better explain DOM accumulation in MBR systems based on the retarded transport of DOM through porous membranes.

1.4 Thesis Program

The thesis itself consists of 8 chapters. Chapter 2 provides a comprehensive literature review, including an overview of MBR application in wastewater treatment and a summary of the main findings with respect to the characteristics and fouling behaviors of DOM based on model compounds or natural organic matter. Chapter 3 describes the materials and methods used in this study.

The characteristics and fouling behaviors of DOM in the pilot MBR systems were investigated in Chapter 4 with specific emphases on: (i) examination of the hydrophobic/hydrophilic and charge properties of DOM, and (ii) quantification of the fouling potential of different fractional DOM components. Chapter 5 focused on development of a fouling model for submerged MBR systems, in which DOM is speculated as the key contributor to irreversible fouling whereas MLSS is mainly responsible for reversible fouling.

Chapter 6 examines the characteristics and behaviors of DOM during operation of the lab-scale MBR system. Measurements were conducted for various DOM parameters

with special attention given to the composition, accumulation, and fouling potential of DOM at different SRTs. DOM accumulation was further investigated both experimentally and theoretically in Chapter 7. The retarded transport of DOM through porous medium was postulated as a new mechanism for a better explanation of DOM accumulation in MBR systems. Finally, Chapter 8 summarizes the key findings of this study and gives some recommendations for future research in this area.

CHAPTER 2

LITERATURE REVIEW

2.1 MBR Technology for Wastewater Treatment and Reclamation

2.1.1 Limitations of Conventional Treatment Processes

The use of biological treatment can be traced back to the late nineteenth century. By the 1930s, it became a standard method for wastewater treatment (Rittmann, 1987; Forster, 2003). Since then, both aerobic and anaerobic biological treatment processes have been commonly used to treat domestic and industrial wastewater (Arceivala, 1981; Ray, 1995; Metcalf and Eddy, 2003). During the course of these processes, organic pollutants, mainly in soluble form, are converted into H_2O, CO_2, NH_4^+, CH_4, NO_2^-, NO_3^-, and biological cells. After removal of the soluble organic pollutants in the biological process, suspended solids must be separated from the liquid stream to produce the required effluent quality (Dignac et al., 2000; Ellis et al., 2004).

One of the most widely used wastewater treatment processes is the conventional activated sludge system. It is a cost effective treatment system under optimal conditions. However, the final effluent quality of the activated sludge system is highly dependent on hydrodynamic conditions in the secondary settling tank and the settling properties of the sludge (Rittmann and McCarty, 2001). A large-size settling tank offering several hours of residence time is usually required to obtain adequate solid/liquid separation. At the same time, close control of the biological treatment unit is necessary to avoid conditions that lead to poor settleability and/or bulking of sludge (Cheremisinoff, 1994; Bitton, 1999). Very often, however, economic constrains limit such options. Even with such controls, further treatment processes such as microfiltration and ultrafiltration are normally needed for most applications of wastewater reclamation. Therefore, a more effective solid/liquid separation method different from the conventional gravity settling method is needed to improve the treatment efficiency (Yamamoto et al., 1989; Xing, et al., 2001).

2.1.2 Overview of Membrane Processes

According to International Union of Pure and Applied Chemistry (IUPAC), membrane is termed as "a structure, having lateral dimensions much greater than its thickness, through which mass transfer may occur under a variety of driving forces" (IUPAC, 1996). More specifically, membrane can be defined as a semi-permeable thin film, which acts as a selective barrier between two phases. Membrane processes can be classified by the driving force and the nature of the membrane. The driving forces in membrane processes can be gradients of concentration, pressure, temperature, and electrical potential (Mulder, 1996; Baker, 2004). Other than driving forces, the nature of a membrane i.e., its structure and material, determines the type of

application, ranging from the separation of microscopic particles to the separation of molecules of an identical size or shape (Hillis, 2000). In Figure 2.1, an overview of the membrane processes commonly used in water and wastewater treatment, namely, microfiltration (MF), ultrafiltration (UF), nanofiltration (NF), and reverse osmosis (RO) as well as the sizes of solutes and particles of interest is presented.

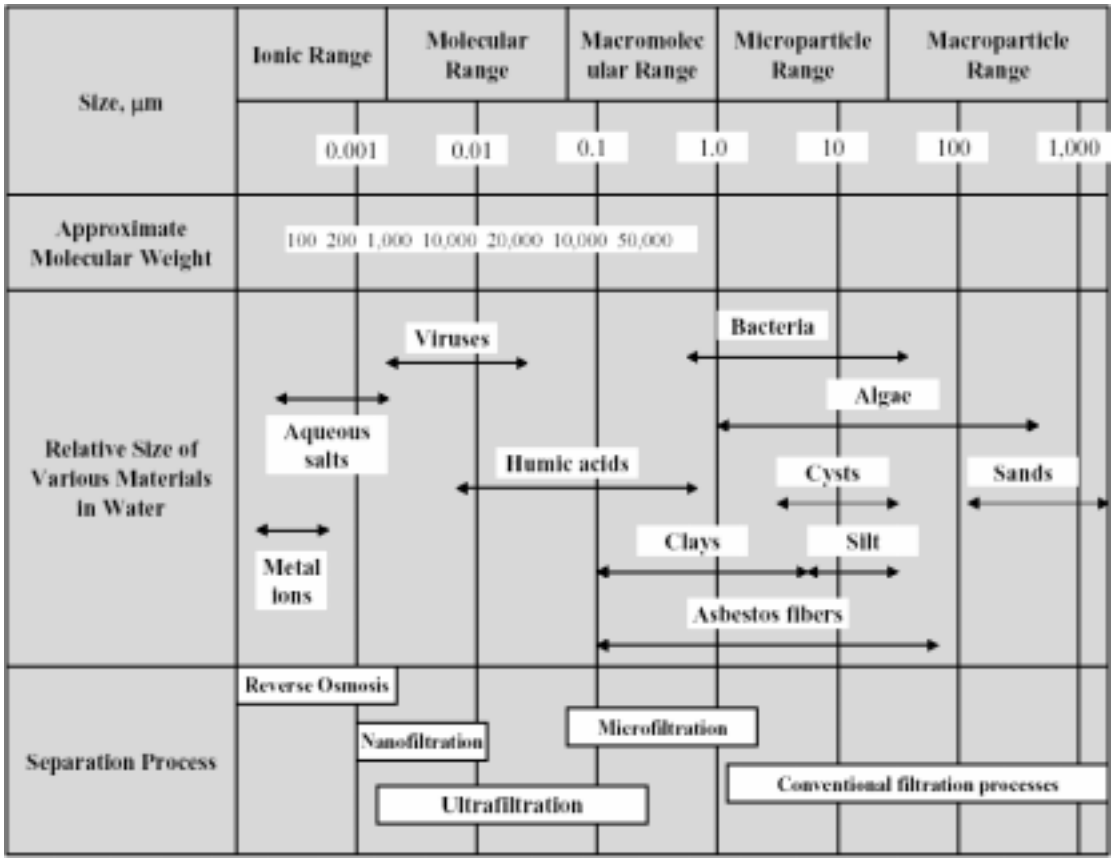

Figure 2.1 Overview of pressure-driven membrane processes commonly used in water and wastewater treatment and dimensions of various impurities found in waters (Jacangelo et al., 1989)**.**

As shown in Figure 2.1, membrane processes cover the entire size range from suspended solids to small organics and mineral salts. Of particular interest, MF and UF are the two membrane processes widely applied in membrane bioreactor (MBR) systems (Fan et al., 1999; Chang et al., 2002). MF is defined as a pressure-driven membrane-based separation process in which particles and dissolved macromolecules

larger than 0.1 μm are rejected (IUPAC 1996). UF is a separation process whereby a solution containing a solute of molecular size significantly greater than that of the solvent molecule is removed from the solvent by the application of a hydraulic pressure which forces only the solvent to flow through a suitable membrane, usually having a pore size in the range 0.001–0.1 μm (IUPAC 1996). The selectivity of MF and UF membranes is determined primarily by the ratio between the hydrodynamic diameter of the solute and the apparent pore diameter. Factors such as the shape and dissociation of the macromolecules also influence the separation performances (Mulder, 1996; Hillis, 2000).

All membrane processes are designed to achieve a certain separation purpose. Owing to the semi-permeability of membranes, some components in solution could transport through membranes more readily than the others (Schultz, 1980). The stream containing penetrants that passes through the membrane is called “permeate”; while the stream that has been depleted of penetrants and leaves the membrane modules without passing through the membrane to the downstream is called “retentate” (or the concentrate) (IUPAC 1996). Generally, there are two configurations of membrane processes as shown in Figure 2.2. Dead-end filtration can be compared with conventional cake filtration. The flow direction of the feedwater is orthogonal to membrane surface. All matters that are rejected by membranes remain on the surface and contribute to the formation of a cake layer. The thickness of this cake layer increases proportionally to the permeate flux. The permeate flux decreases according to the increasing thickness of the cake layer (Rautenbach and Albrecht, 1989; Mulder, 1996). The alternative to dead-end filtration is crossflow filtration, in which the feedwater flows parallel to the membrane surface and so expedites the removal of

accumulated materials from membrane surface. Equilibrium arises between the cleaning effects and the deposit effects, making the cake layer thickness constant. The permeate flux decreases in the initial phase because of the unavoidable cake layer formation and achieves a stable end point in the equilibrium phase. This state is also designated as a steady state in cross flow microfiltration (Mulder, 1996; Song, 1998).

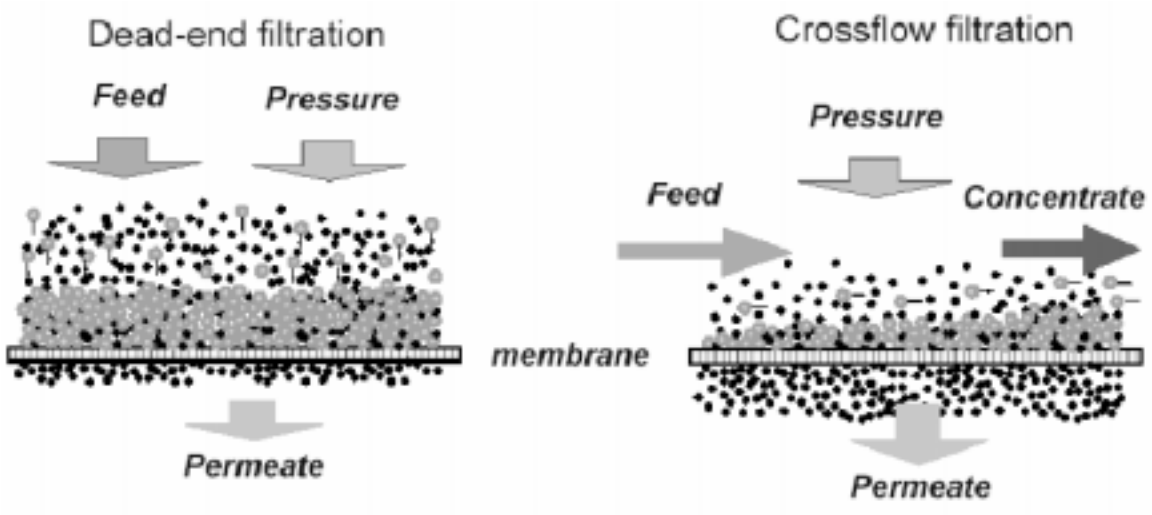

Figure 2.2 Configuration of membrane processes: Dead-end Filtration (left) and Cross-flow Filtration (right).

2.1.3 Development of MBR Technology

Membranes have been finding wide application in water and wastewater treatment ever since the early 1960s when Loeb and Sourirajan invented an asymmetric cellulose acetate membrane for reverse osmosis (Visvanathan et al., 2000). Many combinations of membrane solid/liquid separators in biological treatment processes have been studied since (Hillis, 2000). When the need for wastewater reuse first arose, the conventional wastewater treatment plants were extended by utilizing some advanced treatment processes to meet the more stringent effluent standard for reuse. For irrigation, this treatment may be limited to filtration and disinfection, whereas for building reuse or ground water recharge it may also include RO (Rittmann and

McCarty, 2001; Metcalf and Eddy, 2003). The progress of membrane manufacturing technology and its applications could lead to the eventual replacement of tertiary treatment steps by MF/UF. Parallel to this development, MF/UF was used for solid/liquid separation in the biological treatment process and the secondary settling tank could also be eliminated (Fan et al., 1999; Gunder, 2001). Application of membrane separation (MF/UF) techniques for suspended solid separation can overcome the inherent disadvantages rising from both sedimentation and biological treatment steps. The membrane offers a complete barrier to suspended solids and permits the extraction of a high quality effluent (Cicek et al., 1999).

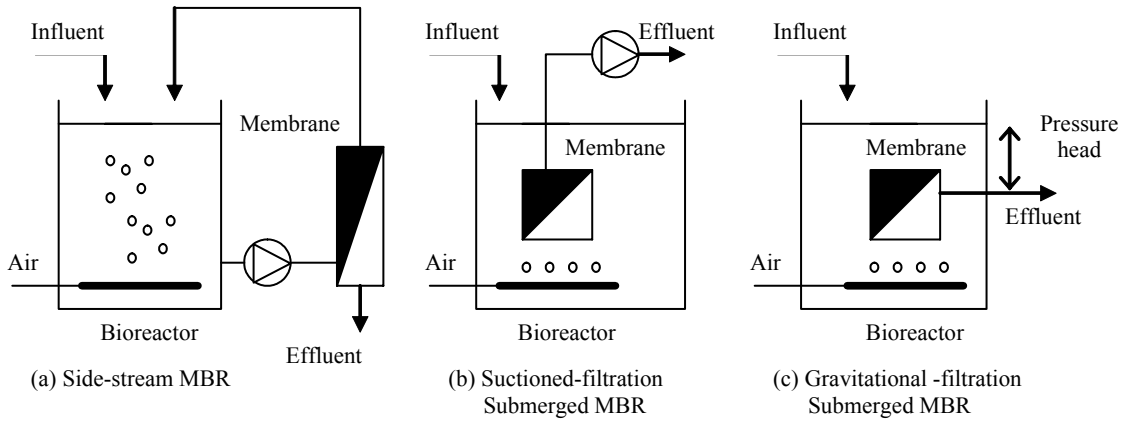

Figure 2.3 Configuration of MBR systems: (a) Side-stream MBR, (b) Suctioned-filtration submerged MBR, and (c) Gravitational-filtration submerged MBR.

Although the concept of an activated sludge process combined with ultrafiltration was commercialized in the late 1960s, the application has only recently started to attract serious attention. There has been considerable development and application of membrane processes in combination with activated sludge processes over the last 15 years (Fleischer et al., 2005). The membrane device can be configured in the external circuit of a bioreactor, as in side-stream operation, or directly submerged in a bioreactor (Figure 2.3). In the case of a side-stream system, the membrane device is

independent of the bioreactor. Feedwater enters the bioreactor where organic matters are biodegraded by biomass. The mixed liquor in the bioreactor is then pumped around a recirculation loop containing a membrane unit where the permeate is discharged and the retentate is returned back to the bioreactor. The transmembrane pressure (TMP) and crossflow velocity of the membrane device are both generated from a pump (Hillis, 2000; Kim et al., 2001).

However, higher energy cost to maintain the crossflow velocity in a side-stream MBR led to the next stage of development: submerged MBR systems (Yamamoto et al., 1989). In this development, membranes were suspended in the bioreactor above the air diffusers. There is no recirculation loop as the separation occurs within the bioreactor itself (Liu et al., 2000). Under these circumstances, the TMP is derived from the hydraulic head of the water above the membrane. This is supplemented by a suction pump, in some systems, to increase the TMP (Bouhabila et al., 1998). Fouling control is achieved by a scour at the membrane surface, usually from aeration with the movement of bubbles close to the membrane surface generating the necessary liquid shear velocity (Chang et al., 2002; Howell et al., 2004).

Full-scale commercial aerobic MBR systems first appeared in North America in the late 1970s and then in Japan in the early 1980s, with anaerobic systems entering the industrial wastewater market at around the same time in South Africa (Visvanathan et al., 2000; Hillis, 2000). The introduction of aerobic MBR systems into Europe did not occur until the mid-1990s. There are over 1000 commercial MBR systems in operation worldwide, with many more proposed or currently under construction (Daigger et al., 2005). Commercial MBR systems have proliferated in Japan, which

has approximately 66% of the world's systems. The rest are predominately either in North America or Europe (Gunder, 2001). Over 90% of these systems couple the membrane separation process with aerobic biological systems rather than with anaerobic bioreactors (Chang et al., 2002). Approximately 70% of these commercial systems have the membrane device submerged within the bioreactor while the remainder has the membrane device external to the bioreactor (Visvanathan et al., 2000).

2.1.4 Advantages of MBR Technology

The coupling of membranes to bioreactors has attracted increasing interest both academically and commercially because of the inherent advantages the system offers over conventional biological wastewater treatment systems. Of these, the prime ones are the excellent effluent quality, easy management, high biomass concentration, and less sludge production (Xing et al., 2000; Fleischer et al., 2005). More detailed descriptions of these advantages are provided below:

i) MBR systems can provide high-quality effluents (free of solids and bacteria) that can be directly reused for municipal watering, toilet flushing, and car washing. Therefore, large quantities of urban wastewater can be effectively harnessed with MBR for reuse. The development of water industry would be more sustainable (Huang et al., 2001; Xing et al., 2001).

ii) Because suspended solids are completely retained by membranes in MBR systems, settling problem caused by poor flocculation of microorganisms or proliferation of filamentous bacteria has no more effect on the quality of effluent (Bai and Leow, 2002). Consequently, operation and maintenance of

MBR systems is much easier than conventional activated sludge systems. This is important with industrial wastewater, in which a lack of nutrients tends to lead to excessive growth of filamentous organisms resulting in poor settlement (Visvanathan et al., 2000).

iii) The elimination of secondary settlement stage allows the use of high activated sludge concentration in a small volume tank. Some authors have investigated MBR system with MLSS ranging between 10,000 and 23,000 mg/L (Dijk and Roncken, 1997; Churchouse et al., 1998). Bouhabila et al. (1998) found critical fluxes for the operation of the MBR with MLSS concentration of up to 15,000 mg/L. High biomass concentration in the reactor enabled MBR to produce high quality effluent at short hydraulic retention time (Gunder, 2001).

iv) The combination of high biomass concentrations and the complete retention of biosolids allows MBR systems to be operated at low organic loading rates. These characteristics promote the development of slow growth bacteria, such as nitrifiers, and result in lower sludge production as compared with conventional aerobic treatment processes (Chang et al., 2002). Bouhabila et al. (1998) reported sludge production in the range of 0.2-0.34 kg MLSS/kg COD removal using the MBR system as compared with sludge production of 0.3-0.5 kg MLSS/kg COD removal using conventional processes. Eikelboom et al. (1993) found zero sludge production when an MBR was used for treating municipal wastewater.

2.2 Membrane Fouling in MBR Systems

Notwithstanding the many advantages of MBR systems, their widespread application is constrained by membrane fouling. In some recent reviews covering membrane applications to bioreactors it has been shown that, as with other membrane processes, membrane fouling is the most serious problem affecting system performance (Visvanathan et al., 2000; Kim et al., 2001). Though numerous investigations of membrane fouling have been published, the diverse range of operating conditions and feedwater matrices employed, and the limited information reported in most studies on the mixed liquor composition, have made it difficult to establish any generic behavior with respect to membrane fouling in MBR systems (Chang et al., 2002). Unified and well-structured theories regarding MBR fouling are not currently available. However, it is evident that the nature and extent of fouling are strongly influenced by three factors: characteristics of mixed liquor, operating conditions, and membrane properties (Chang and Lee, 1998; Chang et al., 1999; Bouhabila et al., 2001). These factors are discussed in turn below.

2.2.1 Characteristics of Mixed Liquor

MBR mixed liquor is a complex and heterogenous suspension containing both feedwater components and metabolites produced during biological reactions as well as microorganisms. Many individual components of the mixed liquor, ranging from suspended solids to dissolved polymers such as EPS and SMP can contribute to membrane fouling with different mechanisms (Defrance et al., 2000; Lee et al., 2003). As soon as a membrane surface comes into contact with the mixed liquor, deposition of suspended solids onto the membrane takes place that leads to cake formation and flux decline. Since this cake layer is largely readily removable from the membrane if

an appropriate physical cleaning protocol is employed, it is often classified as reversible fouling (Chang et al., 2002). On the other hand, internal fouling caused by the adsorption of dissolved polymers into membrane pores and pore blocking is considered irreversible and is generally only removed by chemical cleaning (Mulder, 1996; Carroll et al., 2000).

2.2.1.1 Mixed Liquor Suspended Solids

At the early stages of MBR development, many researchers have given attention to the effects of mixed liquor suspended solids (MLSS) on membrane fouling. Fane et al. (1981), for example, reported membrane resistance to increase linearly with MLSS concentration, and Yamamoto et al. (1989) also reported that the flux decreased abruptly if the MLSS concentration exceeded 40,000 mg/L in a submerged MBR system. MLSS concentration is considered to impact directly upon cake layer resistance, as surmised from conventional cake filtration theory, the cake resistance, R_c, often being expressed as (Shimizu et al., 1993; Chang et al., 2001)

$$R_c = \alpha \cdot v \cdot C_b \tag{2.1}$$

where α is the specific cake resistance, v is the permeate flux, and C_b is the bulk MLSS concentration. MLSS concentrations for aerobic MBR systems typically range from 3,000 to 31,000 mg/L (Brindle and Stephenson, 1996). However, Lubbecke et al. (1995) showed MLSS concentrations up to 30,000 mg/L to be not directly responsible for irreversible fouling, and that viscosity and dissolved matter more significantly impact on flux. Ueda et al. (1996) observed the increase in viscosity to yield a substantial suction pressure increase, which consequently causes the MBR system to fail.

Based on the tremendous research efforts made in this regard, several fouling control techniques including sub-critical flux operation, high shear slug-flow aeration in submerged configuration, periodical air or permeate backflushing, intermittent suction operation or addition of powdered activated carbon have been established as some kinds of standard operating protocols to guarantee the successful application of MBR systems (Visvanathan et al., 2000; Gunder, 2001; Bai and Leow 2002).

2.2.1.2 Dissolved Organic Matter

Dissolved macromolecules, on the other hand, impact both on internal and external fouling, the latter being promoted by concentration polarization and solute-solid interactions. Ishiguro et al. (1994) proposed the following general correlation between permeate flux (J) and DOC:

$$J = a + b \cdot \log(DOC) \tag{2.2}$$

where a and b are empirical constants. Although the concentration of DOM is several orders of magnitude lower than suspended solids, it has been shown that this dissolved fraction of mixed liquor plays a significant role in membrane fouling (Wisniewski and Grasmick, 1998; Bouhabila et al., 2001).

Lee et al. (2001) conducted a comparative study on the fouling characteristics between attached and suspended growth submerged MBR systems. As suspended solids have been thought as the main contributor to membrane fouling in MBR systems, the authors attempted to remove one of the primary sources of suspended solids, which are the microorganisms in the bioreactor. An attached growth MBR system was thus designed to reduce the effect of suspended solids on membrane fouling, in which most of the microorganisms were attached on support media with

only a negligible amount of microorganisms in the bulk. The MLSS concentration in the suspended growth MBR system was 3000 mg/L, while the attached growth MBR system contained only 100 mg/L of MLSS while 2000 mg/L of microorganisms were attached on the looped cord media. Other operating conditions being equal, the extent of fouling was believed to vary according to the mixed liquor composition in the MBR system.

However, contrary to expectations, membrane fouling proceeded much faster with the attached growth system than with the suspended growth system although the latter had suspended solids 30 times higher than the former. Consequently, soluble fraction, not suspended solids was thought to be more responsible for membrane fouling in the MBR system. It is clearly demonstrated that the suspended solids are only partially responsible for the resistance increase during membrane filtration and the relative contribution of DOM to the filtration resistance is significant, especially to the irreversible part leading to long-term flux decline (Kimura et al., 2005).

2.2.1.3 Particle Size Distribution

Many researchers have sought to establish the influence of particle size on the cake layer resistance. According to the well known Carmen–Kozeny equation applied to conventional filtration, specific resistance (α) is a function of particle diameter (d_p), porosity of cake layer (ε), and particle density (ρ) as follows (Baker et al., 1985):

$$\alpha = \frac{180 \cdot (1-\varepsilon)}{\rho \cdot d_p^2 \cdot \varepsilon^3} \tag{2.3}$$

Combination of Eqs. 2.1 and 2.3 leads to Eq. 2.4:

$$R_c = \frac{180 \cdot (1-\varepsilon) \cdot v \cdot C_b}{\rho \cdot d_p^2 \cdot \varepsilon^3} \quad (2.4)$$

Eq. 2.4 shows that R_c is inversely related to cake particle size. In general, the particle size of an activated sludge floc ranges from 1.2 to 600 μm (Jorand et al., 1995). However, the breakup of biological flocs by the shear force during crossflow filtration results in the formation of a denser cake layer on the membrane (Wisniewski and Grasmick 1998; Kim et al., 2001). According to Wisniewski et al. (2000), the suspension produced after the floc breakup consists mainly of particles having a size of around 2 μm corresponding to flux declines. Cicek et al. (1999) revealed the average diameter of particles in a side-stream MBR system to be around 3.5 μm, with 97% of the particles being smaller than 10 μm, whereas the mixed liquor in conventional activated sludge systems contained flocs ranging from 20 to 120 μm in size. The resulting α values, measured by vacuum filtration, of the MBR sludge were determined as 2.4×10^{15} m/kg compared to 2.1×10^{12} m/kg for that of the conventional activated sludge systems. On the other hand, the floc size in the submerged MBR (20–40 μm) appears to be greater than that of side-stream (7–8 μm) due to the reduced shear stress (Zhang et al., 1997).

2.2.2 Operating Conditions

2.2.2.1 Hydraulic Retention Time and Loading Rate

An indirect action of hydraulic retention time (HRT) on fouling in a submerged hollow fiber MBR system has been reported by Visvanathan et al. (1997), who noted reduced fouling (i.e., no TMP increase) at higher HRT values, postulating that a rapid formation of a compact layer on the membrane surface took place at shorter HRTs.

Given that the MLSS concentration was reported to change from 3 g/L for an HRT of 12 h to 7 g/L for 3 h HRT, it is evident that the accompanying change in hydraulic resistance is related to the MLSS: a shorter HRT provides more nutrients to the biomass, and leads to a greater biological growth and so a higher MLSS (Dufresne et al., 1998). MLSS is also directly influenced by organic loading rate (OLR), though Nagaoka et al. (1998) concluded, from their study of the effect of loading rate on the operation of a flat-sheet MBR system, that fouling was not greatly influenced by threefold change in OLR for flux and OLR values of around 4 L/m^2 h and 2 g/L d respectively.

2.2.2.2 Sludge Retention Time

Sludge retention time (SRT) is directly linked to the net production of excess sludge and significantly affects biological performance by altering sludge composition (Urbain et al., 1998; Bouhabila et al., 2001). The most obvious result of SRT variation is on MLSS concentration. By increasing SRT from 5 to 30 days, Xing et al. (2000) noted an apparent MLSS concentration increase from 2.5 to 15 g/L. Decreases in bulk EPS concentration (Chang et al., 1998) and slight increases in mean particle size (Huang et al., 2001) have been reported at longer SRTs, though these effects both appear to be very small. Though longer SRTs inevitably lead to higher MLSS concentration, increasing from 3 to 7.5 g/L on increasing the SRT from 5 to 20 days according to Fan et al. (1999), reduced fouling rates at the longer SRTs have been reported (Fan et al., 1999; Bouhabila et al., 1998). However, high viscosity mixed liquors associated with high MLSS concentrations can lead to excessive fouling (Ueda et al., 1996).

Like HRT, SRT cannot be varied without important changes in sludge composition. The direct effect of SRT on fouling is once again not very clear at this moment. As a general trend, it was shown and now accepted that the shorter the HRT and the longer the SRT, the higher the MLSS concentration (Rittmann and McCarty, 2001; Metcalf and Eddy, 2003). It is then suggested that HRT and SRT cannot be considered as direct fouling causes but rather like parameters influencing factors like MLSS, DOM, and particle size distribution, which can then be directly related to fouling rates (Chang et al., 2002). Clearly, as with HRT, SRT only indirectly impacts on fouling.

2.2.3 Membrane Properties

Membrane properties such as pore size, porosity, surface energy, charge, roughness, and hydrophilicity/hydrophobicity, etc., directly affect membrane fouling (Mulder, 1996). Effects of pore size on membrane fouling strongly depend on the feed solution characteristics, in particular, particle size distribution. Shimizu et al. (1990) correlated the flux with the pore size for a side-stream MBR system treating methanogenic wastes. The authors showed that 0.05–0.2 μm pore sized membranes produced the maximum flux among membranes ranging from 0.01–1.6 μm in pore size. Larger pore size does not always lead to greater flux due to internal fouling. Chang et al. (1994), investigating the effect of pore size on flux from alcohol-distillery wastes, found the flux produced from a membrane of 0.05 μm pore size to be higher than that from 0.4 μm membrane for otherwise comparable filtration conditions. Choo and Lee (1996) determined the optimum pore size based on the particle size distribution of anaerobic broth. These reports all emphasize the importance of pore clogging by fine particles during membrane filtration.

Ceramic and polymeric membranes are commonly available for MBR applications (Visvanathan et al., 2000). Ceramic materials such as aluminum, zirconium, and titanium oxides (Al_2O_3, ZrO_2, and TiO_2, respectively), show superior hydraulic, thermal, and chemical resistance (Ghyoot et al., 1997). Although application of ceramic membranes to aerobic or anaerobic MBR has been studied (Shimizu et al., 1989; Ahn et al., 1998; Scott et al., 1998; Cicek et al., 1999; Defrance and Jaffrin, 1999; Tardieu et al., 1999; Wen et al., 1999a, b; Defrance et al., 2000), polymeric membranes are more commonly used due to the much higher cost of the ceramic membranes, which are also largely limited in geometry to tubular monoliths.

Several studies have demonstrated the importance of hydrophobicity of membrane materials in determining membrane performance. It is known that hydrophilic membranes yield the higher fluxes because of the hydrophobic nature of the interaction between the membrane and biomass (Chang et al., 1999; Futumura et al., 1994; Madaehi et al., 1999). This demands that the naturally hydrophobic polymeric materials, such as polyethylene, polypropylene, polyvinilydene fluoride, and polysulfone, are surface modified with some hydrophilic functional group (Knoell et al., 1999; Wang et al., 2000). Experimental results showed that the modified polyethersulfone membrane (with hydrophilic monomers) presented a 25% increase in hydrophilicity, a 49% decrease in (bovine serum albumin) biofouling, and a 4% increase in albumin retention compared with the unmodified membrane (Pieracci et al., 1999).

2.3 Characterizing Dissolved Organic Matter

Dissolved organic matter (DOM) can range in molecular weight from a few hundred to ten thousand daltons (Da), which is in the colloidal size range (Leenheer and Croué, 2003). Aquatic humic substances (AHS) have been regarded as macromolecular, but recent studies of aqueous humic extracts from soil, lignite, and water found relatively small primary molecular structures (100–2000 Da) with macromolecular characteristics resulting from aggregates formed by hydrogen bonding, nonpolar interactions, and polyvalent cation interactions (Leenheer et al., 2001; Piccolo et al., 2002).

DOM is a complex mixture of aromatic and aliphatic hydrocarbon structures that have attached amide, carboxyl, hydroxyl, ketone, and various minor functional groups (Hong and Elimelech, 1997; Schäfer et al., 2001). Heterogeneous molecular aggregates in natural waters increase DOM complexity. It has been concluded by some researchers that humic substances cannot be well characterized at the molecular level (MacCarthy, 2001). However, recent findings that show small primary structures compose the majority of DOM raise molecular characterization to a tractable problem. DOM research can be divided into two categories: whole water studies, in which DOM is characterized in water and its inorganic constituents, and studies of DOM fractions isolated from water and inorganic constituents (Leenheer and Croué, 2003).

2.3.1 DOM Profiling by Resin Sorbents

DOM can be fractionated into various components with distinct properties using resin sorbents. A protocol with XAD-8 resin has been widely used to isolate humic substances (i.e., humic and fulvic acids) and is the basis of a simple DOM analysis

that determines the so-called humic/nonhumic distribution (DOM profiling) of raw and treated waters (Thurman and Malcolm, 1981; Lin et al., 2000). Another fractionation approach requires a serial two-column array of resins, in which the nonhumic DOM fraction is operationally defined as "transphilic DOM" (Fan et al., 2001). Two small serial resin columns requiring only a few hundred milliliters of water have been used to determine DOM distribution between operational categories based on polarity (Imai et al., 2001; Hu et al., 2003). The terms "hydrophobic", "hydrophilic", "acidic", "basic", and "neutral" refer to the predominant property of a DOM fraction while recognizing that many DOM molecules are both amphiphilic and amphoteric (Leenheer and Croué, 2003). A third anionic exchange resin column can further fractionate the hydrophilic DOM into charged and neutral components (Leenheer, 1981; Imai et al., 2002). In addition, spectrophotometric measurements, such as ultraviolet (UV) absorbance and fluorescence measurements, can complement DOC measurement in DOM profiling studies.

2.3.2 Spectrophotometric Measurements

Absorption of both visible and UV light is widely attributed to the aromatic chromophores present in DOM molecules–primarily humics–dissolved in the water (Weishaar et al., 2003). As shown by numerous studies, UV–visible spectra of DOM are typically broad and nearly featureless because the number of possible types of chromophores is large and none possess an easily distinguishable spectrum (Her et al., 2002; Jackson et al., 2005). Several UV–visible absorbance ratios have been proposed to characterize the spectrometric profile of DOM in soil. However, most aquatic research has limited data collection to the absorbance at 254 nm, which serves as a rough indicator of overall DOM concentration (Leenheer and Croué, 2003).

Specific UV absorbance (SUVA or $SUVA_{254}$) is defined as the sample's UV absorbance at 254 nm divided by the DOC concentration of the solution (Imai et al., 2001; Hu et al., 2003). Carbon-13 nuclear magnetic resonance (^{13}C-NMR) was used to determine a strong correlation between SUVA and the aromatic carbon contents of a large number of DOM fractions (Wong et al., 2002). High SUVA samples are generally enriched in hydrophobic NOM, such as humic substances (Fan et al., 2001). Therefore, SUVA indicates aromatic compounds in the DOM and can be used to estimate the chemical nature of the DOC at a given location. SUVA is also used in water industry as a surrogate parameter to monitor sites for disinfection byproducts precursors (Croué et al., 2000; Imai et al., 2003). It should be noted, however, that high nitrate content in low DOC waters may interfere with this measurement (Leenheer and Croué, 2003).

2.3.3 Size Analysis

Methods to characterize DOM by size are highly dependent on their aggregation state and interactions with media used for size separations. Sequential ultrafiltration is used for low-resolution separations and size exclusion chromatography (SEC) is used for higher-resolution size separations (Amy et al., 1987; Barker and Stuckey, 1999). A cascade of ultrafiltration membranes was used to characterize DOM by size with the understanding that the apparent molecular weight distributions are strongly influenced by a number of parameters, such as pH, ionic strength, membrane type, pressure, and calibration standards (Aiken, 1984; Logan and Jiang, 1990). Schäfer et al (2002) showed that membranes with a smaller molecular weight cutoff produce permeates with a lower UV/DOC ratio, suggesting that the more aromatic components of natural organics are removed by the lower molecular weight cutoff membranes. Variation in

ionic strength has little effect on the rejection of humic acid fractions but does significantly influence the rejection of low molecular weight acids. pH and organic concentration do not affect DOC rejection significantly over the pH range of 4.5-10 and the DOC concentration range of 15-60 mg/L.

2.3.4 Fractionation and Characterization

A comprehensive, tiered approach to DOM characterization was initially developed as a DOC fractionation method that classified dissolved organic macromolecules based on their polarity (hydrophobic/hydrophilic), acid/neutral/base properties, compound-class characteristics, specific compound characteristics, and compound complex characteristics (Leenheer, 1981; Thurman and Malcolm, 1981). This fractionation approach was improved into a preparative fractionation method in which DOM fractions can be quantitatively isolated as desalted, freeze-dried preparations and subsequently characterized (Leenheer et al., 2000; Leenheer and Croué, 2003). This preparative fractionation method led to the isolation of bacterial cell-wall peptidoglycan colloids that constitute significant percentages of DOC in most surface water samples. The DOM classification scheme is presented in Figure 2.4.

These DOM fractions are operationally defined. For a previously filtered water sample, the hydrophobic base and neutral fractions are isolated by selective sorption/desorption on Amberlite XAD-8 resin (Lin et al., 2000). Colloids can be isolated by dialysis of the evaporated concentrate through a 3500 Da membrane. Those hydrophilic DOM fractions that do not adsorb on Amberlite XAD-8, and Amberlite XAD-4 resins are desalted from the sample by selective precipitation and evaporation methods, allowing the hydrophilic acid fraction to be separated from the

hydrophilic neutral fraction by selective adsorption/desorption on a Duolite A-7 anion exchange resin. DOM fractions are frequently coisolated depending on the objectives of the study (Hu et al., 2003).

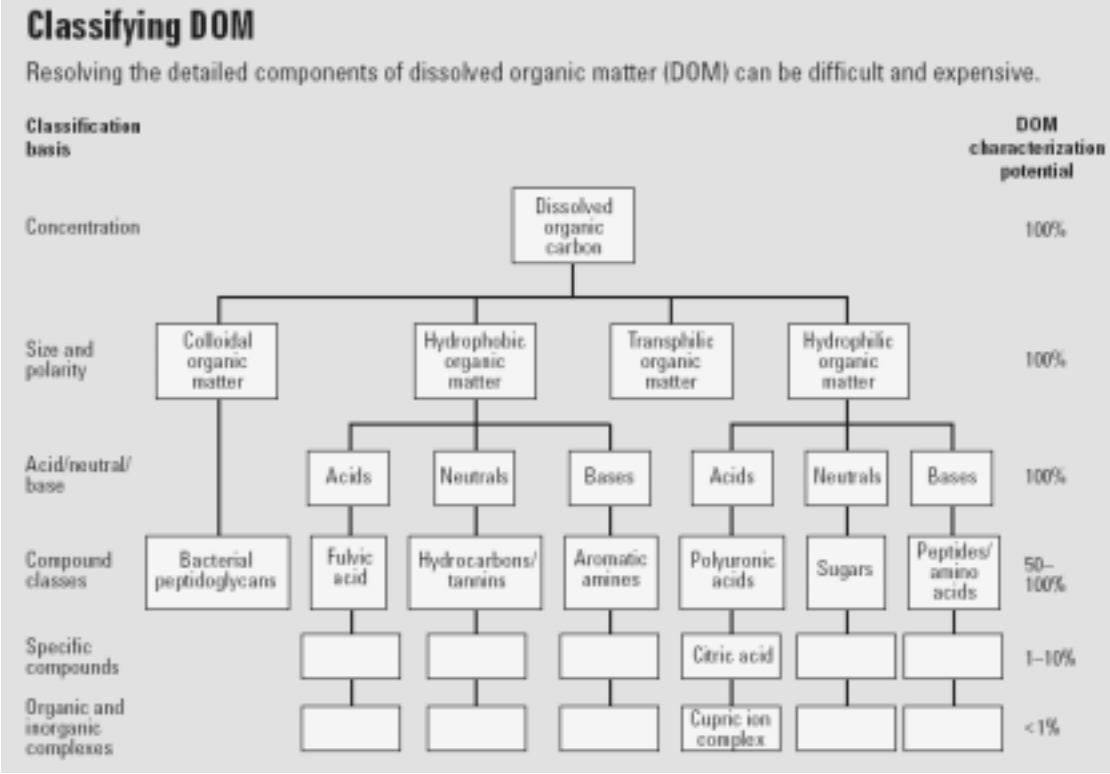

Figure 2.4 Schematic of DOM classification (Leenheer and Croué, 2003)**.**

As indicated in Figure 2.4, specific compound characterization of natural DOM typically can identify only 1–10% of the DOM. Mixture complexity and molecular complexity have defeated previous attempts to resolve natural DOM into discrete components. Nevertheless, the representative compound classes in each category of hydrophobic and hydrophilic organic matter have been successfully identified. In general, the carbohydrate-like compounds belong to HiN, whereas proteinaceous components (i.e., peptides and amino acids) are classified into HiB. Similar results have also been reported by other researchers (Thurman, 1985; Imai et al, 2001; Schäfer, 2001; Imai et al, 2002).

2.4 Organic Fouling during Membrane Filtration

2.4.1 Organic Foulants

Organic fouling depends on the organic characteristics. Research to date focuses on the identification of a "critical" organic fraction, which then can be eliminated to prevent fouling. Wiesner et al. (1992) identified four NOM categories which are strong foulants: proteins, aminosugars, carbohydrates, and polyhydroxyaromatics. DiGiano et al. (1994) found that organic compounds with a molecular weight greater than 30 kDa were responsible for NF fouling. The flux history indicated a change in the fouling mechanism after 20 h operation, possibly due to an interaction of the hydrophobic and hydrophilic fraction. Maartens et al. (1998) observed greater fouling for a more heterogeneous organic sample in UF, which consisted of a mixture of smaller and larger compounds, compared to a sample that contained only larger compounds. Amy and Cho (1999) identified carbohydrates as dominant foulants in UF and NF. However, carbohydrate concentration in surface waters is relatively low. Kaiya et al. (1996) found compounds larger than 100 kDa to be major foulants in MF. Mackey (1999) studied the fouling of UF and NF membranes (cellulose ester) by various model compounds, such as carbohydrates, polyhydroxyaromatics, and proteins. The larger compounds (carbohydrates and proteins) were observed to cause more serious fouling.

Berg and Smolders (1989) studied protein fouling and attributed higher fouling potential of protein mixtures to molecular charge, rather than size effects and resulting differences in molecular packing. This is of interest in surface water treatment, since natural organics are a mixture of compounds with extremely varied characteristics. A study with Suwannee River NOM showed a very high flux decline at low pH. This

was explained by a higher macromolecular packing density (gel-layer), due to the spherocolloidal shape of NOM at this pH, while at neutral pH the effect was low and mainly a long term phenomenon (Braghetta and DiGiano, 1994). Nilson and DiGiano (1996) measured little fouling due to the hydrophilic fraction in NF. However, the unfractionated sample showed greater flux decline than the hydrophobic fraction alone. The proposed reasons for this difference were given as an interaction between the two fractions, modification due to fractionation, or the loss of a specific fraction to the XAD resin. Although the largest molecular weight fraction was responsible for fouling, the large size of the foulants prevented them from penetrating into the pores, and fouling was therefore reversible (Lin et al., 2000).

2.4.2 Membrane Characteristics and Operating Conditions

The above results emphasize the importance of solute-solute interaction. Membrane characteristics and operating conditions also affect fouling. DiGiano et al. (1994) studied fouling with a hollow fiber NF membrane (1000 Da). The membrane surface was treated to be hydrophilic. An increase in crossflow velocity greatly decreased flux decline, and the same effect was observed by decreasing DOC concentration. The membrane resistance was directly related to the amount of DOC removed from the fouled surface. Thorsen et al. (1993) recommended the use of highly hydrophilic membranes with a pore size of 1-2 nm and low operating pressure to reduce fouling in the filtration of soft waters high in organics. Fouling was worst for positively charged membranes which interact strongly with the negatively charged organics (Nyström et al., 1996). In a later study Thorsen et al. (1997) found hydrophilic membranes to be more fouling resistant, while pore size did not affect fouling.

Reversible fouling was caused by cake formation and irreversible fouling by organics adsorption. The static adsorption test showed that the hydrophobic membranes suffered a high pure adsorptive flux loss, whereas the hydrophilic membranes were almost unaffected by adsorption (Chang et al., 2002). Hollow fiber studies showed a high irreversible fouling for polysulfone membranes, but coagulation significantly enhanced flux recovery (Clark and Heneghan, 1991).

NOM was found to be less important for fouling than previously considered, following experiments with extracted NOM spiked into the feed. Six different membranes were tested and fouling was modeled using reversible and irreversible fouling coefficients, calculated from mass transfer coefficients (Champlin and Hendricks, 1995). The results seem to contradict most other studies in finding a lesser extent of fouling. A possible explanation might be a lack of inorganics in the sample used.

Inorganic ions worsen NOM fouling during water treatment with membranes. The inorganic deposit was determined to be mainly calcium, phosphorus (due to pretreatment), and minorities of aluminium and iron (Baker et al., 1995). Hong and Elimelech (1997) showed that fouling by NOM was increased in the presence of calcium ions, at decreased pH, and increased ionic strength. Additionally, the authors noted that permeation drag and electrostatic double layer repulsion control fouling. The addition of a strong chelating agent (EDTA) to feed water reduced NOM fouling significantly by removing free and NOM-complexed calcium ions. EDTA treatment of NOM-fouled membranes also improved the cleaning efficiency dramatically by disrupting the fouling layer structure through a ligand exchange reaction between

EDTA and NOM-calcium complexes. Hiemstra et al. (1997) concluded from pilot trials that iron deposition and humic acid adsorption were the main causes of NF fouling.

Calcium can be expected to create a more compact fouling layer and thus to exaggerate flux decline. Mallevialle et al. (1989) used various MF and UF membranes to evaluate the irreversible fouling of humic substances. Flux decreases of up to 90% were observed in the initial stages of filtration. An analytical scheme to analyze water and the deposit was established. Fouling could be linked to the organic matrix of humic substances, and carbohydrates. Proteins and polyhydroxy aromatic compounds were believed to be the major contributors.

Yuan and Zydney (1999) found that humic substances, despite their small size, can cause a significant flux decline of MF membranes. This was attributed to aggregates deposited on the membrane surface. Prefiltration improved flux decline, but reaggregation occurred at increased calcium concentrations and initial deposit of organics facilitated further deposition.

In summary, a number of organic fouling mechanisms occur. The most important ones are initial adsorption, precipitation and gel formation, and the interaction with multivalent cations (Hong and Elimelech, 1997). Large organics appear to possess relatively high fouling potential, and for mixtures fouling is consistently worse, indicating the importance of solute-solute interactions in fouling layer formation. Organic fouling has been studied mostly for UF and NF, with MF being rarely studied (Schäfer, 2001).

2.4.3 Adsorption Fouling

Adsorption is the physico-chemical interaction between solutes and membranes. The adsorption of organics, or more specifically humic substances, is considered a major fouling mechanism in water treatment (Fan et al., 2001; Howe and Clark, 2002). NOM can adsorb either in the structure of the cake, or in the bulk of the membrane. These interactions are strongly influenced by membrane solute affinities and the reversibility is slow (Chang et al., 2002). However, it is not well established to what extent adsorption can account for the fouling observed.

Adsorption can vary membrane charge. Jucker and Clark (1994) measured zeta potentials of hydrophobic UF membranes before and after adsorption. Hydrophobic compounds exhibited a preferential adsorption and zeta potentials became less negative after adsorption. The change in contact angle of the membranes before and after adsorption was also measured and was smaller. Humic acid and fulvic acid were on the same curve for the adsorption/contact angle relationship. Adsorption kinetics showed that fulvic acid adsorbed more quickly than humic acid due to a higher diffusivity, whereas humic acid adsorbed to a greater extent as a result of a greater number of attachment sites on the larger molecules. Adsorption increased with concentration. Calcium interacted between humic acid and the membrane, and more calcium was required at a higher pH due to the larger pH difference. Adsorption seemed to first appear in pores (high energy sites), and then on the skin.

Adsorption isotherms of Suwannee River fulvic acid and humic acid were also determined for UF membranes by Clark and Jucker (1993). The effect of calcium was greater for humic acid. More porous membranes showed a greater flux decline.

Phosphate groups from the buffer solution competed with calcium for adsorption. The study illustrated the importance of the choice of an appropriate background solution, as ions from a buffer solution can compete for adsorption and result in different effects. Adsorption was also dependent on the solubility of the organics, and a lower solubility led to higher adsorption. The increased adsorption at low pH was attributed to the decrease in solubility (Clark and Lucas, 1998). Braghetta and DiGiano (1994) found a greater adsorption of organics on the membrane at low pH due to a higher packing density. Adsorption also increased with ionic strength.

The effect of humic acid adsorption on hydrophilic (cellulose acetate and thin film composite) membranes for a pH range of 2-10 was investigated by Elimelech et al. (1994). The surface charge became more negative over the entire pH range for both membrane types and reached values of -30 mV at pH 2, down to -45 mV and -50 mV at pH 10 for the cellulose acetate and thin film composite membranes, respectively. This suggested that adsorption is not limited to hydrophobic surfaces. The work of Childress and Elimelech (1996) showed that humic substances also adsorbed on hydrophilic membranes very rapidly, and that the membrane surface potential became more negative due to the humic substances. Calcium facilitated the adsorption of negatively charged organics onto negative surfaces. This indicated some charge neutralization effect or specific interaction. Childress and Elimelech (1997) studied adsorption of humic substances and surfactants on NF membranes using streaming potential measurements. Large humic substances adsorbed preferentially, especially in the presence of calcium. Surfactants formed hemicelles at the surface. The results are closely relevant for humic substances as some natural organics may have surfactant characteristics.

Crozes et al. (1993) found that the adsorption on a hollow fiber membrane was much higher than that on a flat sheet of the same material. Adsorption occurred after contacting the membranes with the solutes in the absence of flux. This indicated a higher adsorption with a larger membrane area. Maartens et al. (1998) found that larger organics adsorbed faster to UF membranes and reduced the pore size more effectively. Non-polar groups were the main cause of protein fouling, arising from adsorption on polysulfone and polyethersulphone monopolar membranes. Hydrophilic membranes were expected to be more resistant to fouling problems (Gourley et al., 1994).

The adsorption of organic compounds is an important process. However, adsorption alone would only be responsible for a relatively thin deposit layer. After this initial adsorption, the solutes see the "new" membrane characteristics, which are determined by the solute (Schäfer, 2001). It appears as if gel formation or cake deposition are more important long-term problems.

2.4.4 Precipitation and Gel Formation

Concentration polarization can become irreversible if a gel is formed, which can be the case when solute solubilities are exceeded (Song and Elimelech, 1995). Concentration polarization depends strongly on solute concentration and operational conditions, such as pressure and stirring (Song, 1998). Fouling of "tight" UF and NF membranes tends to occur more on the surface than in the pores in contrast to MF and "loose" UF. Cake formation is usually reversible and can, as in MF, form a second membrane (Schäfer, 2001). Surprisingly, Odegaard and Thorsen (1989) demonstrated that humic substance concentration and transmembrane pressure, which influence

precipitation and gel formation, had no much influence on flux. The fouling layer thickness was calculated with pressure drop and permeate flux. The film was soft, dark brown, and loosely connected to the surface.

Wijmans et al. (1984) indicated that osmotic pressure limitations were more likely in the UF of low molecular weight organic solutes, whereas for high molecular weight solutes, gel formation was more important. Gill et al. (1988) showed that viscosity effects in the boundary layer are more important than diffusivity. Concentration factors in UF of macromolecules were 40 to 400 times. A similar effect can be expected for large natural organic molecules. Kim et al. (1992) showed cake formation for low initial fluxes and aggregation for high initial fluxes during UF of proteins. This demonstrated that solute-solute interactions in the boundary layer were important. Tu et al. (1997) predicted NF flux by incorporating a gel-layer into the concentration polarization model. Results corresponded well to filtration experiments with tannic acid.

The mass transfer coefficient (MTC) describes the accumulation of solute at membrane surface. It is mainly determined by the hydrodynamic conditions at the surface. Duranceau and Taylor (1993) modeled the MTC and found a direct relationship of MTC with solute charge and molecular weight. Nyström et al. (1994) filtered humic acid with 3 mg/L iron and while a gel layer was formed, flux decline occurred at pH 7, but not at pH 10. The low fouling at high pH was attributed to the absence of pore penetration. Nyström et al. (1995) found that tighter NF membranes fouled less, and that charge repulsion between membrane and foulants also reduced fouling. Gel formation was described as a symbiotic effect of salts and organics.

Multivalent ions fouled the UF membrane when combining with organic compounds. Humic acid fouled the membrane at lower pH values when it was partly undissociated. A gel layer formed on the membrane surface if a high concentration was applied (Aoustin et al., 2001).

While gel formation and precipitation are reported frequently as the source of fouling in all membrane processes, only a small amount of work has been done on a quantitative determination of gel layer concentration and the solubility of natural organics (Mulder, 1996; Schäfer, 2001). Naturally, flux or transmembrane pressure is important for concentration polarization, which seems to be the major factor in gel formation. The MTC can also describe this, as was shown above. Organic characteristics such as solubility and hydrophobicity require further investigation as do their interaction with ions. Unfortunately, the solubilities of humic substances and their complexes with salts are relatively unknown (Chang et al., 2002).

2.4.5 Pore and Surface Fouling

Many authors attempted to distinguish between pore and surface fouling (Yuan and Zydney, 2000; Howe and Clark, 2002). Cleaning is more effective if fouling occurs on the membrane surface. However, in many cases it is difficult to distinguish between the two mechanisms. The blocking laws have limited applications in distinguishing between pore and surface fouling in MF and UF processes (Bowen et al., 1995; Kim et al., 1993). By definition, these models are limited for applications in dead-end, unstirred filtration. Song (1998) described the initial rapid flux decline in MF and UF as pore blocking, whereas a slower, more gradual flux reduction process was attributed to cake formation.

Mackey (1999) observed a greater fouling in UF than NF, and proposed both pore and surface fouling. The fluxes of UF at the end of the experiments were close to those of NF. The greater fouling in the UF case was attributed to pore fouling, as evidenced by an initial steep decline in flux. Pore blocking requires an initial low retention of solutes. While retention may increase due to cake formation, this increase in retention especially at early stages of filtration can indicate pore fouling.

2.4.6 Fouling with Multivalent Cations

Multivalent ions have been reported to increase adsorption and fouling in general. Possible interactions are bridging and charge neutralization between membrane and organic compounds (both are usually negatively charged), chelation, complexation, and aggregation (in the bulk and boundary layer), and co-precipitation of organic compounds and inorganic precipitates (Hong and Elimelech, 1997). Speth et al. (1996) investigated foulants on NF membranes after conventional treatment. Foulants had a specific fingerprint, different to the organics in the feedwater. The deposit was also rich in aluminium, calcium, iron, magnesium, sodium, and silica. Mallevialle et al. (1989) analyzed membrane deposits and found a higher ash content in the deposits compared to the raw water.

Multivalent ions are believed to enhance natural organics adsorption. The effect depends on the organic type. Clark and Jucker (1993) determined that the effect of calcium on fulvic acid is lower than on humic acid. Binovi (1983) found that the gel layer formed on RO membranes was composed primarily of organics and iron. Nyström et al. (1994) filtered humic acid with 3 mg/L iron and while a gel layer was formed, the rate of flux decline was reduced. Mackey (1999) studied the effect of iron

(5 mg/L or 0.09 mM) and calcium (50 mg/L or 1.25mM) on fouling of polygalacturonic acid. Surprisingly, addition of calcium and iron did not significantly increase fouling. Aggregation was suggested as a fouling mechanism for the concentrations which were close to the solubility limit.

CHAPTER 3

MATERIALS AND METHODS

The experimental work reported here was conducted in two phases. In Phase 1, experiments were performed with DOM in three pilot MBR systems, where a sufficient amount of sample can be obtained. A series of fouling experiments were carried out in a stirred-cell filtration system to gain a more fundamental understanding of the complicated DOM fouling phenomenon. In Phase 2, the lab-scale MBR system was operated for readily biodegradable synthetic wastewater treatment over 250 days. The characteristics, composition, and fouling potential of DOM both in the MBR and in the effluent were investigated and compared at different SRTs to elucidate the effect of SRT on DOM fouling and accumulation.

3.1 Experiments with DOM in Pilot MBR Systems

3.1.1 Sample Source and Collection

The mixed liquor samples were collected from three local pilot submerged MBR systems treating municipal wastewater. The MBR systems all had an effective volume of 75 m^3 and consisted of both an anoxic chamber for denitrification and an aerobic chamber for organic carbon oxidation and nitrification. The overall system specifications are given in Table 3.1. Each time, about 240 L of mixed liquor was collected from the aerobic chamber of the MBR system and stored at 4°C in the laboratory until use. After an overnight quiescent settlement of the mixed liquor, 120 L of supernatant, where DOM resides, was carefully isolated from the settled solids using Masterflex® pumps (Model 7553-85, Cole-Palmer, Vernon Hills, IL, USA). The extracted supernatant was subsequently subjected to 0.4 μm membrane filters (Type 203, Kubota, Osaka, Japan) for further removal of particulate matter.

Table 3.1 Specifications of pilot MBR systems

	MBR 1	**MBR 2**	**MBR 3**
Membrane Unit			
Total surface area, m^2	480	1008	1120
Type (UF/MF)	MF	UF	MF
Nominal pore size, μm	0.4	0.035	0.4
Materials	Chlorinated PE	PVDF	PE
Configuration	Flat plate	Hollow fiber	Hollow fiber
Operating Conditions			
TMP, kPa (initial)	4	10	17
Permeate flux, L/m^2 day	630	300	270
HRT, hours	6	6	6
SRT, days	21	21	21
DO in aeration tank, mg/L	2-4	2-4	2-4
Aerobic tank pH	~6.3	~5.9	~6.6
Anoxic tank pH	~5.7	—	~6.9
Temperature, °C	30-32	30-32	30-32

3.1.2 DOM Fractionation

According to the procedure adapted from Namour and Müller (1998), DOM in the extracted supernatants was fractionated into four more homogeneous components on the basis of hydrophobic/hydrophilic and charge properties, namely, hydrophobic aquatic humic substances (AHS), hydrophilic bases (HiB), hydrophilic acids (HiA), and hydrophilic neutrals (HiN). The fractionation experiment was performed using borosilicate glass chromatography columns (006-CC-35-15-FF, Omnifit, Cambridge, UK) with a series of resin adsorbents, including non-ionic DAX-8 resin (Supelco, Bellefonte, PA, USA), AG MP-50 cation exchange resin (Bio-Rad, Hercules, CA, USA) and IRA-96 anion exchange resin (Rohm and Haas, Philadelphia, PA, USA).

Prior to the fractionation process, the DAX-8 resin was purified and conditioned as described by Leenheer (1981). Both AG MP-50 and IRA-96 resins were Soxhlet-extracted with methanol for 24 hours, and stored in methanol until use. The columns, endpieces, connection tubings, and the accompanying frits for uniform water distribution were cleaned with acid to remove trace carbon and then rinsed three times with deionized (DI) water. The frits were replaced after each run. The flow rate was set at 10 and 15 ml/min for non-ionic DAX-8 resin and ionic AG MP-50/IRA-96 resins, respectively. DI water was used as system blank. Blank samples were taken from each column immediately after conditioning to evaluate the interference of the bleed DOC. Through the entire fractionation process, DOC concentrations of the blank samples collected from DAX-8, AG MP-50, and IRA-96 columns were successfully controlled to < 0.5 mg/L.

The flow chart of the DOM fractionation procedure is outlined in Figure 3.1. The column containing conditioned DAX-8 resin was alternatively washed with 0.1 M NaOH and 0.1 M HCl. DI water washing was implemented between each run. The column was rinsed with 500 ml DI water just before sample application. The pH 2 acidified MBR supernatant was then pumped through DAX-8 column. One bed volume of 0.01 M HCl was used to flush out the residue DOM left in the tubings. The sorbed substances, defined as hydrophobic aquatic humic substances (AHS), were eluted in reverse direction with 0.1 M NaOH.

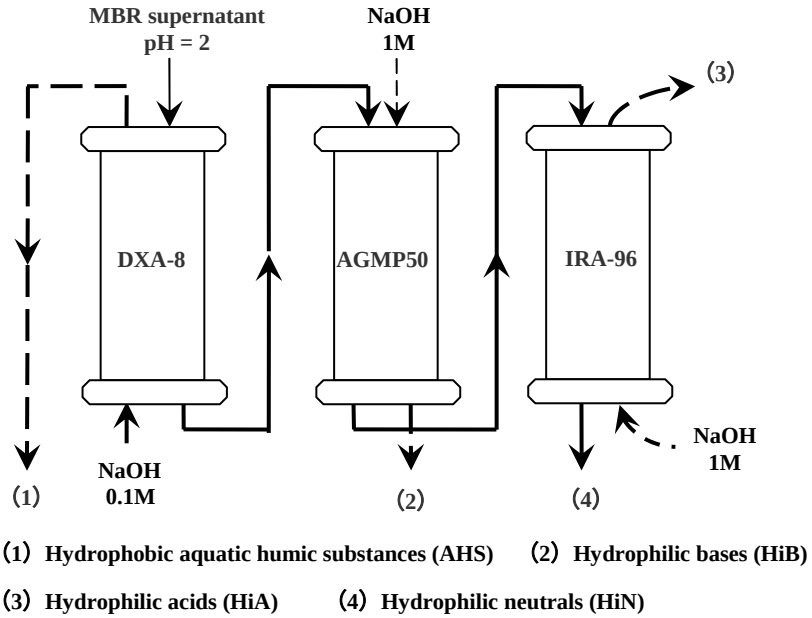

Figure 3.1 Procedure for fractionation of DOM in MBR systems.

The DAX-8 column effluent was subsequently pumped through the hydrogen saturated AG MP-50 column. After rinsing with one bed volume of DI water, the sorbed substances were forward eluted with 1 M NaOH. The eluate is defined as hydrophilic bases (HiB). Finally, the effluent from AG MP-50 column was run through the IRA-96 column containing conditioned resin which has been converted to the free-base-form using 1 M NaOH. After rinsing with one bed volume of DI water,

the sorbed substances were backward eluted with 1 M NaOH. The desorbed substances are defined as hydrophilic acids (HiA). Finally, the non-sorbed substances in the effluent passing through all three columns are defined as hydrophilic neutrals (HiN). The recovery rate of each fractional DOM component was calculated based on mass balance principle. It is indicated by the ratio of the DOC value of desorbed components to that of sorbed components. The data summarized in Table 3.2 were the average values obtained from duplicate measurements.

Table 3.2 Recovery rate of fractional DOM components

Recovery (%)	AHS	HiB	HiA	HiN
Supernatant 1	67.5	67.4	83.3	100
Supernatant 2	63.1	73.7	79.6	100
Supernatant 3	68.2	76.5	75.8	100

3.1.3 Membranes

Two types of flat-sheet microfiltration membranes, hydrophobic GVHP and hydrophilic GVWP with the same nominal pore size of 0.22 μm (Millipore, Bedford, MA, USA) and filtration area of 28.7 cm^2, were employed in the fouling experiments. They have very similar morphological structure but significantly different surface chemistry. The properties of these two membranes reported in the literature are summarized in Table 3.3 (Schäfer et al., 2000; Fan et al., 2001). The bulk of the experiments were performed with GVHP membranes because DOM fouling was observed to be much more serious with GVHP membranes than GVWP membranes. Limited data were obtained with GVWP membranes, which provide additional information with respect to the effect of membrane hydrophobicity on DOM fouling.

The hydrophilic GVWP membranes were cleaned and conditioned with DI water for 2 h, whereas the hydrophobic GVHP membranes were soaked in ethanol solutions for 1 h to wet the pores and then thoroughly rinsed with DI water. Prior to fouling experiments, the membranes were further cleaned by filtration of 800 ml of DI water to remove any impurities left over from the manufacturing process or additives used for stabilization. A fresh membrane was used for each run.

Table 3.3 Characteristics of GVHP and GVWP membranes

Parameter	GVHP	GVWP
Nominal pore size (μm)	0.22	0.22
Material	PVDF	Surface-modified PVDF
Surface property	Hydrophobic	Hydrophilic
Protein binding capacity (μS/cm^2)	150	4
Pure water flux (7.5 Psi) (L/m^2 h)	3580±260	3350±230
Mean thickness (μm)	125	125
Porosity (%)	75	70
Surface charge at pH 4/7/9 (mV)	-4.5/-18/-22	-16/-21/-22

3.1.4 Stirred-cell Filtration System

Fouling experiments were performed in a stirred-cell filtration system comprising a 64 mm diameter stirred-cell (Model 8200, Amicon, Beverly, MA, USA) and an external reservoir for increase of feed volume (Figure 3.2). The transmembrane pressure was maintained constant at 51.7 kPa (7.5 Psi) using nitrogen gas and the stirring speed was set at 180 rpm. All experiments were conducted at a temperature of 25 ± 1 °C. Membrane fouling, indicated by flux decline, was monitored by weighing membrane filtrate on a top-loading digital mass balance (PG8001-S, Mettler Toledo, Greifensee, Switzerland) at preset time intervals with computerized data acquisition.

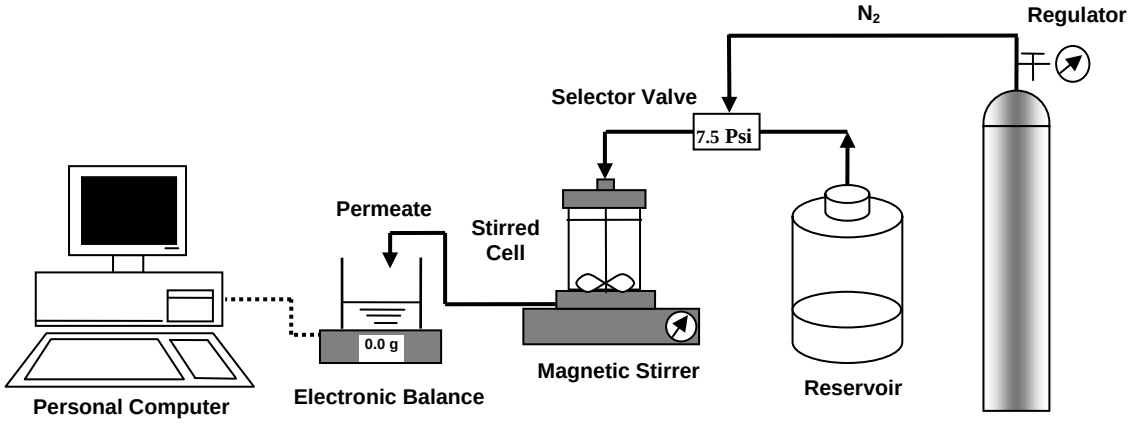

Figure 3.2 Schematic diagram of stirred-cell filtration system.

3.1.5 Experimental Procedure

The stirred-cell filtration system was initially filled with DI water. The pure water flux of a clean membrane (J_0) was measured as a function of time until the consecutively recorded values were considered constant (i.e., differed by less than 2%). The stirred-cell and reservoirs were then emptied and refilled with a certain feed solution depending on the experimental purpose. The stirred-cell filtration system was repressurized and the permeate flux was continuously monitored for 35 min. Separate reservoirs were used for feed solutions and DI water to avoid contamination of the DI water reservoir.

At the end of the experiment, the stirred-cell filtration system and the fouled-membrane were rigorously rinsed three times with DI water. After physical cleaning, the stirred-cell and reservoirs were emptied again and refilled with DI water to determine the pure water flux of the cleaned fouled-membrane (J_0'). The resistance-in-series model was applied to evaluate the fouling characteristics. The permeate flux of a membrane is governed by the basic membrane filtration equation as follows:

$$J = \frac{\Delta P}{\mu R_t} \tag{3.1}$$

where J is the permeate flux, ΔP is the transmembrane pressure (TMP), μ is the permeate viscosity, R_t is the total membrane resistance. The total membrane resistance, typically, includes three parts, i.e.

$$R_t = R_m + R_r + R_i \tag{3.2}$$

where R_m is the intrinsic membrane resistance, R_r is the resistance due to reversible fouling caused by the cake layer deposited over the membrane surface, and R_i is the resistance due to irreversible fouling caused by solute adsorption into the membrane pores. Based on the experimental data, the values of R_m, R_r, and R_i can be determined as follows:

$$R_m = \frac{\Delta P}{\mu J_0} \tag{3.3}$$

$$R_i = \frac{\Delta P}{\mu J_0'} - R_m \tag{3.4}$$

$$R_r = \frac{\Delta P}{\mu J_f} - R_m - R_i \tag{3.5}$$

where J_0 is the pure water flux of a clean membrane, J_0' is the pure water flux of the fouled-membrane after physical cleaning, and J_f is the quasi-steady state permeate flux with feed solutions.

3.1.6 Calculation of Fouling Potential

The fouling potential of DOM was determined according to the normalization method initially developed by Song et al. (2004), which is rigorously defined by the following equation:

$$R_t = R_0 + k_f \int_0^t J dt \tag{3.6}$$

where R_t and R_0 are the total membrane resistance at time t and 0, respectively. k_f is the fouling potential of DOM. The physical meaning of k_f is the incremental resistance due to a unit volume of permeate passing through a unit membrane surface area. The permeate flux J at any time can be calculated from experimental data.

The fouling potential of DOM in MBR systems was graphically determined by choosing the value of k_f for the best fit of the flux data with the following equation:

$$J_{i+1} = J_i - \frac{k_f}{\Delta P} J_i^3 \Delta t \tag{3.7}$$

The optimal fouling potential can be obtained by trial and error or more rigorously with optimization technologies. More details of the method can be found elsewhere (Song et al., 2004; Singh and Song, 2005).

3.2 Experiments with DOM in Lab-scale MBR System

3.2.1 MBR System Description

In this phase, experiments were performed in the lab-scale submerged MBR system as illustrated in Figure 3.3. The MBR system consisted of a rectangular tank having an operating volume of 16 L and a flat-sheet membrane module submerged in the tank. The membrane module was made of polyolefin with a pore size of 0.4 μm and an effective filtration area of 0.1 m^2 (Type 203, Kubota, Osaka, Japan). Two water level sensors were installed at the high and low water level respectively to maintain a constant water level in the bioreactor.

Aeration was done through the air diffuser installed directly beneath the membrane module to maintain desired dissolved oxygen (DO) concentration and to mix activated

sludge in the MBR. The air bubbles generated during aeration, on the other hand, induced a crossflow scouring the membrane surface and so suppressing membrane fouling to some extent. Two baffle plates were mounted above the air diffuser to optimize the contact between air bubbles and the membrane surface.

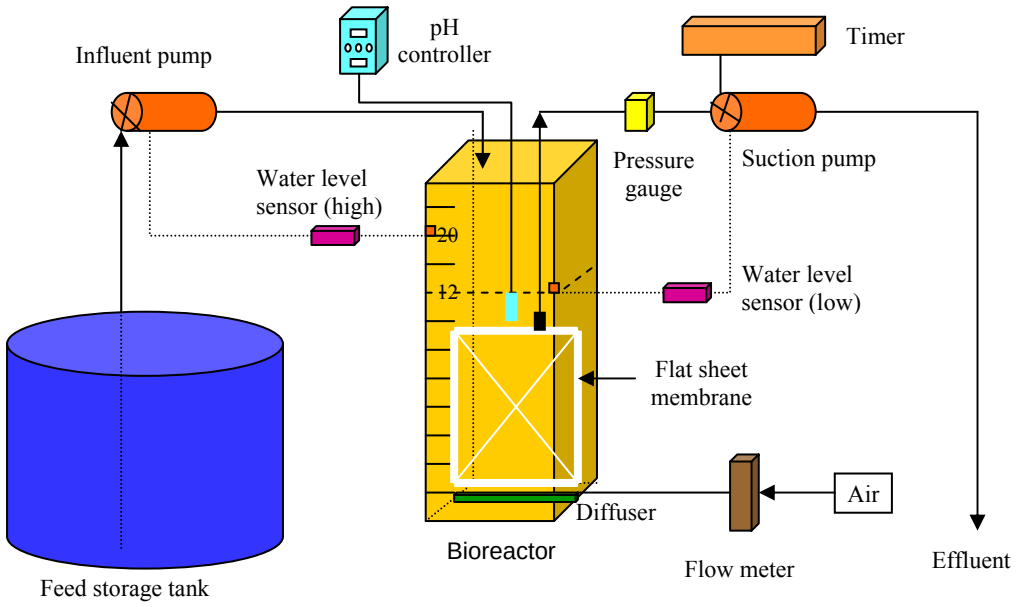

Figure 3.3 Schematic diagram of lab-scale MBR system.

Both the bioreactor and the storage tank were initially filled with the synthetic wastewater. The storage tank with an effective volume of 50 L was reloaded everyday with the fresh wastewater to ensure the continuous supply to the MBR over the entire experimental period. The wastewater was fed into the MBR with a peristaltic pump (Model 7553-85, Cole-Palmer, Vernon Hills, IL, USA), whereas membrane-filtered effluent was extracted by a pump of the same model operating intermittently with a cycle of 8 min on and 2 min off. To minimize the variation of wastewater characteristics, the temperature of the storage tank was maintained as low as possible

using a water bath containing ice blocks. Moreover, the storage tank was thoroughly cleaned every two days to suppress the growth of microorganisms.

3.2.2 Synthetic Wastewater and Operating Conditions

The composition of the synthetic wastewater used in this study is listed in Table 3.4. The carbon source is mainly from sodium acetate which is simple and readily biodegradable. The concentration of residual acetate in the MBR was measured and found to be negligible. Nitrogen and phosphorus were provided by ammonium sulfate and monopotassium phosphate, respectively. The influent COD concentration was 600±20 mg/L with the ratio of COD: N: P maintained at 100: 10: 1.

Table 3.4 Composition and concentration of synthetic wastewater

Components	Molecular weight (Da)	Concentration (mg/L)
CH_3COONa	82.0	768.75
$(NH_4)_2SO_4$	132.1	284
KH_2PO_4	136.1	26
$CaCl_2 \cdot 2H_2O$	147.0	0.368
$MgSO_4 \cdot 7H_2O$	246.5	5.07
$MnCl_2 \cdot 4H_2O$	197.9	0.275
$ZnSO_4 \cdot 7H_2O$	287.5	0.44
$FeCl_3$	162.2	1.45
$CuSO_4 \cdot 5H_2O$	249.7	0.391
$CoCl_2 \cdot 6H_2O$	237.9	0.42
$Na_2MoO_4 \cdot 2H_2O$	242	1.26
Yeast extract		30

Seed sludge was obtained from the aeration tank of the local pilot MBR system for municipal wastewater treatment. After transferring into the lab-scale MBR, the sludge

was allowed to acclimate to the synthetic wastewater for five weeks. During this start-up period, the MBR was operated at the same condition as that used in the experimental period except no sludge wastage. The experiments were performed in three phases according to the change of SRT in the order of 40 days, 20 days and 10 days. The SRT of 40 days was investigated first in consideration of minimizing the loss of acclimated sludge. Before transferring to a new phase, a period of at least two times of the new SRT was provided for MBR stabilization. In each phase, a steady-state of four weeks was maintained, during which measurements were evenly conducted for parameters of interest.

The hydraulic retention time (HRT) of 10 hours and DO concentration of around 5 mg/L were maintained during the entire experimental period of 256 days. The MBR was operated under ambient temperature (28 ± 2 °C) and the pH was controlled within a range of 7.0-8.0. Fouling development, indicated by the increase in suction pressure, was monitored using a digital pressure switch (ZSE50F-T2-22L, SMC, Japan). Membrane cleaning was required in about 35-50 days when the suction pressure increased beyond 35 kPa. Typically, the interval between two membrane cleanings became shorter as SRT decreased indicating membrane fouling was more serious at short SRTs. The membrane module was taken out of the MBR. It was rigorously rinsed with tap water to remove the attached cake layer followed by backwashing with 0.05% sodium hypochlorite solution for 2 h to further remove the foulants adsorbed within membrane pores. The membrane module was thoroughly cleaned again with tap water before it was mounted back in the MBR. Since no significant irreversible fouling was observed, the same membrane was used during the steady-state at all investigated SRTs for a fair comparison.

3.2.3 DOM Fouling Experiment

The fouling potential of DOM at the investigated SRT was examined for both supernatant and effluent at the end of each experimental phase. Fouling experiments were conducted in the same stirred-cell filtration system as that described in section 3.1.4. The supernatants and effluents, where DOM resides, were filtered through flat-sheet membranes made of the same material as that used in the lab-scale MBR system. The sample volumes used for fouling experiments were 4 L and 5 L for supernatant and effluent, respectively, and the filtration time was 25 min. The experimental conditions (i.e., transmembrane pressure, stirring speed, and temperature) were the same as those applied in the filtration tests for the DOM in the pilot MBR systems. Based on the experimental data, the fouling potential of DOM can be calculated according to the normalization method stated before.

3.3 Analytical Methods

COD, NH_4^+-N, mixed liquor volatile suspended solids/suspended solids (MLVSS/SS), and specific oxygen uptake rate (SOUR) were measured in accordance with the Standard Methods (APHA-AWWA-WEF, 1998). Supernatant samples in the lab-scale MBR were obtained by centrifuging MBR mixed liquor at 10,000 rpm (11,000 g) for 10 min at 4°C and then filtering through 0.45 μm membranes. Measurement of acetate concentration was conducted using a Gas Chromatograph (GC-14B, Shimadzu, Japan).

DR/4000U Spectrophotometer (HACH, Loveland, CO, USA) was employed to measure UV absorbance at 254 nm (UVA_{254}) (Figure 3.4). The dissolved organic carbon (DOC) concentration was determined by 1010 Total Organic Carbon Analyzer

(O. I. Analytical, College Station, TX) using computer software package WinTOC®1010 for Windows (Figure 3.4). The specific UVA_{254} (SUVA), indicating the aromaticity of DOM, was calculated as the ratio of UVA_{254} to DOC.

Figure 3.4 DR/4000U Spectrophotometer (left) and 1010 TOC Analyzer (right).

The phenol-sulfuric acid method (Dubois et al., 1956) was used to measure the content of carbohydrate in DOM with glucose as the standard reference, whereas the modified Lowry method (Lowry et al., 1951; Hartree, 1972) was used for protein determination with bovine serum albumin (BSA) as the standard reference. Total dissolved solids and conductivity were measured with WTW Conductivity Meter (LF538, WTW, Weilheim, Germany) and pH was determined by F-24 pH/ion meter (HORIBA, Kyoto, Japan). DX500 ion chromatography system (Dionex, Sunnyvale, CA, USA) was used for measurement of calcium concentration (Figure 3.5).

Apparent molecular weight distribution of DOM was determined using the ultrafiltration fractionation method as described by Huang et al (2000). Fractionation

experiments were conducted in the stirred-cell (Model 8050, Amicon, Beverly, MA, USA) using YM series UF membranes with nominal molecular weight cut-offs of 3, 10, and 30 kDa (Millipore, Bedford, MA, USA). The filtration was performed at a constant pressure of 100 kPa. The filtrate permeating through each membrane with a different molecular weight cut-off was collected and the DOC concentration was measured. The fractional amount of DOM within a certain molecular weight range was calculated from the difference in DOC concentration between adjacent filtrate samples. The hydrophobic/hydrophilic and charge properties of DOM in the lab-scale MBR system were investigated using the fractionation method as described in section 3.1.2. The fractionation was performed with small columns (006-CC-15-15-FF, Omnifit, Cambridge, UK) to scale down the resin volume for processing 800 ml sample.

Figure 3.5 DX500 ion chromatography system.

CHAPTER 4

CHARACTERISTICS AND FOULING POTENTIAL OF DOM IN MBR SYSTEMS

Despite the advantages and potential of MBR systems, membrane fouling is still a major problem that hinders their more widespread and large-scale application. The purpose of this chapter is to contribute to a more fundamental understanding of the characteristics and fouling behaviors of DOM in MBR systems. The experiments were conducted with the supernatant samples obtained from the pilot MBR systems according to the procedure as described in section 3.1.1. The common parameters of the MBR supernatants were analyzed as shown in Table 4.1. It can be seen that the general characteristics of the supernatant samples were significantly different from each other. The supernatant in MBR 2 had the highest concentration of DOM in terms of DOC, whereas the supernatant in MBR 3 exhibited the highest value of UVA_{254}. The differences among the samples were reasonably expected in view of the

fluctuation of influent characteristics and the specific configuration of each MBR system.

Table 4.1 General characteristics of MBR supernatants

Parameter	Supernatant 1	Supernatant 2	Supernatant 3
DOC(mg/L)	12.15	15.11	10.65
pH	7.39	6.92	7.83
TDS (mg/L)	593	526	658
Conductivity (μS/cm)	1562	1210	1811
Ca^{2+} (mg/L)	33.2	24.8	42.6
UVA_{254} (cm^{-1})	0.298	0.263	0.335
SUVA (L/m·mg)	2.45	1.74	3.15

The characteristics of DOM, implicated in membrane fouling, were investigated such as molecular size, hydrophobic/hydrophilic and charge properties. The complex DOM mixtures in MBR systems were, at the first time, fractionated into four more homogeneous components using classical DOC preparative fractionation method. The fractionation result, on the other hand, enables a more detailed study of DOM fouling at fractional level. Microfiltration experiments were carried out in the stirred-cell filtration system as described in section 3.1.4, where the fouling potentials of various types of DOM (i.e., original, prefiltered, and fractionated) were examined with either hydrophobic or hydrophilic membranes. In particular, the fouling potentials of fractional DOM components were quantified and compared at equivalent conditions in order to investigate the main foulants of DOM in MBR systems. It is believed that the knowledge of the characteristics and fouling potential of DOM at fractional level would greatly strengthen our capability to alleviate or minimize membrane fouling in MBR systems.

4.1 Characteristics of DOM in MBR Systems

4.1.1 Hydrophobic/hydrophilic and Charge Properties

Hydrophobic and electrostatic interactions are two important fouling processes commonly observed during microfiltration of DOM. As a consequence, the hydrophobic/hydrophilic and charge properties of DOM in MBR systems are of particular interest in membrane fouling. The DOM fractionation results according to these two characteristics are shown in Figure 4.1. It was noted that hydrophobic AHS were the most abundant fraction in all samples, accounting for 43.8-65.7% of the total DOM measured as DOC. This suggests that DOM in MBR systems is mainly composed of humic and fulvic acids rather than proteins and carbohydrates, which are considered hydrophilic in nature. In contrast, however, the proportion of hydrophilic fractions, HiA, HiB, and HiN, differed substantially among the samples and no general trend can be observed. This indicates that the amount and properties of hydrophilic DOM components in MBR systems are variable and greatly affected by the characteristics of the membranes used in each MBR system.

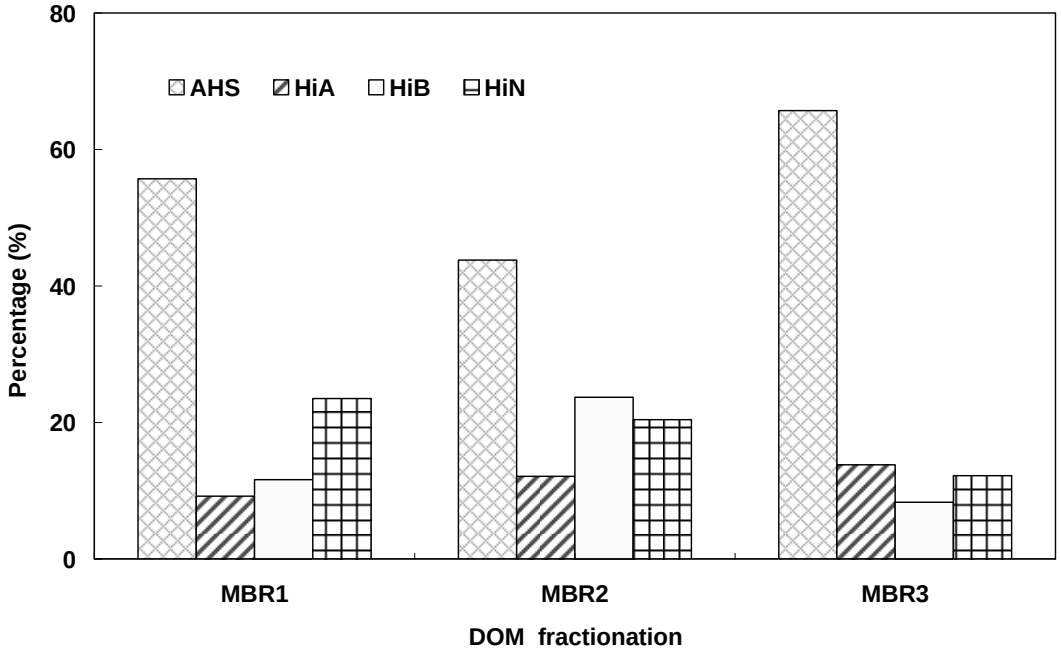

Figure 4.1 Fractionation results of DOM in pilot MBR systems.

Unlike the situation of natural organic matter (NOM) characterization where a huge database has been successfully established based on a great number of fractionation results, DOM in wastewater treatment systems has rarely been fractionated on the basis of hydrophobic/hydrophilic and charge properties. In a recent study, Imai et al. (2002) attempted to fractionate DOM in several conventional activated sludge systems treating domestic sewage. However, in sharp contrast to our results, HiA were found to be the most abundant fraction, accounting for 40-54% of DOM, whereas AHS constituted merely 18-28% of the DOM, which is much lower than the values reported here. It appears that the fractionation results of DOM in conventional activated sludge systems are not applicable to MBR systems, though the characteristics of DOM in MBR systems is fundamentally related to the coupled activated sludge process. The dominance of AHS in MBR systems can be attributed partly to the extended SRT, which favors the production of more hydrophobic components (Lee et al., 2003; Shin and Kang, 2003).

On the other hand, it is noteworthy that, in most cases, hydrophobic AHS in the MBR system can pass through the membranes more readily than other DOM components and consequently constituted the majority of DOM in the MBR effluent. The dominance of AHS in MBR effluents would, therefore, present a serious problem for the potential downstream disinfection process, as it has been generally accepted that AHS exhibit high DBP formation potential and represent the main source of DBP precursors (Norwood and Christman, 1987; Reckhow et al., 1990).

4.1.2 Molecular Size of DOM

The molecular size of DOM, commonly measured as molecular weight, is another important characteristic in terms of membrane fouling. Figure 4.2 shows the apparent molecular weight distributions (AMWD) of DOM in the three pilot MBR systems. It can be seen that there was not much difference in the AMWD of DOM in different MBR systems. The majority of DOM in MBR systems, accounting for about 70%, had a molecular weight of less than 3 kDa. The components of large molecular weights (> 30 kDa) formed the second largest fraction, constituting 12-23% of DOM, whereas each of the two fractions in the range between 3 kDa and 30 kDa merely represented <10% of DOM.

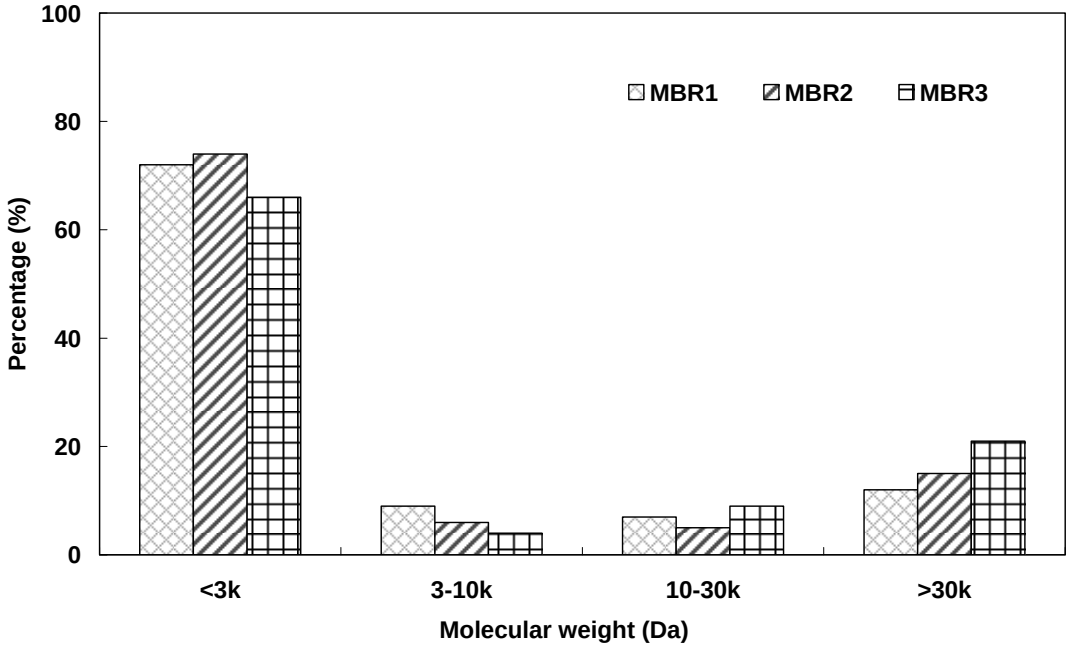

Figure 4.2 Apparent molecular weight distributions of DOM in MBR systems.

Table 4.2 compares our results with those measured in MBR systems treating readily biodegradable synthetic wastewaters, where the DOM is basically soluble microbial products (Huang et al., 2000; Lee et al., 2003). It should be noted that the composition of DOM examined here was much more complex than those characterized in the

previous studies, including not only soluble microbial products but also various refractory dissolved organic components contained in the feedwater. It can be seen that the DOM in MBR systems for synthetic wastewater treatment tends to have a smaller fraction of small molecules but larger fractions of intermediate and large molecules. This implies that the majority of large DOM components may have a microbial origin. The proportion of large molecules, on the other hand, is most likely to be overestimated when readily biodegradable synthetic wastewater is used as a surrogate of real wastewater.

Table 4.2 Apparent molecular weight distributions of DOM in MBR systems

Wastewater	Apparent Molecular Weight Distributions			References
	< 3 kDa	3 – 30 kDa	> 30 kDa	
Synthetic	27-30%	31-36%	45.5-56.5%	Lee et al. (2003)
Synthetic	34-52%	22-34%	35-37%	Huang et al. (2000)
Municipal	67-74%	10-16%	12-23%	Our result

4.2 DOM Fouling with Hydrophilic/Hydrophobic Membranes

Figure 4.3 shows the decline of normalized permeate flux as a result of membrane fouling during the filtration of supernatants (containing DOM) from the three pilot MBR systems with hydrophilic GVWP and hydrophobic GVHP membranes, respectively. It can be seen that the permeate flux declined more rapidly and greatly with hydrophobic membranes than hydrophilic membranes in all cases. The flux dropped about 85% for hydrophobic membranes, but only 35% for hydrophilic membranes after 35 min of filtration. The fouling experiments were performed in duplicate runs with the reproducibility better than 10% in all cases. The results clearly

show that the hydrophobic membrane is more susceptible to fouling by DOM in MBR systems.

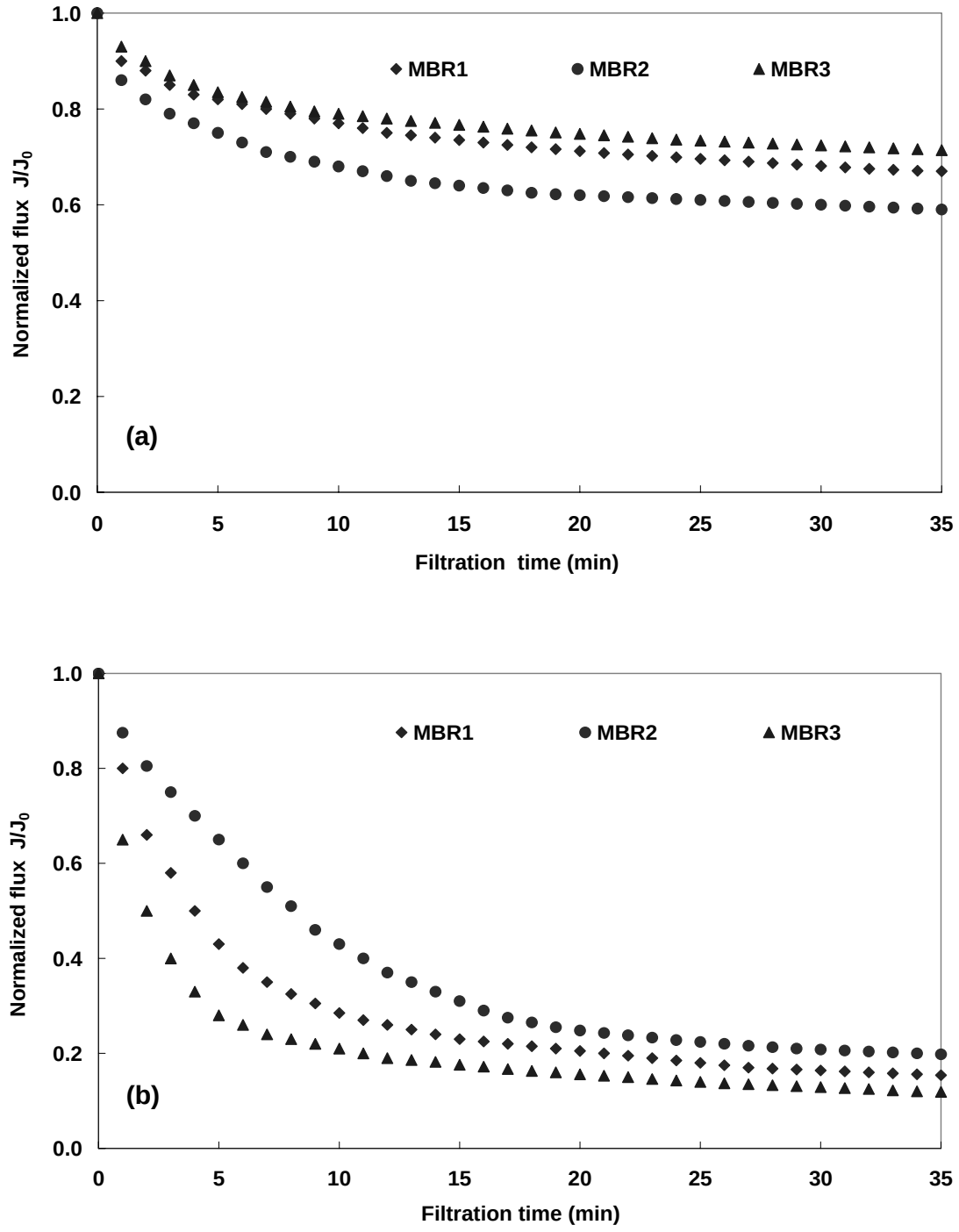

Figure 4.3 Normalized permeate flux for the filtration of MBR supernatants with (a) hydrophilic GVWP membranes and (b) hydrophobic GVHP membranes.

Fouling strength of each DOM sample can be more accurately assessed with its fouling potential, which is defined as the increment in membrane resistance per unit volume of permeate collected per unit membrane surface area (Song et al. 2004). The fouling potential (k_f) of DOM determined from the experimental data is presented in Table 4.3. It was noted that the fouling potentials of DOM for hydrophobic GVHP membranes were about 1 to 2 orders of magnitude higher than for hydrophilic GVWP membranes.

Table 4.3 Fouling potential of DOM for GVWP and GVHP membranes

Samples	MBR 1	MBR 2	MBR 3
k_f (Pa s/m^2) — GVWP	1.26×10^7	2.30×10^7	1.20×10^6
k_f (Pa s/m^2) — GVHP	2.40×10^8	1.38×10^8	3.20×10^8

With respect to hydrophilic membranes, the fouling potential of DOM increased with its total DOC concentration. On the contrary, for hydrophobic membranes, however, the DOM from MBR3 caused the most serious flux decline, even though its DOC concentration was much lower than that of DOM from MBR2. Apparently, the fouling potential of DOM for the hydrophobic membrane was not proportional to its DOC concentration. This implies that DOM from MBR3 contains a higher fraction of components responsible for serious membrane fouling, and DOC is not always an effective fouling indicator for DOM in MBR systems.

Figure 4.4 shows the fouling characteristic of DOM in the three pilot MBR systems with hydrophilic GVWP and hydrophobic GVHP membranes, respectively. It can be seen that the resistance during filtration with GVWP membranes was mainly from the membrane itself, whereas the majority of filtration resistance was induced by DOM fouling for GVHP membranes.

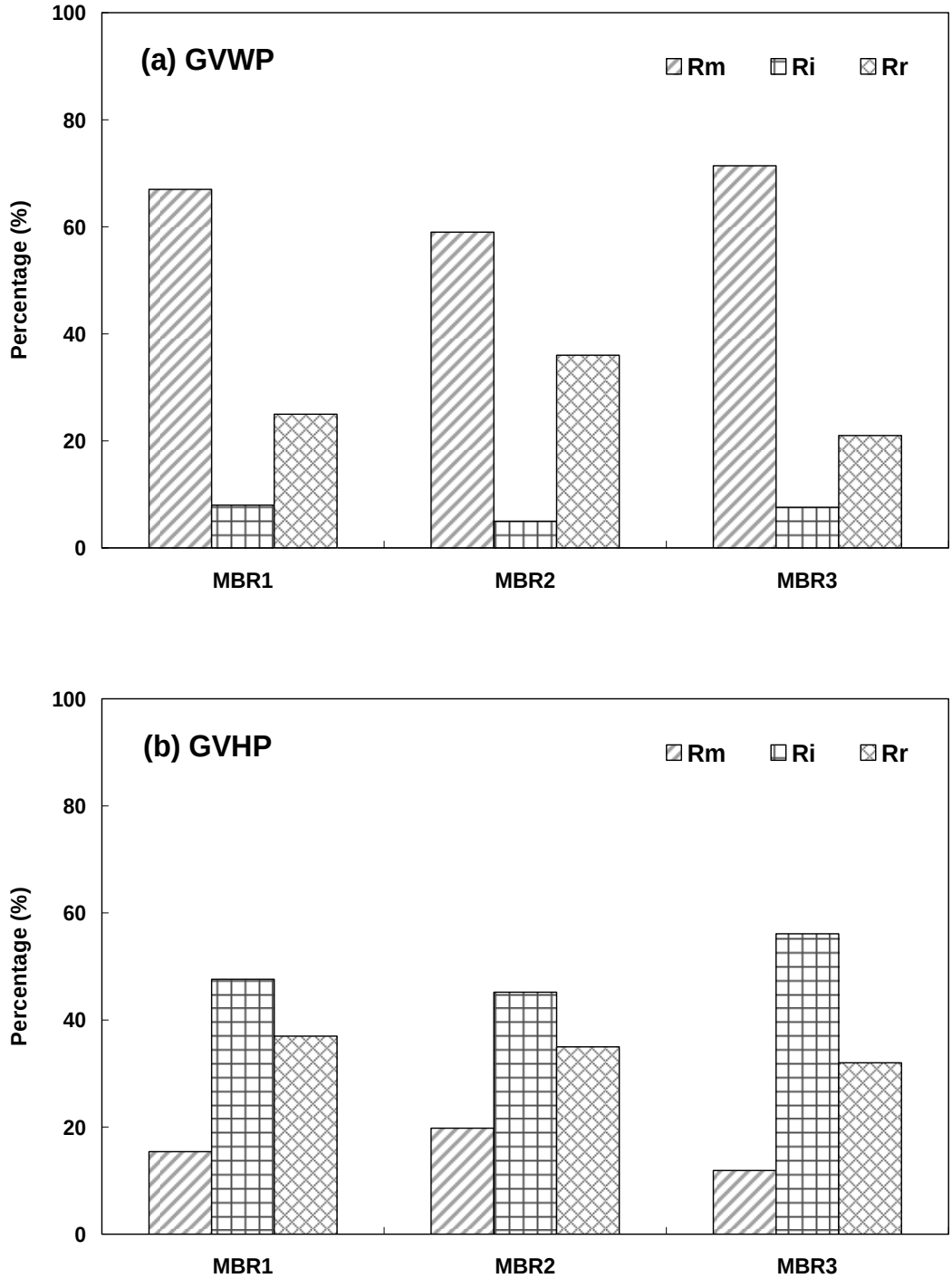

Figure 4.4 Characteristics of fouling resistance caused by DOM in the three pilot MBR systems during filtration with (a) hydrophilic GVWP membranes, and (b) hydrophobic GVHP membranes. R_m, membrane resistance; R_i, resistance of irreversible fouling; R_r, resistance of reversible fouling.

Moreover, it was noted that the major part of fouling for GVWP membranes is reversible. In contrast, however, over 55% of fouling for GVHP membranes can be classified as irreversible, which cannot be easily removed by simple physical cleaning. It is therefore inferred that more chemical cleanings may be required for hydrophobic membranes during the long-term operation in MBR systems.

4.3 Effect of Prefiltration on DOM fouling

The DOM from MBR3 was prefiltered with either hydrophilic or hydrophobic membranes with the purpose of obtaining some clues about the major DOM foulants responsible for the dramatic flux decline during filtration with hydrophobic membranes. The fouling behavior of each filtrate with a fresh GVHP membrane was examined and compared with that of the original DOM in MBR3 (Figure 4.5).

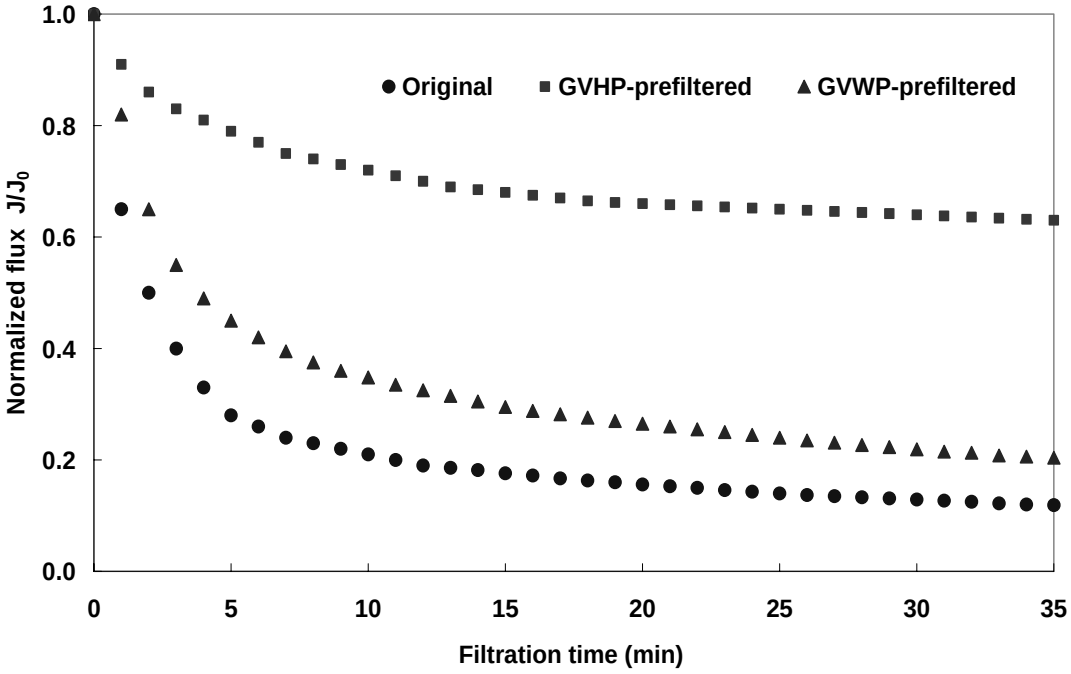

Figure 4.5 Normalized permeate flux for the filtration of three DOM samples, original, GVWP-prefiltered, GVHP-prefiltered with hydrophobic GVHP membranes.

It can be seen that the flux decline was greatly reduced compared to the original DOM after prefiltration with the GVHP membrane, whereas DOM prefiltered with the GVWP membrane still caused substantial flux decline. This was also the case for the DOM in MBR 1 and MBR 2. It appears that the GVHP membrane is more effective than GVWP membrane in terms of reducing DOM fouling potential.

The rejections of DOC by the two membranes were found to be almost identical (GVWP 9.8±1.2%; GVHP 10.1±0.9%), indicating that the difference in fouling reduction by GVWP and GVHP membranes arises from their ability to reject different DOM components. Since the two membranes have the same nominal pore size, the difference in the rejected foulants is less likely related to the molecular size of DOM. It can be seen from Figure 4.6 that the AMWD of DOM after filtration with GVHP membranes are almost identical with those of original DOM.

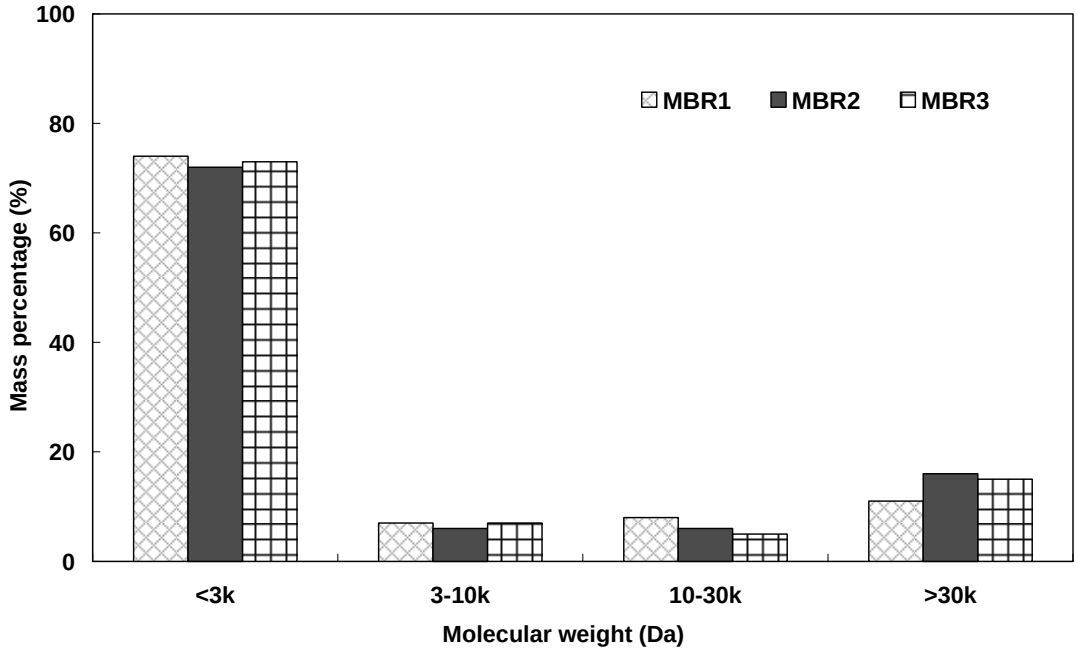

Figure 4.6 Apparent molecular weight distributions of DOM in pilot MBR systems after GVHP membrane filtration.

Unlike the case of DOC rejection, however, it was observed that the GVHP membrane achieved a consistently higher SUVA rejection than the GVWP membrane. It is therefore inferred that DOM components, which have higher SUVA value, may be the major foulants responsible for irreversible organic fouling in MBR systems.

4.4 Characteristics and Fouling Potential of Fractional Components

4.4.1 Characteristics of Fractional DOM Components

In order to obtain more detailed insights into DOM fouling phenomenon, the characteristics of each fractional DOM component, AHS, HiA, HiB, and HiN were examined. Figure 4.7 shows the SUVA value of different fractional DOM components in the pilot MBR systems. It was noted that hydrophobic AHS exhibited the highest SUVA value in all samples. This implies that AHS would have higher fouling potential than hydrophilic DOM components. In addition, because AHS constituted the major fraction of DOM in the pilot MBR systems, it can be inferred that most aromatic components of DOM reside in AHS. The results reported here agree well with the general consensus that AHS comprise the majority of aromatic DOM components. With respect to hydrophilic components, however, HiN were found to have lower SUVA value than HiA and HiB.

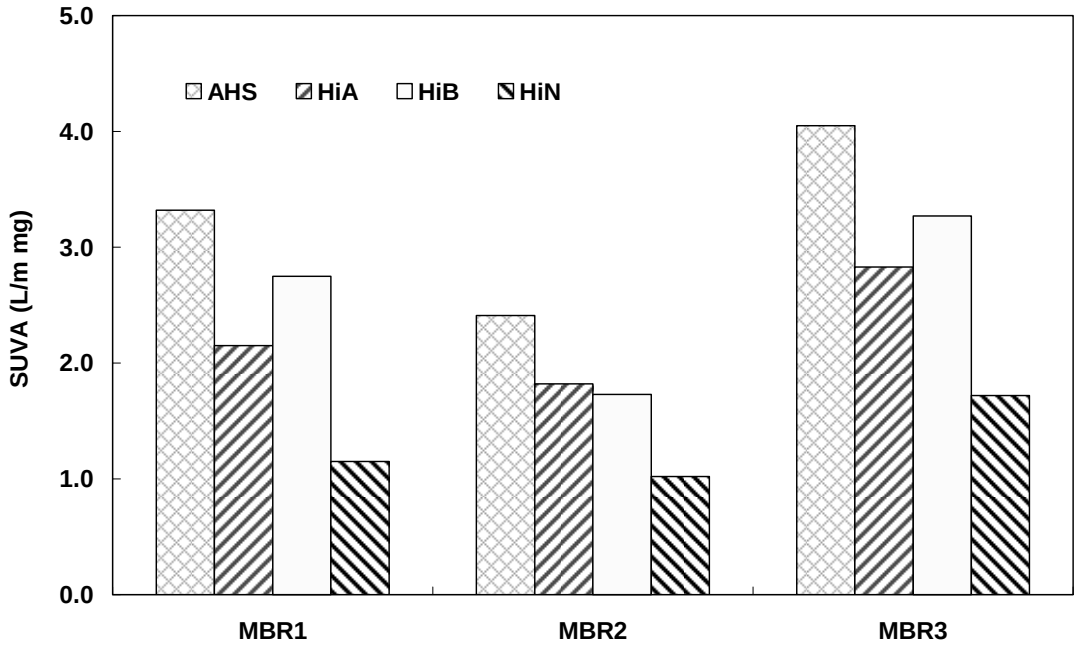

Figure 4.7 SUVA values for different fractional DOM components in pilot MBR systems.

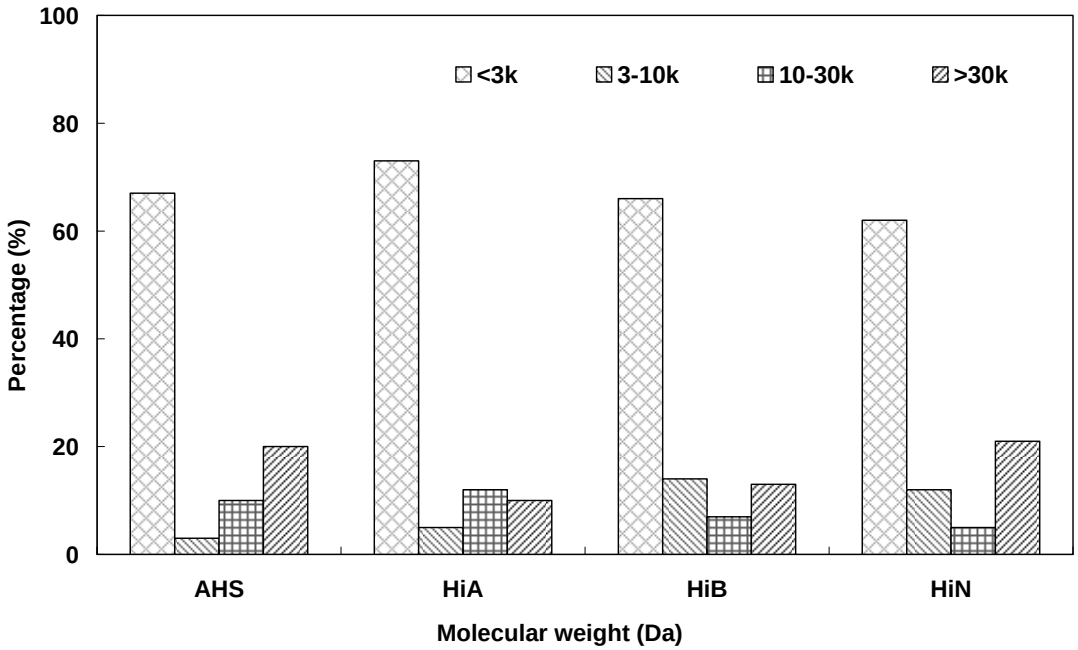

Figure 4.8 Apparent molecular weight distributions for the fractional DOM components in MBR3.

On the other hand, the AWMD of the fractional DOM components were measured and one of the representative results (DOM in MBR3) is shown in Figure 4.8. It can be seen that the AWMD of each individual DOM fraction generally followed the same trend as that observed for unfractionated DOM. Furthermore, it was noted that AHS and HiN contained relatively more large molecules than HiA and HiB.

4.4.2 Fouling Potential of Fractional DOM Components

To further investigate the major foulants of DOM in MBR systems, the relative contribution of each individual DOM fraction to membrane fouling was quantified. Membrane fouling by the fractional DOM components in MBR3 was examined with hydrophobic GVHP membranes at the same DOC concentration of 5 mg/L. As shown in Figure 4.9, each fractional DOM component caused substantial flux decline, resulting in 60-86% loss of the initial flux after 35 min of filtration. However, contrary to our early speculation, it was noted that HiN exhibited the highest fouling potential rather than AHS. The highest fouling potential of HiN can be attributed partly to its high concentration of Ca^{2+}. During the fractionation process, the majority of Ca^{2+} can readily pass through the resin columns and eventually concentrated in HiN. The formation of large organic-Ca^{2+} complexes with the polar groups on HiN would significantly enhance the affinity of HiN to the negatively charged membranes (Fan et al., 2001). However, in the natural environment, complexation of Ca^{2+} with negatively charged hydrophobic AHS is supposed to be more favorable (Hong and Elimelech, 1997; Carroll et al., 2000).

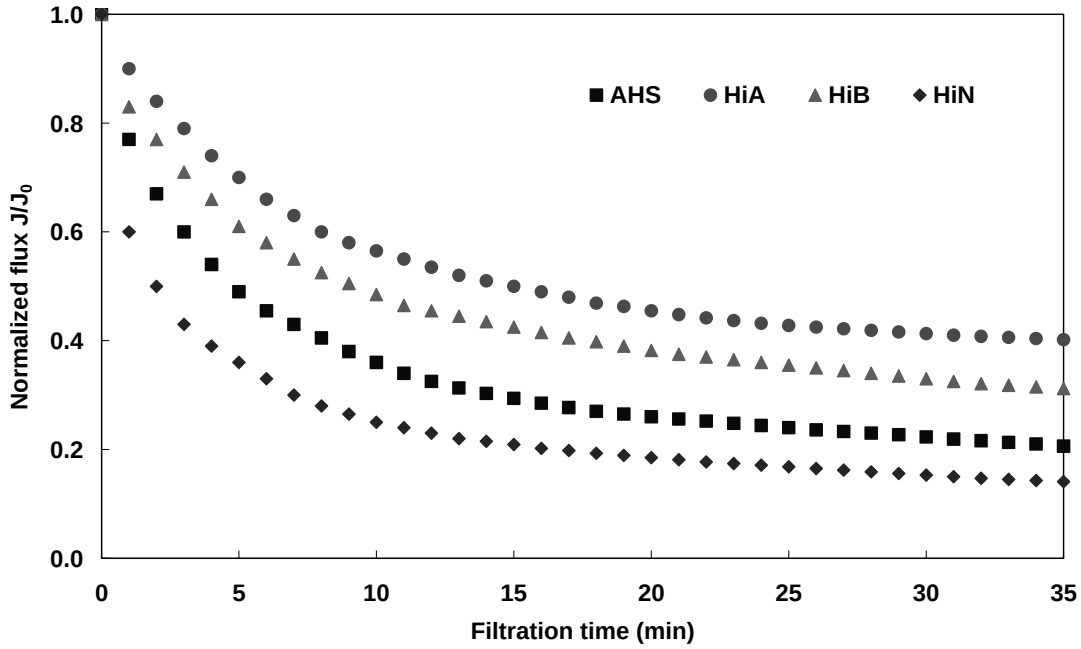

Figure 4.9 Normalized permeate flux for the filtration of the fractional components of DOM in MBR3 with hydrophobic GVHP membranes.

For a more fair comparison of fouling potentials of different fractional DOM components, fouling experiments were repeated with AHS, HiA, and HiB, in which the concentration of Ca^{2+} was adjusted to the same value as in HiN (i.e., 38 mg/L). As shown in Figure 4.10, both fouling rate and extent of AHS, HiA, and HiB significantly increased with the addition of Ca^{2+}. The fouling potentials of fractional DOM components with calcium adjustment are summarized and compared with those without calcium adjustment in Table 4.4. It can be seen that AHS now exhibited the highest fouling potential at the same DOC concentration. This was also the case for the DOM in MBR 1 and MBR 2. Recalling that AHS are also the most abundant components of DOM in the MBR systems, the results clearly show that hydrophobic AHS are the most important foulants of DOM for hydrophobic microfiltration membranes.

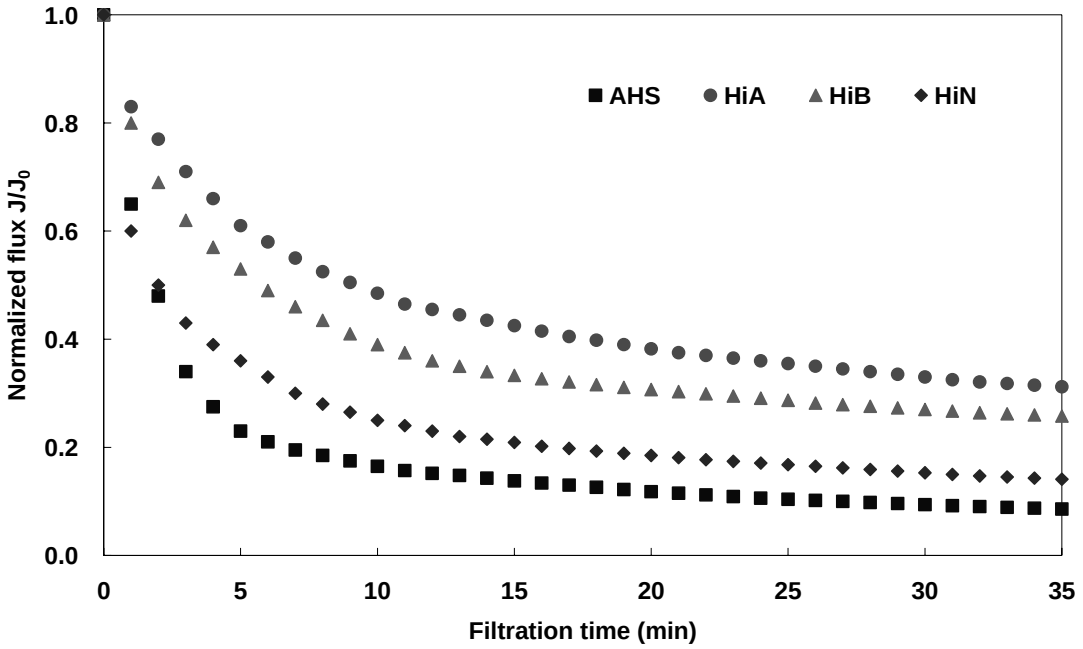

Figure 4.10 Normalized permeate flux for the filtration of the fractional components of DOM in MBR3 at the same level of Ca^{2+} with hydrophobic GVHP membranes.

Table 4.4 Fouling potential of fractional DOM components in MBR3 at DOC concentration of 5 mg/L

Samples	AHS	HiA	HiB	HiN
k_f (Pa s/m^2)	2.28×10^8	7.90×10^7	1.32×10^8	3.58×10^8
k_f (Pa s/m^2); Ca^{2+} = 38 mg/L	3.82×10^8	1.27×10^8	1.81×10^8	3.58×10^8

On the other hand, it was noteworthy that HiN showed much higher fouling potential than the other two hydrophilic DOM components even compared at the same concentration of Ca^{2+}. Since these DOM components are hydrophilic in nature, the higher fouling potential of HiN is probably attributed to the particular chemical structures of these organics, which have higher affinity to the membrane. Figure 4.11 further shows that HiN fouling was mainly irreversible while the major part of HiB and HiA fouling was reversible. This indicates the higher binding capacity of HiN within membrane pores and further confirms the importance of HiN in DOM fouling.

It can therefore be inferred that DOM having more HiN would most likely cause more serious irreversible fouling in MBR systems.

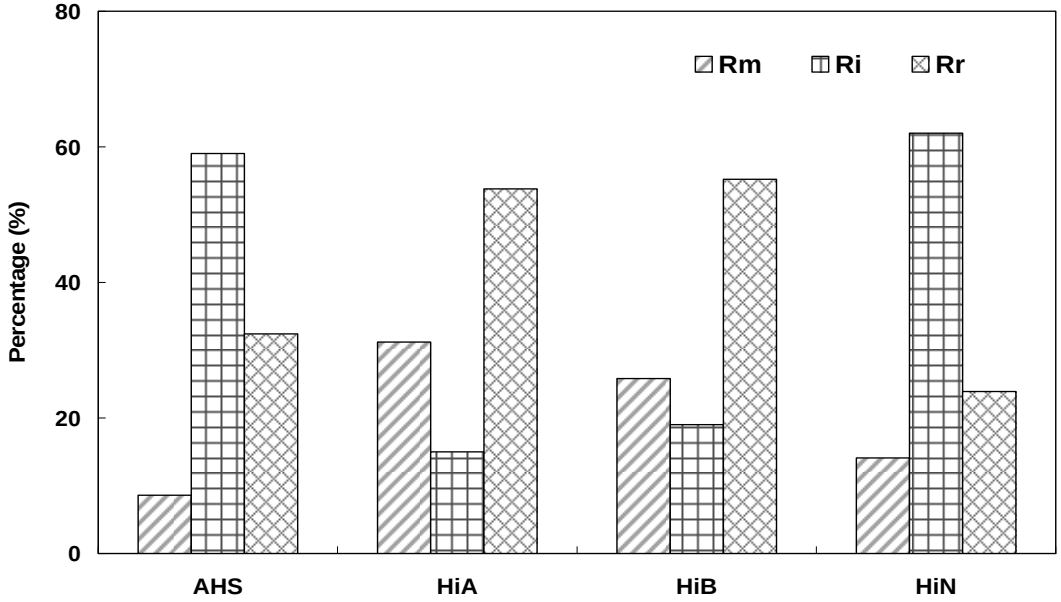

Figure 4.11 Characteristics of fouling resistance caused by the fractional components of DOM in MBR3 during filtration with hydrophobic GVHP membranes. R_m, membrane resistance; R_i, resistance of irreversible fouling; R_r, resistance of reversible fouling.

4.5 Concluding Remarks

The fouling potentials of DOM in the three pilot MBR systems were investigated in a stirred-cell filtration system with hydrophilic GVWP and hydrophobic GVHP membranes, respectively. DOM fouling was much more serious with hydrophobic membranes, and was not always proportional to its DOC concentration. It was found that the DOM having the highest content of AHS induced the severest membrane fouling, suggesting a strong link between the high fouling potential of DOM and its high content of AHS.

The majority of DOM in the MBR systems, accounting for about 70%, had a molecular weight of less than 3 kDa. The components of large molecular weight (> 30 kDa) formed the second largest fraction, constituting 12-23% of DOM, which is smaller than those previously reported in the MBR systems for readily biodegradable synthetic wastewater treatment. The hydrophobic AHS were found to be the most abundant fraction in the DOM, accounting for 43.8-65.7% of the total DOC. In addition, it was noted that AHS exhibited much higher SUVA value than hydrophilic DOM components, implying that the aromaticity of DOM mainly resides in AHS.

It was observed that the fouling potential of DOM was greatly reduced after prefiltration with the GVHP membrane, whereas DOM prefiltered with the GVWP membrane still induced serious fouling. The fact that the GVHP membrane showed higher SUVA rejection than the GVWP membrane during DOM prefiltration implies that AHS having high SUVA value may constitute the major DOM foulants. The order of the fouling potential of the fractional DOM components, evaluated at comparable conditions, was observed to be AHS > HiN > HiB > HiA. This further confirms that hydrophobic AHS were the major components of DOM responsible for fouling of GVHP membranes. In addition, it was noted that HiN also induced significant fouling, which was mainly irreversible. The fouling potential of fractional DOM components was greatly affected by the concentration of Ca^{2+}.

CHAPTER 5

MODELING OF FOULING DEVELOPMENT IN MBR SYSTEMS

As with many other membrane systems, mathematical models can be powerful tools to improve MBR design and operation. However, modeling of fouling development in MBR systems represents a great challenge because of the intrinsic complexity of MBR systems. A large number of components and phenomena are involved in MBR systems, which consists of two mutually influenced and dynamically interrelated, but fundamentally different processes (biodegradation and membrane separation). In addition, there are still many uncertainties or even contradictions over the major foulants and main flux-determining mechanisms regarding membrane fouling in MBR systems (Chang et al., 2002; Wisniewski and Grasmick, 1998).

In most existing models, the role of DOM, which is commonly lumped together with other foulants, has not been sufficiently delineated or speculated. However, the significance of DOM in MBR fouling has been clearly demonstrated in many recent MBR researches (Wisniewski and Grasmick, 1998; Bouhabila et al., 2001; Lee et al., 2003). In MBR systems, DOM may contribute to membrane fouling in two ways; (i) it is a foulant itself that can be adsorbed onto membrane surface and inside membrane pores, and (ii) DOM adsorbed on the membrane may act as glue or cement that holds the particulates on membrane surface, which otherwise would be susceptible to be re-suspended by the shear flow.

The primary objective of this chapter is, therefore, to conceptualize and develop a model to describe membrane fouling in submerged MBR systems for wastewater treatment, in which both reversible and irreversible fouling would be quantified. In particular, DOM is speculated as the key foulant responsible for the long-term irreversible fouling of the membrane module. The validity of the model was verified by comparing model simulation results with the independent operational data from the pilot submerged MBR system that was not used for parameter identification.

5.1 Theories and Models

5.1.1 Resistance-in-series Model

The permeate flux of a membrane is governed by the basic membrane filtration equation, as follows:

$$J = \frac{\Delta P}{\mu R_t} \tag{5.1}$$

where J is the permeate flux, ΔP is the transmembrane pressure (TMP), μ is the permeate viscosity, R_t is the total membrane resistance. The total membrane resistance,

according to the classical resistance-in-series model, includes two parts, as follows:

$$R_t = R_m + R_f \tag{5.2}$$

where R_m is the intrinsic membrane resistance and R_f is the time-dependent resistance resulting from membrane fouling. In this study, the resistance of membrane fouling is further divided into two parts caused by reversible fouling and irreversible fouling, as follows:

$$R_f = R_r + R_i \tag{5.3}$$

where R_r and R_i are the resistance components for reversible fouling and irreversible fouling, respectively.

The precise definition of reversible/irreversible fouling is still open to debate and is heavily dependent on the measurement protocols applied (i.e., vigor of physical cleaning). In the present study, reversible fouling refers to the loose deposition of mixed liquor suspended solids (MLSS) on membrane surface that can be readily removed with an appropriate physical cleaning. On the other hand, irreversible fouling refers to the accumulation of the foulants that is removable only by chemical cleaning. It is speculated that irreversible fouling is related to the accumulation of DOM on the membrane surface and within the membrane pores, and to the other foulants glued or cemented onto the membrane surface by the accumulated DOM.

The following assumptions are made in the development of the mathematical model:

i) MLSS are the major foulants for reversible fouling, while the contribution of DOM to reversible fouling is negligible;
ii) Back-transport of accumulated MLSS on the membrane surface to the bulk solution is mainly by shear-induced diffusion;

iii) Specific resistance of the reversible fouling layer is constant;

iv) The concentration polarization effect of both MLSS and DOM is relatively small compared with both membrane intrinsic resistance and fouling layer resistance (Zhang and Song, 2000); and

v) Irreversible fouling is dependent on the DOM concentration and property.

5.1.2 Reversible Fouling

According to the conventional cake filtration theory, the time-dependent resistance resulting from reversible fouling R_r can be expressed as follows:

$$R_r = \sigma m \tag{5.4}$$

where σ is the specific resistance of reversible fouling layer, and m is the mass of cake layer accumulated on membrane surface. The value of σ can be measured by conducting dead-end filtration experiments at constant pressure with the mixed liquor in MBR systems (Bouhabila et al., 1998). The rate expression of accumulated reversible foulant can be determined by the advection of MLSS with permeate flow to the membrane surface and the back diffusion of MLSS from the membrane surface caused by shear flow over the membrane surface:

$$\frac{dm_r}{dt} = JX_T - k_r m_r \tag{5.5}$$

where m_r is the amount of the reversible foulant, X_T is the concentration of MLSS in the MBR system, and k_r is the detachment coefficient to account for the crossflow effect on removal of accumulated mass from membrane surface. The detachment coefficient k_r is supposed to be an operation-specific parameter, which is influenced by the aeration intensity and adhesive property of MLSS.

Eq. (5.5) can be solved for the initially clean membrane [$m_r(0) = 0$] by integrating over the time interval from 0 to t, as follows:

$$m_r = \frac{JX_T\left(1 - e^{-k_r t}\right)}{k_r} \tag{5.6}$$

where e is the base of natural logarithms. Hence, the resistance R_r resulting from reversible fouling can be calculated by the following:

$$R_r = \sigma \frac{JX_T\left(1 - e^{-k_r t}\right)}{k_r} \tag{5.7}$$

Eq. (5.7) shows that the resistance of the reversible fouling layer is proportional to the specific resistance (σ), permeate flux (J) and MLSS concentration (X_T), but inversely proportional to the detachment coefficient (k_r).

The effect of the detachment coefficient on the accumulation of reversible foulant on the membrane surface is simulated and shown in Figure 5.1. It can be seen that both the maximum amount of mass accumulated on the membrane surface and the time to reach the maximum value are strongly affected by the value of the detachment coefficient. A higher value of detachment coefficient indicates that crossflow is more effective on preventing the membrane surface from biomass attachment. As a result, less biomass would accumulate on the membrane surface. On the other hand, it is noted that there are two stages in the accumulation of biomass on the membrane surface. Biomass accumulates dramatically at the beginning and then reaches a plateau, which means that the two terms on the right side of Eq. (5.5) attained a dynamic equilibrium. In most cases, as illustrated in Figure 5.1, the steady-state situation can be reached within one day.

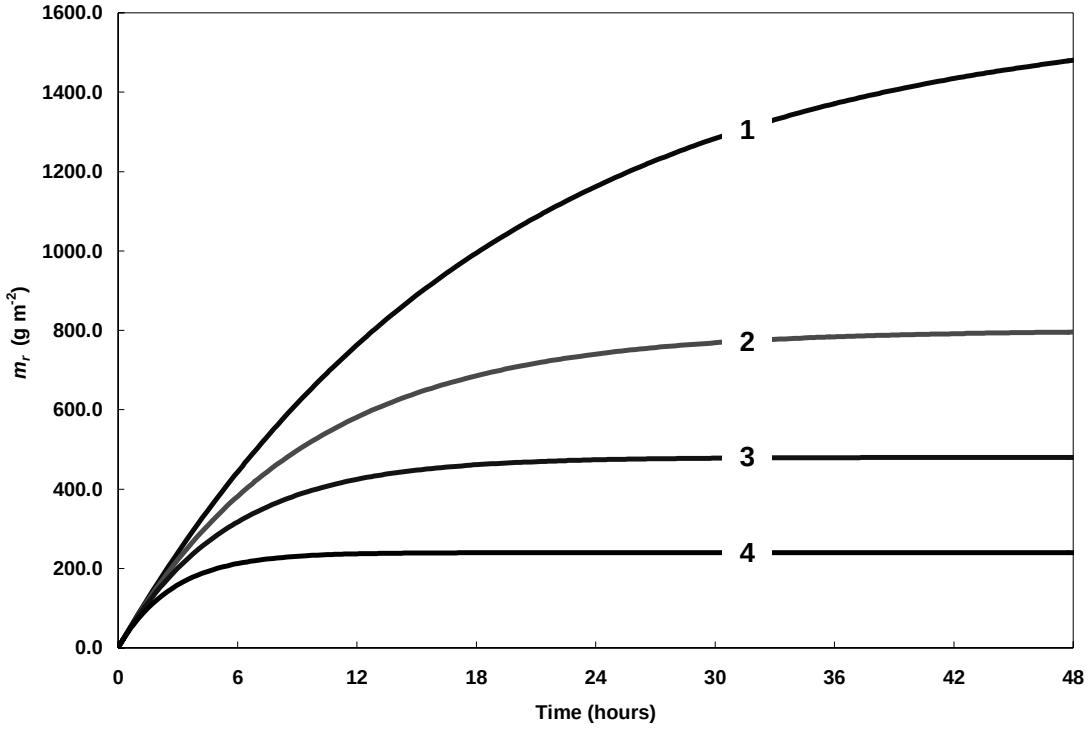

Figure 5.1 Effect of detachment coefficients on time and magnitude of reversible foulant accumulation on the membrane surface (1. $k_r = 1.5\times10^{-5}$ s^{-1}, 2. $k_r = 3.0\times10^{-5}$ s^{-1}, 3. $k_r = 5.0\times10^{-5}$ s^{-1}, 4. $k_r = 1.0\times10^{-4}$ s^{-1}). Other parameters used in calculations: $J = 3.0\times10^{-6}$ m/s; $X_T = 8.0$ kg/ m^3.

5.1.3 Irreversible Fouling

The rate equation for the accumulation of irreversible foulant on or in the membrane is given by the following:

$$\frac{dm_i}{dt} = JC_{MBR} \tag{5.8}$$

where m_i is the amount of the irreversible foulant, and C_{MBR} is the concentration of DOM in the MBR system. Comparing Eq. (5.8) with Eq. (5.5), it can be found that there is only the forward term on the right side of Eq. (5.8). The lack of the backward term is because fouling is irreversible here. Integrating Eq. (5.8) for the initially clean membrane over time interval 0 to t results in the following:

$$m_i = C_{MBR}\int_0^t Jdt \tag{5.9}$$

With a known mass of DOM accumulated on or in the membrane, the resistance resulting from irreversible fouling R_i, similar to the case of reversible fouling, can be calculated by the following:

$$R_i = k_i C_{MBR}\int_0^t Jdt \tag{5.10}$$

where k_i is the fouling strength of DOM, which can be defined as the specific resistance resulting from accumulation of one unit of DOM. Similar to k_r, k_i is also supposed to be operation-specific, probably a function of DOM characteristics and membrane materials of the filtration module. Eq. (5.10) shows that the resistance of the irreversible fouling is proportional to the fouling strength factor (k_i), DOM concentration (C_{MBR}), and the total volume of the filtrate per unit area of the membrane ($\int_0^t Jdt$).

5.1.4 Permeate Flux and Transmembrane Pressure

Substituting Eq. (5.7) and Eq. (5.10) into Eq. (5.3), the time-dependent filtration resistance resulting from membrane fouling R_f can be described as follows:

$$R_f = \sigma\frac{JX_T\left(1-e^{-k_r t}\right)}{k_r} + k_i C_{MBR}\int_0^t Jdt \tag{5.11}$$

Finally, with Eqs. (5.1), (5.2), and (5.11), the instantaneous permeate flux at any time is formulated as follows:

$$J = \frac{\Delta P}{\mu\left[R_m + \sigma\frac{JX_T\left(1-e^{-k_r t}\right)}{k_r} + k_i C_{MBR}\int_0^t Jdt\right]} \tag{5.12}$$

For those MBR systems operated at constant flux conditions, the evolution of TMP

with time is the main focus of interest, which can be described by simply rearranging Eq. (5.12) as follows:

$$\Delta P = \mu\left\{R_m J_0 + \left[\sigma \frac{X_T\left(1-e^{-k_r t}\right)}{k_r} + k_i C_{MBR} t\right] J_0^2\right\} \tag{5.13}$$

where J_0 (instead of J) is used in Eq. (5.13) to indicate the constant permeate flux. The evolution of TMP with operation time, calculated from Eq. (5.13), was simulated for different detachment coefficients, and one of the representative results is plotted in Figure 5.2.

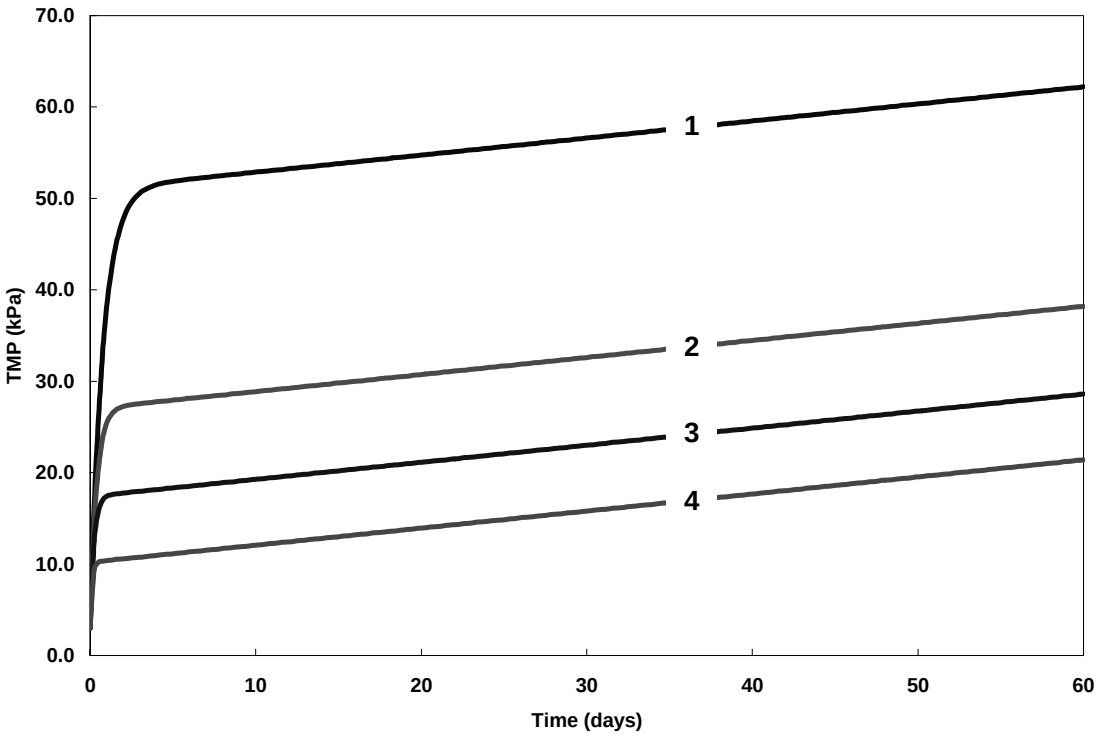

Figure 5.2 Evolution of TMP with operation time for different detachment coefficients (1. k_r = 1.5×10^{-5} s^{-1}, 2. k_r = 3.0×10^{-5} s^{-1}, 3. k_r = 5.0×10^{-5} s^{-1}, 4. k_r = 1.0×10^{-4} s^{-1}). Other parameters used in calculations: J = 3.0×10^{-6} m/s, X_T = 8.0 kg/m^3, σ= 1.0×10^{13} m/kg, R_m = 1.0×10^{12} m^{-1}, μ = 1.0×10^{-3} Pa s, C_{MBR} = 2.0×10^{-2} kg/m^3, k_i = 1.2×10^{13} m/kg.

It can be seen that the TMP goes up steeply at the beginning, after which the TMP increases much more moderately. This fashion of TMP increase can be readily explained with the concepts of reversible and irreversible fouling. The initial steep

increase of TMP is mainly caused by reversible fouling. Because of the extremely high MLSS concentration in MBR systems, it is reasonably expected that dynamic equilibrium can be reached rapidly. The moderate TMP increase thereafter would be the result of irreversible fouling, characterized by a slow accumulation of DOM on or in membranes.

5.1.5 Biological Parameters X_T and C_{MBR}

The total concentrations of MLSS (X_T) and DOM (C_{MBR}) in MBR systems are two key biological parameters that must be determined before the simulation of fouling development in MBR systems. The values of X_T and C_{MBR} are readily measured during MBR operation. Alternatively, in the case of model prediction, these two parameters can be calculated using activated sludge models for the biodegradation process in MBR systems with specified initial conditions.

5.2 Simulations and Discussions

5.2.1 Description of the pilot MBR System

The pilot submerged MBR system of 75 m^3 was operated over 7 months for municipal wastewater treatment. After primary settling and passing through a 1mm fine screen, the wastewater was then supplied into the MBR system. The typical influent characteristics are listed in Table 5.1. The system consisted of both anoxic and aerobic tanks. Microfiltration membrane modules (Mitsubishi Rayon, Japan) were placed in the aerobic tank for solid-liquid separation. The membrane modules were made of polyethylene hollow fibers with an average pore size of 0.4 μm. Permeate flux was suctioned from the membrane modules with an intermittent mode of 13 min on and 2 min off.

Table 5.1 Typical characteristics of influent municipal wastewater

Parameter	Unit	Value
COD	mg/L	265
Soluble COD	mg/L	109
TSS	mg/L	77
TN	mg/L	45
TKN	mg/L	33
NH_4^+-N	mg/L	26
pH	-	7.05

The MBR system was operated at a constant flux condition, and the TMP was continuously monitored. The TMP data for 7 consecutive months (January 1 to August 1, 2004) are presented in Figure 5.3. The following three individual filtration intervals were identified according to the information from the system management: January 1 to February 24, February 27 to June 27, and June 30 to August 1, 2004, respectively. Herein, filtration intervals were defined as the period of filtration time between two in-situ membrane cleaning work. It is noted that there are a few sudden drops of TMP within certain filtration intervals. This is most likely because of the unexpected operating interruptions and the variation of the influent wastewater characteristics. In general, the treatment performance is quite satisfactory and stable. The average removal efficiency of COD remained at 95% or even higher, while approximately 100% nitrification was achieved, which confirms the substantial capacities of MBR systems in wastewater treatment.

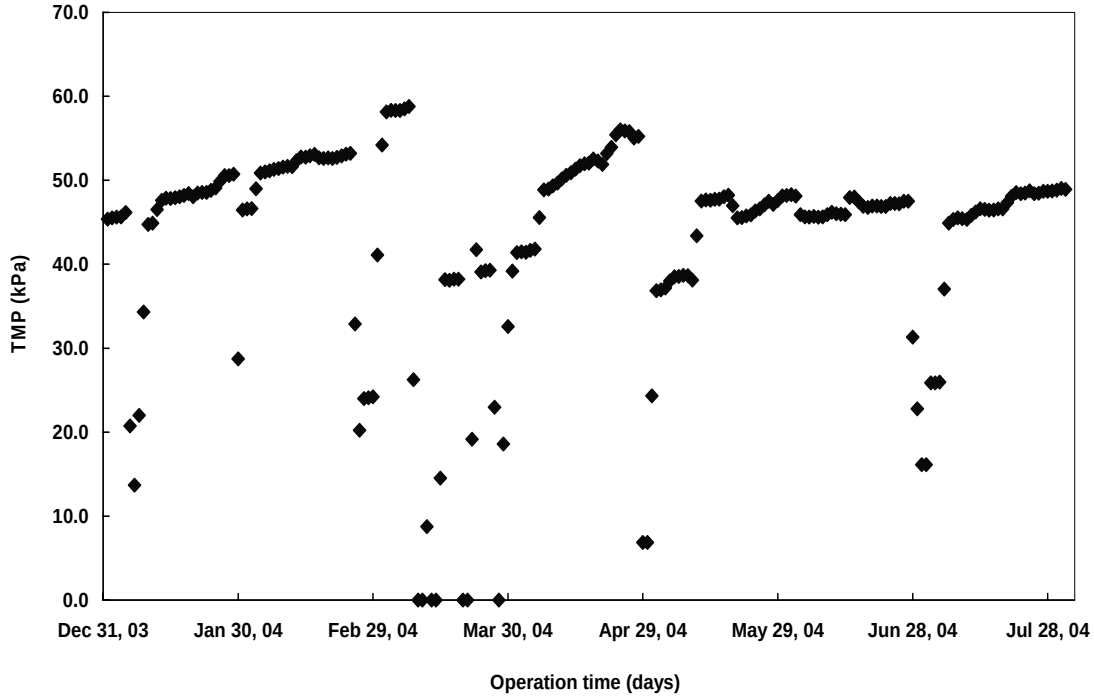

Figure 5.3 Operational data for TMP of the submerged MBR system (January 1 to August 1, 2004).

5.2.2 Model Parameters

The measured values of X_T and C_{MBR} in the pilot MBR system were generally stable, with standard deviations observed less than 15 and 23%, respectively. The mean values of X_T and C_{MBR} used in the model simulation are given in Table 5.2.

Table 5.2 Mean values of X_T and C_{MBR} in the three filtration intervals

Parameter	Unit	Value		
		Interval 1	Interval 2	Interval 3
X_T	gMLSS/m^3	7782	7825	7816
C_{MBR}	mgDOC/L	15.2	18.9	17.8

The specific resistance of the reversible fouling layer, σ, was determined experimentally according to the method as described by Bouhabila et al. (1998). Table 5.3 shows the values of σ for the three different filtration intervals. It is noted that the

specific resistance of the reversible fouling layer is approximately constant throughout the entire operation time, which coincides well with the assumption (iii) made during model development.

Table 5.3 Values of σ in three filtration intervals

Parameter	Unit	Value
σ_1 (Interval 1)	m/kg	1.29×10^{13}
σ_2 (Interval 2)	m/kg	1.12×10^{13}
σ_3 (Interval 3)	m/kg	1.27×10^{13}

Because the detachment coefficient, k_r, and fouling strength factor, k_i, were not directly measurable, their values were determined from experimental TMP data in the first filtration interval by the method of best curve fitting. Further studies are needed to correlate these two parameters to the measurable variables of the MBR system. The TMP data and the best fitting curve for the parameter estimation are presented in Figure 5.4. It can be seen that both the general trend of TMP increase and fluctuations in operating conditions agreed well with the fitting curve.

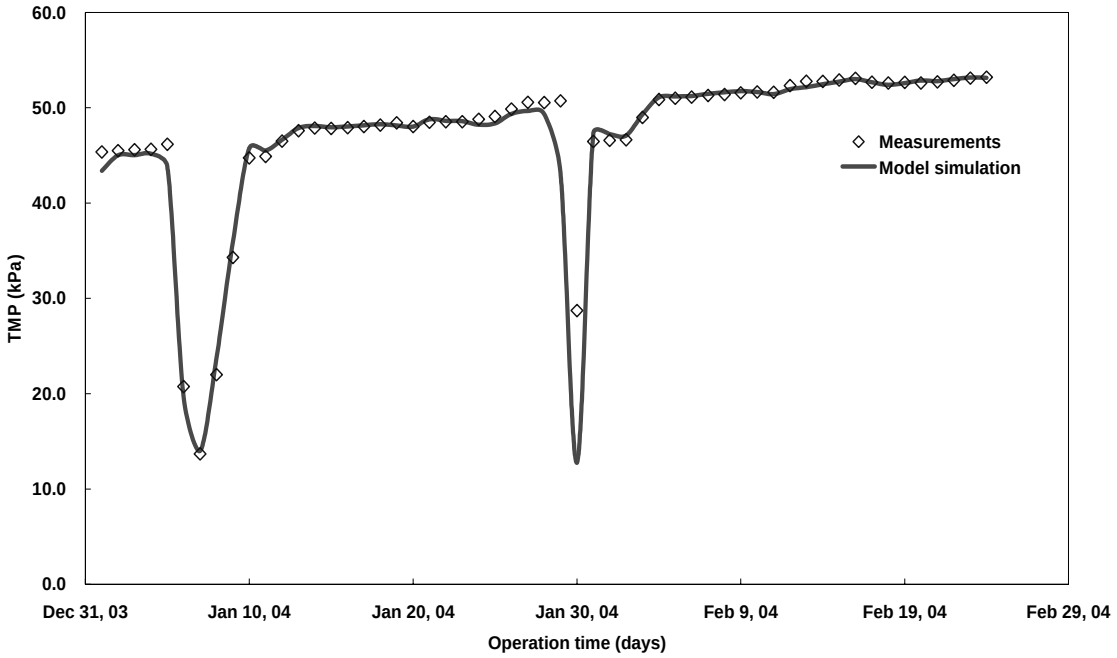

Figure 5.4 Comparison of model simulations with TMP measurements (January 1 to February 24, 2004).).

5.2.3 Performance Simulations and Model Verification

Simulation studies were carried out for the following two filtration intervals with the same set of model parameters as shown in Table 5.4. The validity of these parameters (i.e., k_r and k_i) was verified by comparing the simulation results with the operational data in the corresponding filtration intervals as shown in Figure 5.5 and Figure 5.6, respectively. The average deviations for the simulations of both the second and third filtration intervals are less than 10%. Considering the inevitable measurement errors and fluctuations in operating conditions, a satisfactory simulation performance in terms of the evolution of TMP with operation time can be claimed. The good agreement of the simulation results with operational data, on the other hand, indicates that fouling behavior in the pilot MBR system can be well described with the model developed in this study.

Table 5.4 Values of model parameters used in the simulation study

Parameter	Unit	Value
k_r	s^{-1}	3.24×10^{-5}
k_i	m/kg	1.48×10^{13}

The experimental observations and model simulations for the entire operational period (January 1 to August 1, 2004) are compared in Figure 5.7. The simulations were conducted with a single set of parameters (Table 5.4). Despite two in-situ membrane cleanings during this period, the characteristic evolution of TMP can be adequately described with the model. The results reveal that the fouling characteristics of the mixed liquor in the MBR system are relatively stable. Moreover, the model parameters identified from a short period of operation time can be satisfactorily applied to predict fouling behaviors in the MBR system, even though the system is under the influence of regular cleanings and unexpected interruptions.

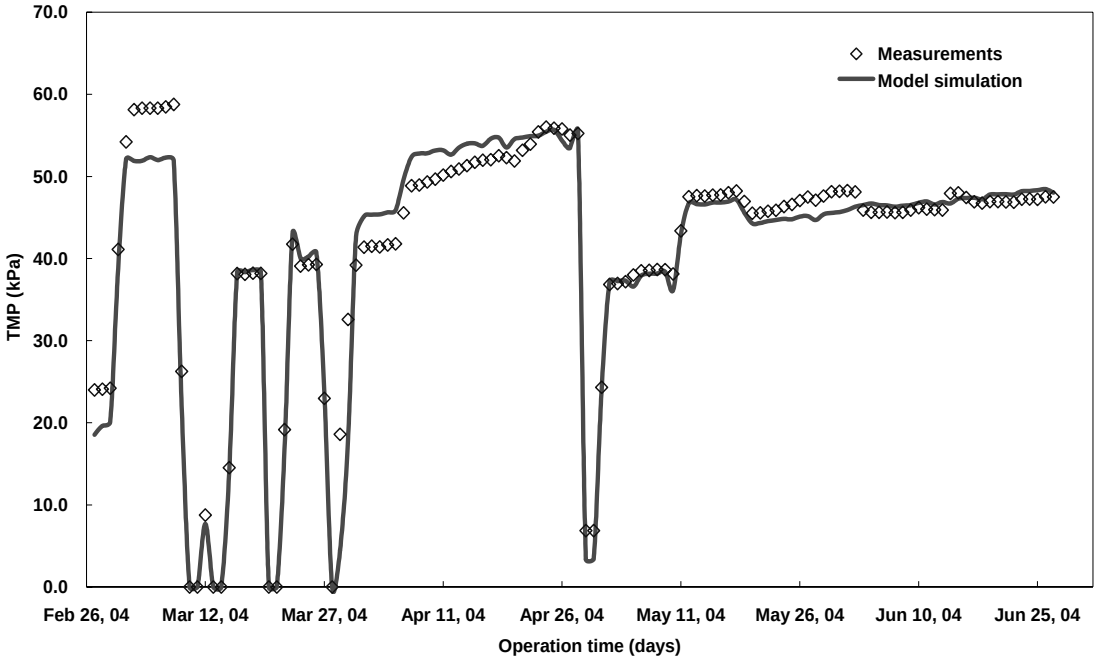

Figure 5.5 Comparison of model simulations with TMP measurements (February 27 to June 27, 2004).

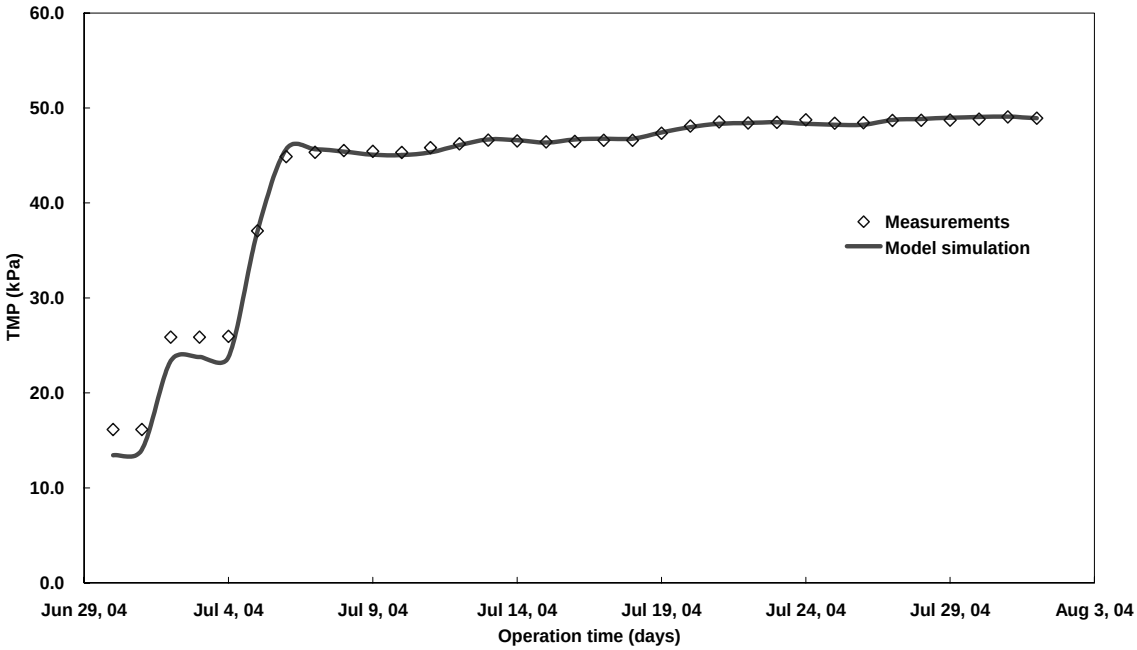

Figure 5.6 Comparison of model simulations with TMP measurements (June 30 to August 1, 2004).

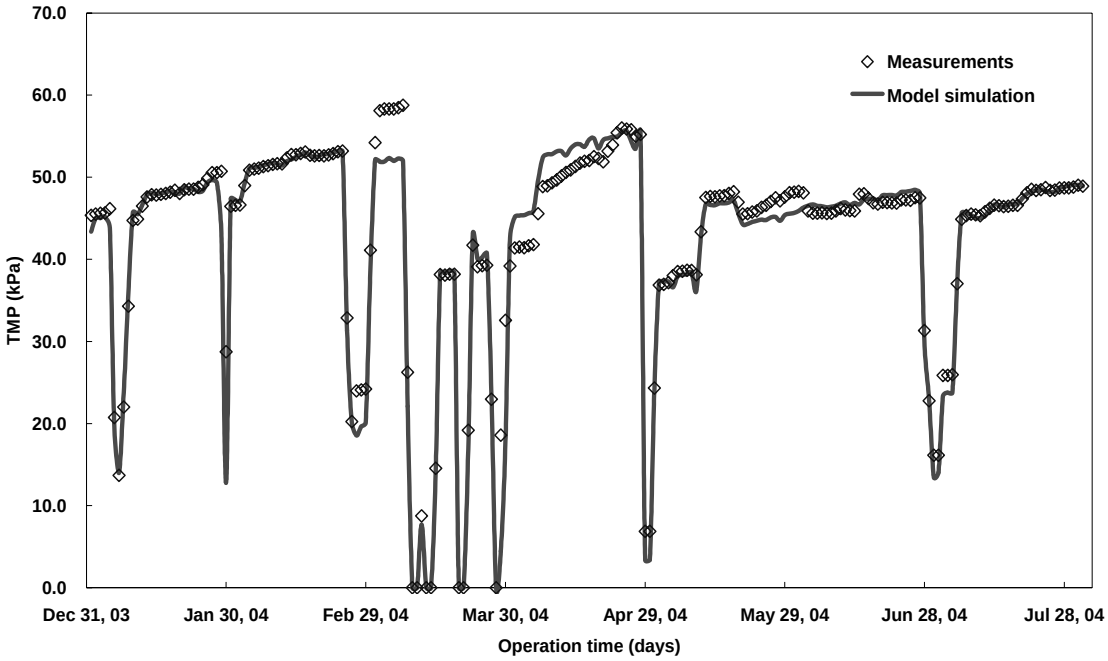

Figure 5.7 Comparison of model simulations with TMP measurements (January 1 to August 1, 2004).

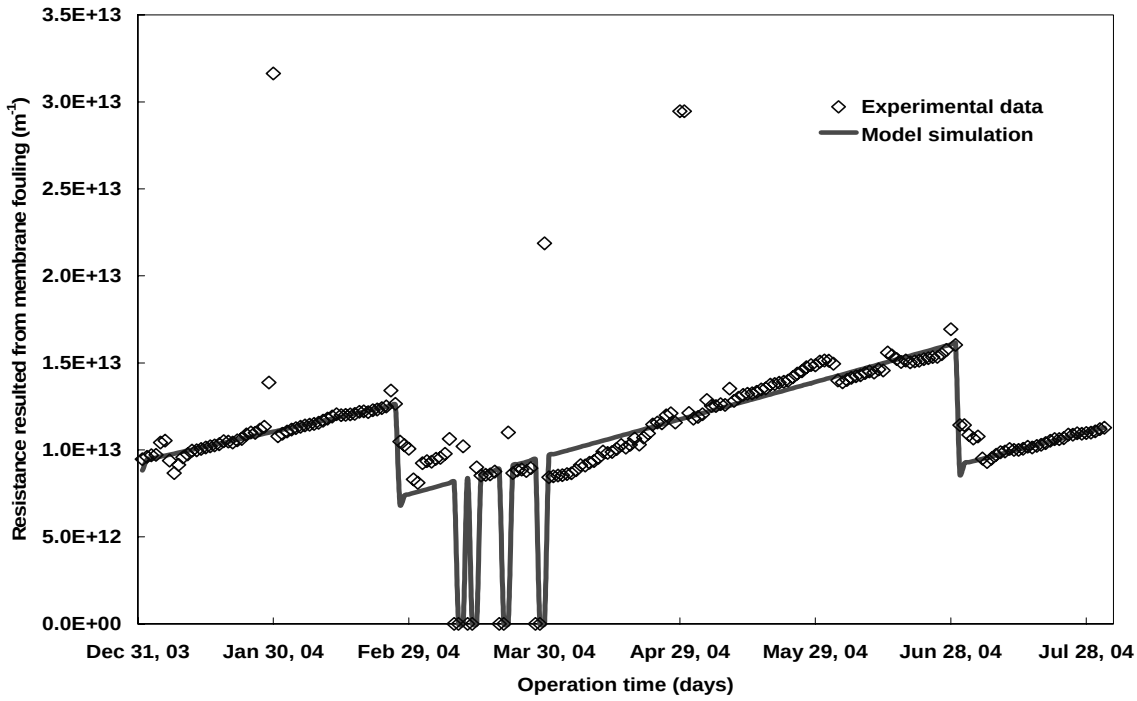

Figure 5.8 Comparison of model simulations with experimental data of filtration resistance resulted from membrane fouling (January 1 to August 1, 2004).

Finally, the comparison of the development of filtration resistance with model simulations is presented in Figure 5.8. The same set of model parameters was used in the simulation study. It is evident from Figure 5.8 that, similar to the simulation results of TMP evolution (Figure 5.7), the model outputs successfully capture all the trends of the development of filtration resistance resulting from membrane fouling with merely one single set of parameters, except for a few irregular points.

5.3 Concluding Remarks

A mathematic model was developed in this chapter for membrane fouling in submerged MBR systems for wastewater treatment, in which both reversible and irreversible fouling were quantified. While the particulate MLSS are mainly responsible for reversible fouling, the DOM is speculated as the key contributor to irreversible fouling. Analytical expressions for both permeate flux and TMP are obtained for prediction of fouling behaviors in MBR systems with constant pressure or constant flux operation modes, respectively.

The MLSS concentration (X_T) and DOM concentration (C_{MBR}) are measured in MBR systems or can be calculated with activated sludge models for predictions. The specific resistance of reversible fouling layer (σ) can be determined experimentally. While the fouling related parameters, detachment coefficient (k_r), and fouling strength factor (k_i), can be determined from a short period of testing data of the pilot MBR system with the curve fitting technique.

The validity of the model was verified by comparing theoretical predictions with the independent operational data of the pilot submerged MBR system that was not used

for parameter identification. The good agreement between theoretical predictions and operational data indicates that membrane fouling in the MBR system could be well described by the model. In addition, the steady values of the specific resistance of the reversible fouling layer, detachment coefficient, and fouling strength factor over the entire operational period revealed that fouling properties maintained consistency, regardless of regular membrane cleaning or unexpected interruptions. However, it should be noted that that fouling properties in an MBR system might change with altered operating conditions, such as variations in aeration intensity, hydraulic retention time, and sludge retention time.

CHAPTER 6

CHARACTERISTICS AND BEHAVIORS OF DOM AT DIFFERENT SRTS

In the previous chapter, it is clearly demonstrated that the fouling potential of DOM is greatly affected by its characteristics and composition. The majority of DOM in the MBR systems had a molecular weight smaller than 3 kDa and was hydrophobic in nature. The AHS and HiN were identified to be the components of DOM having higher fouling potential and inducing mainly irreversible fouling. However, it is reasonable to believe that the characteristics and fouling potential of DOM would be significantly affected by operating conditions such as SRT, which has not been seriously investigated so far. It is noteworthy that, unlike the situation in conventional biological treatment systems, the amount and nature of DOM in MBR systems are not only determined by the biodegradation process but also affected by the membrane filtration process.

The primary objective of this chapter is, therefore, to investigate the characteristics and behaviors of DOM during MBR operation. Experiments were conducted in a lab-scale submerged MBR system treating readily biodegradable synthetic wastewater at different SRTs. The concentration, composition, and fouling potential of DOM were measured both in the MBR and in the effluent. The data presented here were based on the observations obtained in each experimental phase after the MBR reached steady-state. The steady-state, herein, referred to the experimental period approximately after two SRTs when the concentrations of both activated sludge and DOM were generally stable. The error bars in all Figures indicate the sample standard deviations determined from replicate measurements. The results would provide new insights into the characteristics and behaviors of DOM in MBR systems at different SRTs, and would consequently lead to a better understanding of the role of DOM during MBR operation.

6.1 Overall Performance of MBR System

The overall performance of the MBR in terms of COD and NH_4^+-N removal at different SRTs is summarized in Figure 6.1. The COD removal efficiency was excellent and stable with an average over 95% at all investigated SRTs. Our results are generally consistent with those reported in the literature (Huang et al., 2001; Lee et al., 2003). It has been reported that membrane separation plays an important role in maintaining satisfactory organic removal of MBR systems. With respect to NH_4^+-N, average removal efficiency was maintained over 90% even at short SRTs. The high nitrification rate achieved by the MBR can be attributed to the effective membrane retention of slow-growing nitrifying microorganisms, which cannot be fulfilled by gravity clarification in conventional biological treatment systems (Chang et al., 2002).

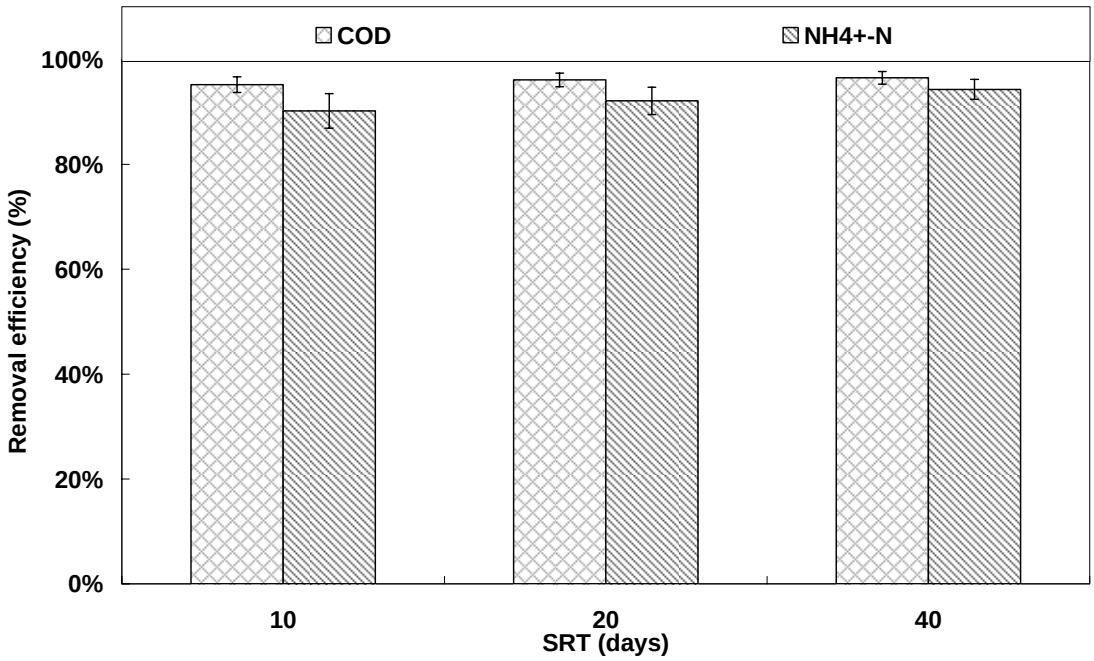

Figure 6.1 COD and NH_4^+-N removal efficiencies of MBR at different SRTs (number of measurements: *n* = 25).

Table 6.1 shows sludge concentrations and properties in the MBR system at different SRTs. It can be seen that, as SRT shortened, the average MLSS concentration decreased accordingly from 7.82 g/L at SRT of 40 days to 3.07 g/L at SRT of 10 days. However, the ratios of VSS/SS were very high with average value over 0.96 and almost independent of SRT. This indicates no considerable accumulation of inorganic matter in the MBR system. On the other hand, it was noted that the metabolic activity of sludge, characterized by SOUR, slightly decreased as SRT lengthened. This can be attributed to the increase of inert biomass (i.e., metabolic products mainly form endogenous respiration) at long SRTs and possibly to the potential inhibition effect of soluble microbial products as observed by Huang et al (2000). Nevertheless, as shown in Figure 6.1, the reduction of specific respiration rates of activated sludge had no significant effect on the general performance of the MBR system.

Table 6.1 Biomass concentration and metabolic activity at different SRTs[a]

Parameters	SRT		
	10 days	20 days	40 days
MLSS (g/L)	3.07±1.28	4.98±1.16	7.82±1.22
VSS/SS (%)	97.1±2.3	97.2±1.9	96.3±3.2
SOUR (mgO_2/gVSS h)	13.95±2.05	11.23±1.58	9.58±1.57

[a]Sample mean ± standard deviation, number of measurements: n = 25 (MLSS and VSS/SS); n = 18 (SOUR).

6.2 Concentration of DOM at different SRTs

Figure 6.2 shows total concentrations of DOM, indicated by DOC, in the MBR and in the effluent at different SRTs. It was noted that the concentration of DOM in the MBR significantly increased as SRT shortened, implying that the potential effect of DOM on system performances (e.g., membrane fouling) might be more striking at short SRTs. In comparison, the concentration of DOM in the effluent was relatively stable with merely slight increases at short SRTs. Furthermore, it was found that the concentration of DOM in the MBR was always higher than that in the effluent. This means that a certain portion of DOM was retained by the membrane, and thus accumulated in the MBR system. DOM accumulation in MBR systems has also been observed by Huang et al (2001). It was suggested that the accumulated DOM would be inhibitory to the metabolic activity of activated sludge and would also exert negative impact on membrane permeability due to organic fouling.

As an interesting and complicated phenomenon, DOM accumulation in MBR systems is fundamentally determined by the characteristics of DOM and the properties of membranes. Although it is usually attributed to the sieving effect (size exclusion) of the membranes (Huang et al. 2000; Shin and Kang, 2003), no experimental evidence

has been shown so far. To our knowledge, there has been no in-depth study aimed at elucidating the underlying mechanisms governing DOM accumulation in MBR systems. This issue is further addressed in the next chapter, where a new mechanism (i.e., retarded transport of DOM through porous membranes) is postulated for a better understanding of DOM accumulation in MBR systems.

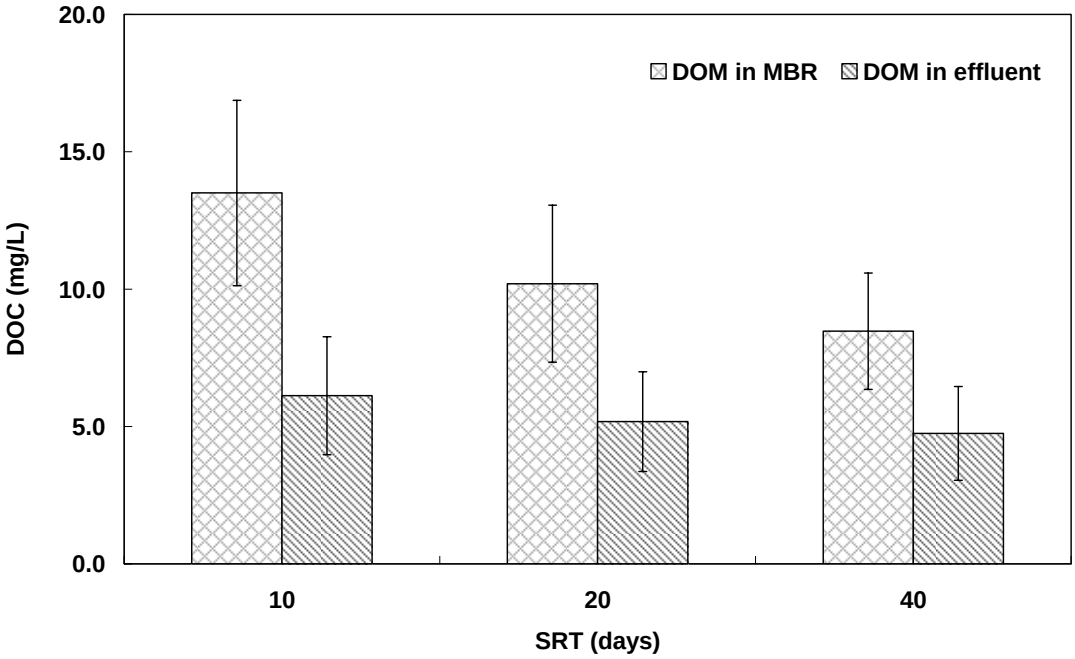

Figure 6.2 Concentrations of DOM in the MBR and in the effluent at different sludge retention times (number of measurements: n = 26).

Figure 6.3 shows the ratio of DOM concentration in the effluent to that in the MBR (C_e/C_{MBR}) at different SRTs. The higher the ratio is, the less the DOM accumulates. It can be seen that DOM accumulation was more salient at short SRTs. The normalized effluent DOM concentration, C_e/C_{MBR}, can be linearly correlated to SRT with the following equation:

$$C_e/C_{MBR} = 0.003\theta_s + 0.427 \quad (6.1)$$

where θ_s is the sludge retention time. The regression coefficient, R^2, is equal to 0.96. Since the same type of membrane was used through the entire experimental period,

the extent of DOM accumulation is primarily determined by the characteristics of DOM. It appears that DOM generated at short SRTs is more prone to accumulate in the MBR system.

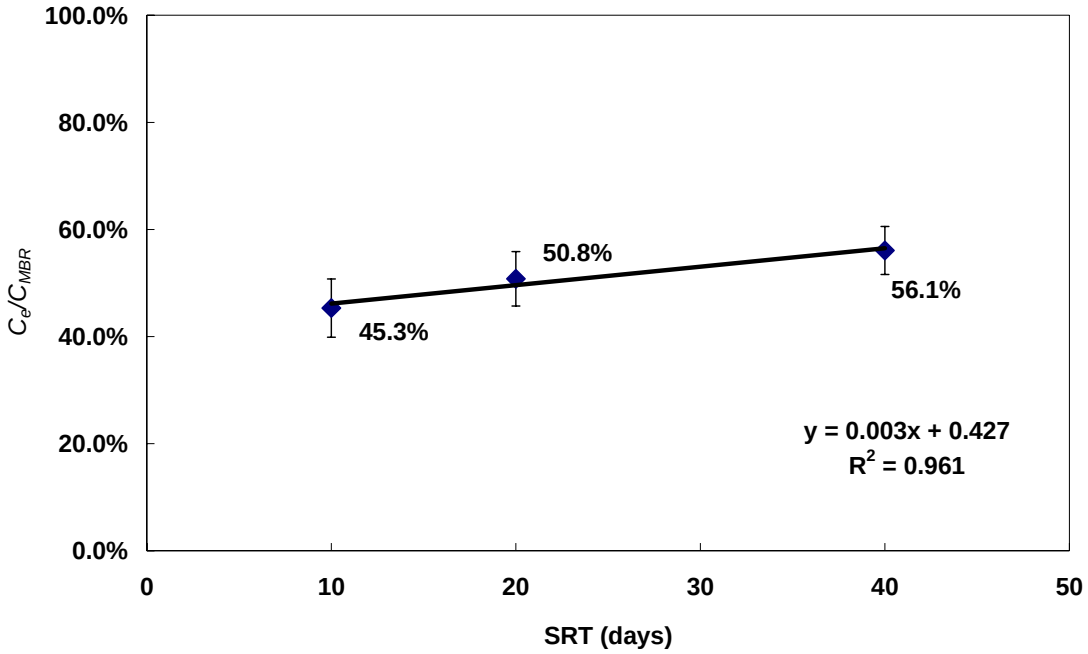

Figure 6.3 Relationship between C_e/C_{MBR} and SRT.

6.3 Composition of DOM at different SRTs

It is well known that DOM represents a myriad of structurally complex organics with distinctly different characteristics. In addition to measuring the gross concentration of DOM, the concentrations of carbohydrate and protein, the known components of DOM, were examined in order to get more detailed insights into the composition of DOM at different SRTs. As shown in Figure 6.4 and Figure 6.5, concentrations of both carbohydrate and protein varied with SRT following the trend quite similar to that observed for the concentration of total DOM. It can be, therefore, inferred that the proportions of both carbohydrate and protein in total DOM maintain approximately the same at different SRTs. Furthermore, similar to the case of total DOM

concentration, concentrations of both carbohydrate and protein in the MBR were found to be always higher than those in the effluent. This indicates that carbohydrates and proteins are the components of DOM accumulating in the MBR.

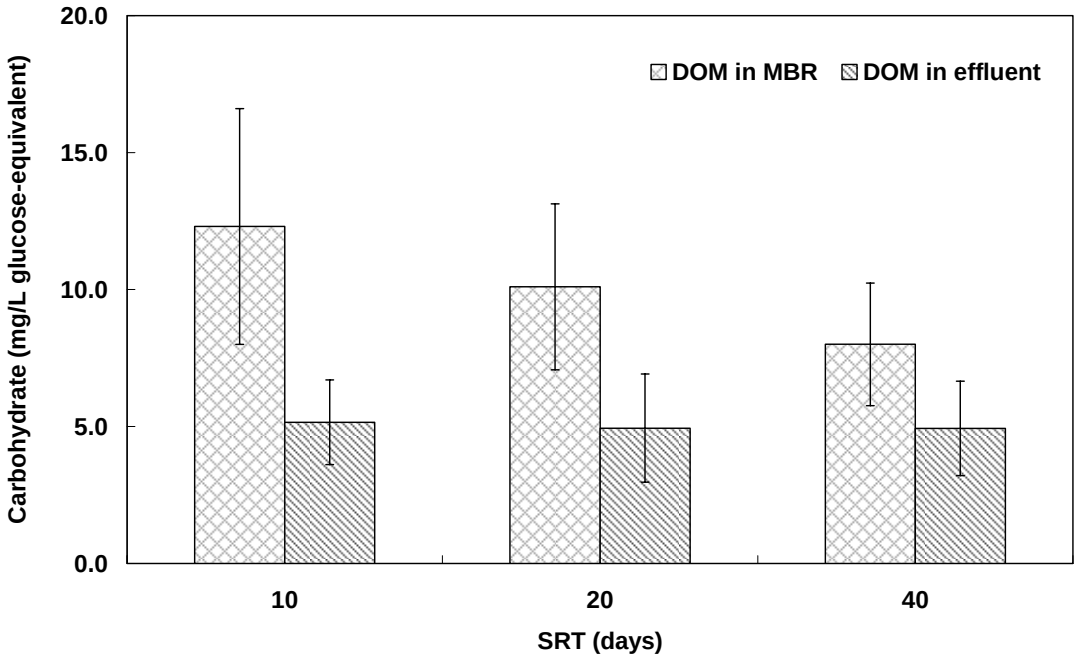

Figure 6.4 Concentrations of carbohydrate in the MBR and in the effluent at different sludge retention times (number of measurements: *n* = 25).

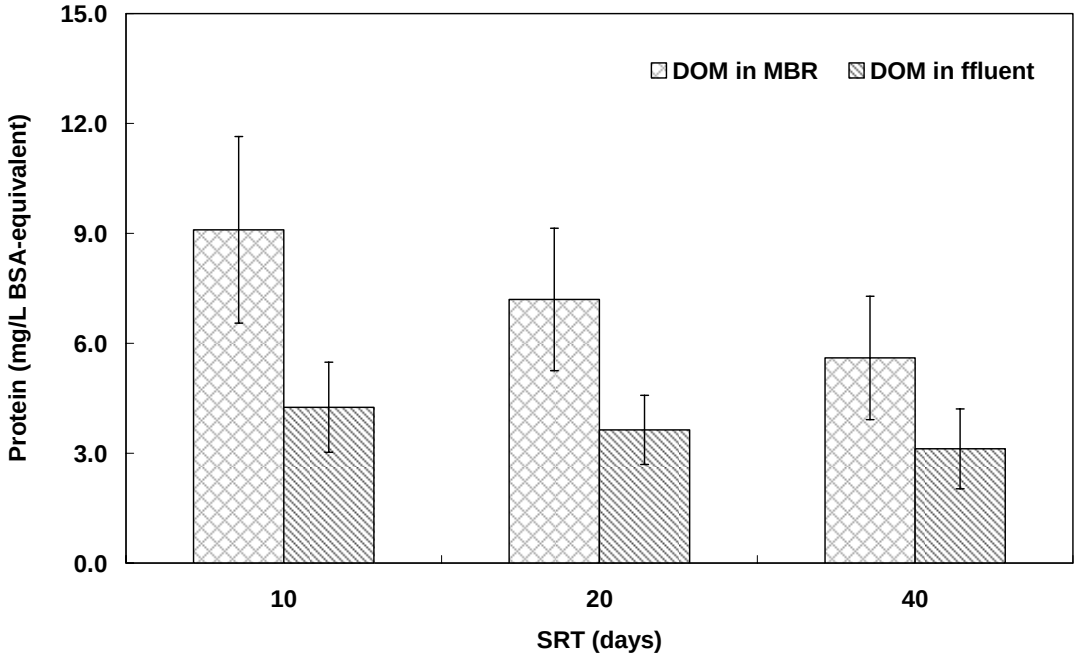

Figure 6.5 Concentrations of protein in the MBR and in the effluent at different sludge retention times (number of measurements: *n* = 25).

On the other hand, the aromaticity of DOM in the MBR and in the effluent was measured at different SRTs. The results are presented in Figure 6.6. It was interestingly noted that the SUVA value decreased as SRT shortened, though the total DOM concentration was higher at short SRTs. Lee et al. (2003) also observed the decrease of SUVA value of MBR supernatant as SRT shortened from 40 to 20 days. This implies that the DOM generated at short SRTs contains smaller percentage of aromatic compounds. It appears that production of aromatic DOM components is more favored at long SRTs where the food-to-microorganism ratio is low. Furthermore, it was found that DOM in the effluent exhibited higher SUVA values than that in the MBR. This means that the percentage of aromatic compounds in DOM increased after passing through the membrane. It is therefore inferred that, unlike carbohydrates and proteins, aromatic DOM seem much less prone to accumulate in the MBR.

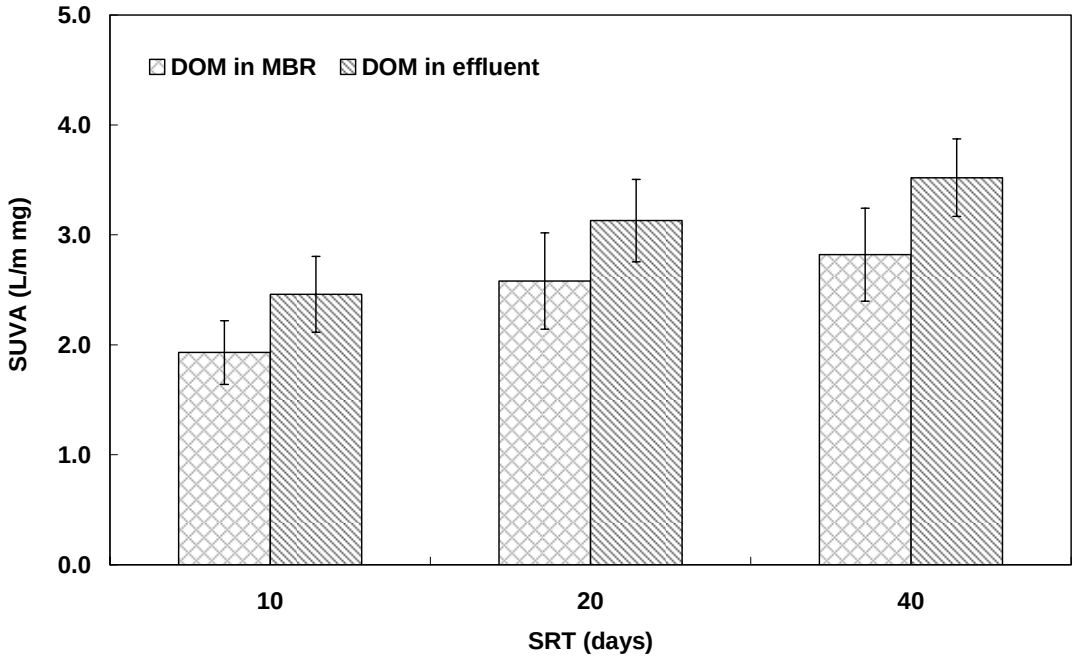

Figure 6.6 SUVA values of DOM in the MBR and in the effluent at different sludge retention times (number of measurements: *n* = 26).

6.4 Molecular Size of DOM at different SRTs

Figure 6.7 shows the apparent molecular weight distributions (AMWD) of DOM in the MBR and in the effluent at different SRTs. It can be seen that DOM in the MBR systems had a broad spectrum of molecular weight. The majority of DOM, accounting for around 57%, had molecular weight of less than 3 kDa, whereas the components with high molecule weights (> 30 kDa) formed the second largest fraction, constituting 23-32% of DOM. Each of the two fractions with molecule weights in the range between 3 kDa and 30 kDa, however, only represented a very small amount of DOM. It is noteworthy that the results shown here are well consistent with the previous finding that the DOM in MBR systems for readily biodegradable synthetic wastewater treatment has a smaller fraction of small molecules but larger fractions of large molecules.

In addition, it was noted that AMWD of DOM were quite similar at each SRT, even though the concentrations of DOM were significantly different. The results are somewhat inconsistent with those reported in conventional biological treatment systems where the AMWD of DOM have been found to be greatly affected by SRT with high molecular weight components becoming more evident at long SRTs (Barker and Stuckey, 1999). It is clear that the findings with respect to DOM in conventional biological treatment systems are not directly applicable to the case of MBR systems. Moreover, it was found that AMWD of DOM in the MBR and in the effluent were almost identical at all investigated SRTs. This indicates that membrane sieving does not work for the majority of DOM. It is therefore inferred that DOM accumulates in the MBR system based not mainly on their molecular size but on other characteristics.

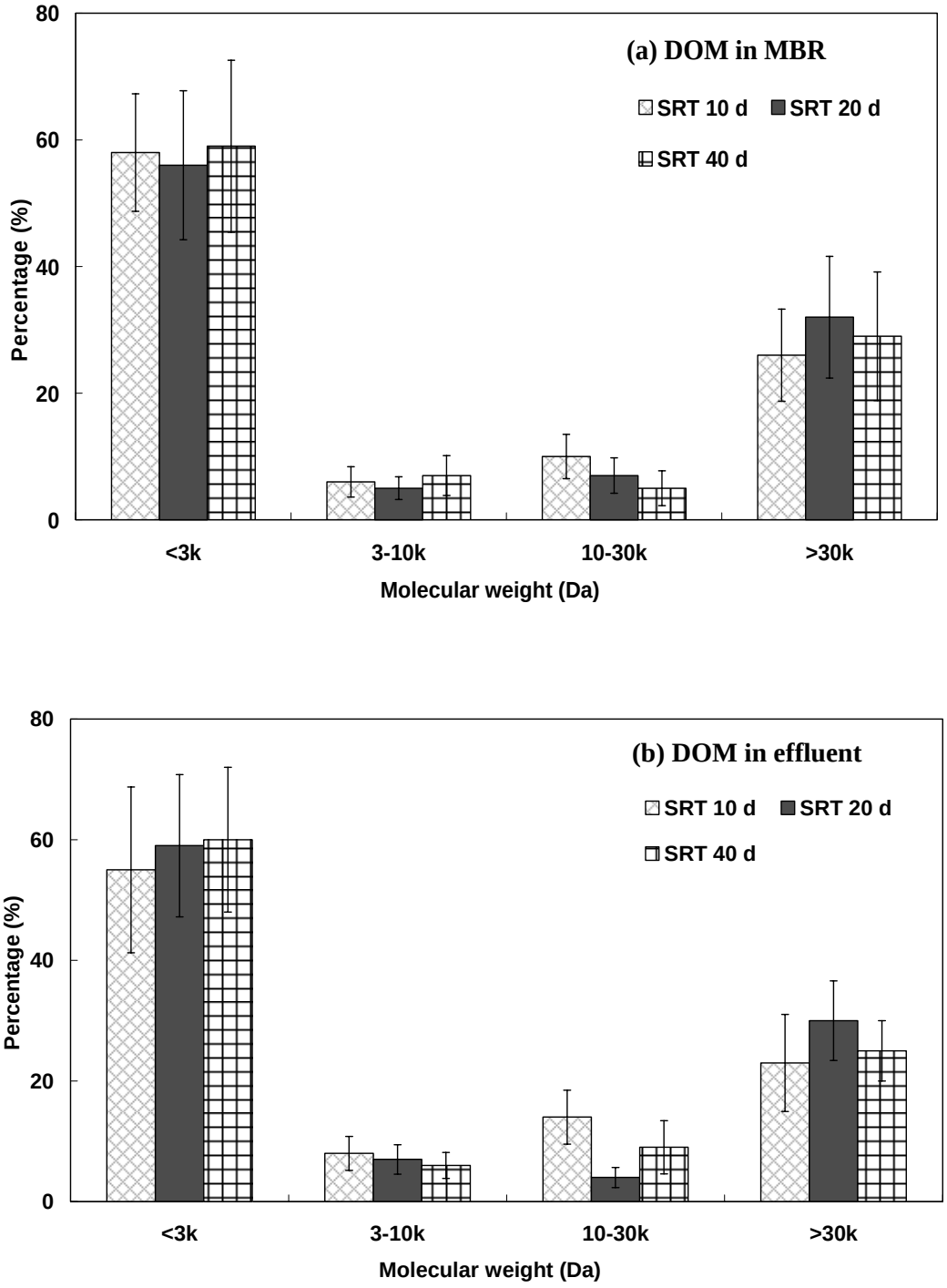

Figure 6.7 AMWD of DOM at different sludge retention times (a) AMWD of DOM in the MBR; (b) AMWD of DOM in the effluent (number of measurements: n = 15).

6.5 Hydrophobic/hydrophilic and Charge Properties of DOM at different SRTs

Apart from molecular size, hydrophobic/hydrophilic and charge properties of DOM are of particular interest in studying the filtration behaviors and accumulation of DOM in MBR systems. It has been well accepted that hydrophobic/hydrophilic and charge properties of DOM have great effects on their interactions with membranes (Carroll et al., 2000; Fan et al., 2001). The DOM fractionation results according to these two characteristics are shown in Figure 6.8. It can be seen that hydrophobic AHS were the most abundant fraction of DOM, though their proportion significantly varied at different SRTs. This implies that DOM in MBR systems is mainly composed of hydrophobic components, probably humic and fulvic acids. The results obtained here are well consistent with those presented in the previous chapter regarding DOM in the pilot MBR systems. In addition, it was noted that the proportion of AHS in total DOM gradually increased as SRT lengthened, suggesting that DOM generated at long SRTs tend to be more hydrophobic.

The distributions of hydrophilic components, on the other hand, were quite complex. As shown in Figure 6.8(a), neutral components constitute the major fraction of hydrophilic DOM in the MBR, especially at short SRTs. However, the proportion of HiN in total DOM decreased significantly as SRT lengthened. In contrast, proportions of HiA and HiB were relatively stable and independent of SRT. Since most MBR systems are operated at long SRTs in the real world, the distributions of hydrophilic components at SRTs of 20 days and 40 days may be closer to the real case.

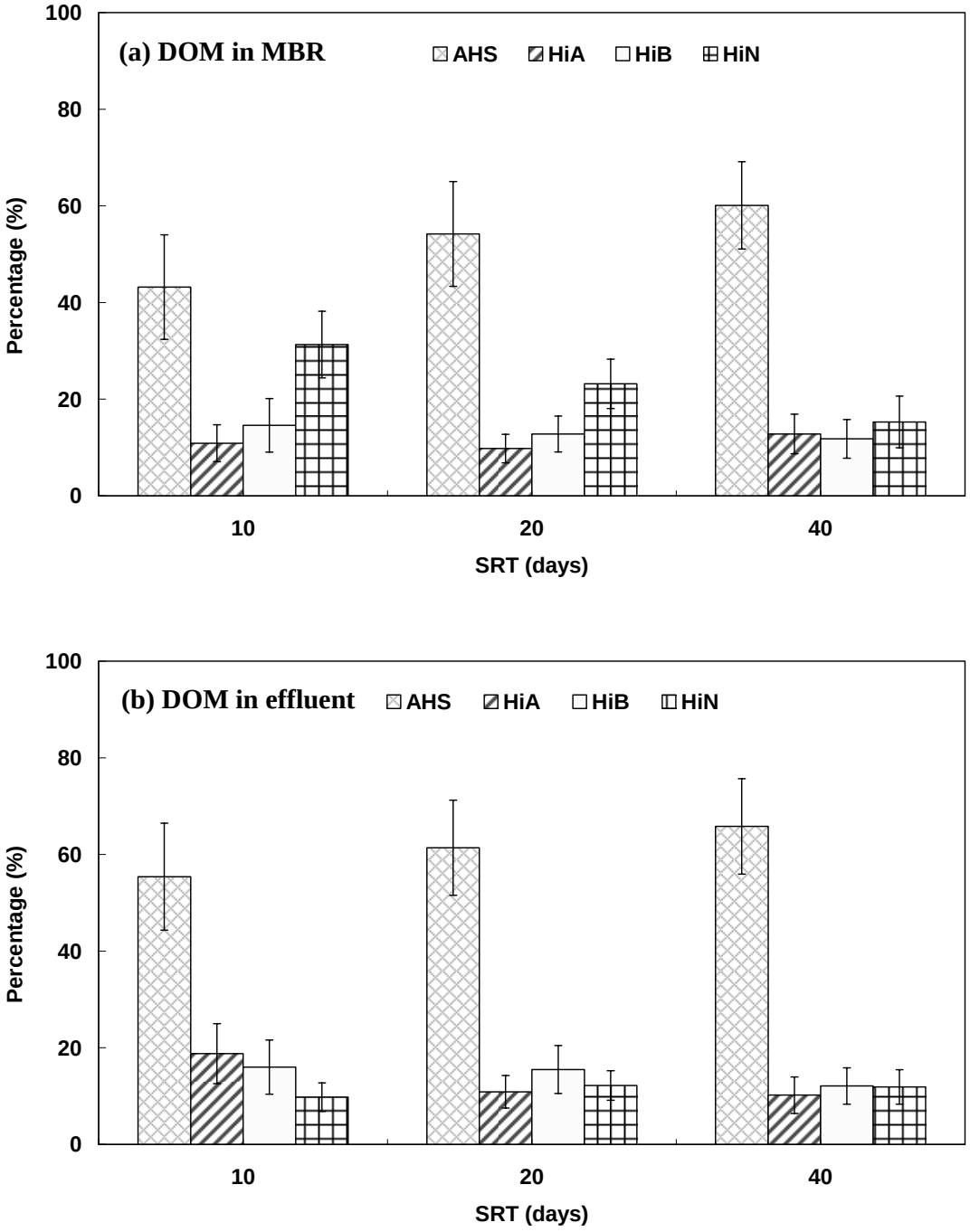

Figure 6.8 Hydrophobicity and charge property of DOM at different sludge retention times: (a) Hydrophobicity and charge property of DOM in the MBR; (b) Hydrophobicity and charge property of DOM in the effluent (number of measurements: *n* = 13).

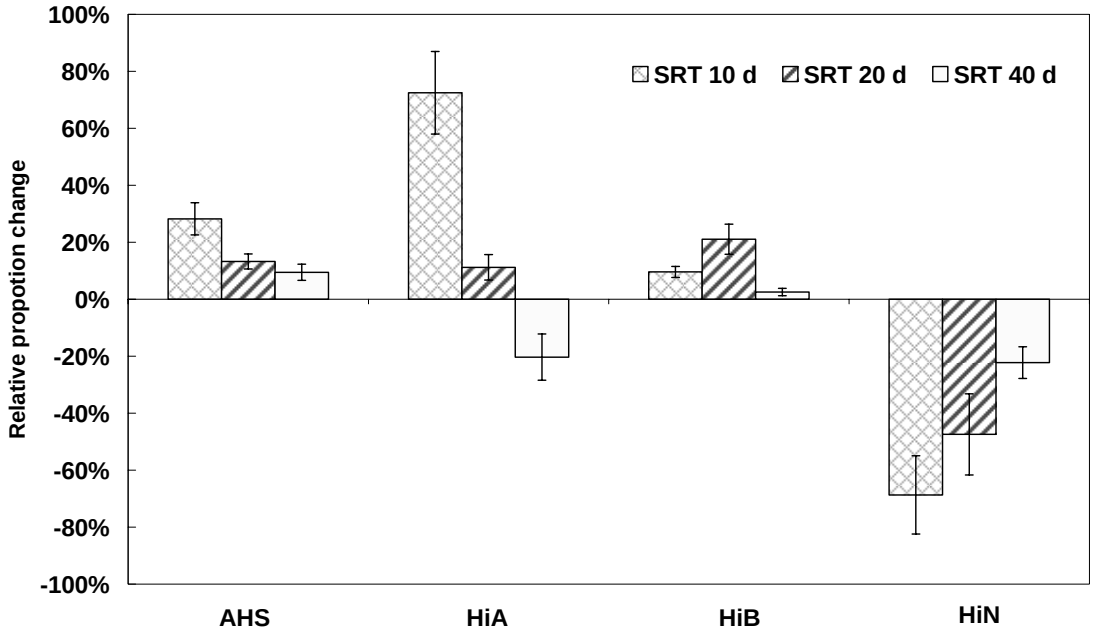

Figure 6.9 Relative proportion change of different fractional DOM components after passing through membrane at different sludge retention times (number of measurements: *n* = 13).

It was noted from Figure 6.8 that, unlike the AMWD of DOM, the proportions of different fractional DOM components significantly changed after passing through the membrane. This means that hydrophobic/hydrophilic and charge properties are two important characteristics greatly affected DOM accumulation in the MBR systems. The relative proportion change (RPC) of each fractional component can be quantified as follows:

$$RPC = \frac{P_{Effluent} - P_{MBR}}{P_{MBR}} \times 100\% \qquad (6.2)$$

where $P_{Effluent}$ and P_{MBR} are the proportion of certain fractional DOM component in the effluent and in the MBR, respectively. As shown in Figure 6.9, the proportion of fractional DOM component, except HiN, generally increased after passing through the membrane. This suggests that HiN are more prone to accumulate in the MBR than other fractional DOM components. It can be inferred that HiN may have relatively

high affinity to membranes and thus low transport rate through membranes. The high affinity of HiN to membranes may be attributed to their low aromaticity. It is generally believed that aromatic compounds are less attracted to hydrophilic membrane surface (Mulder, 1996; Schäfer, 2001). Nevertheless, a more detailed chemical identification of the HiN components is necessary for a more fundamental understanding of their interactions with membranes.

6.6 Fouling Potential of DOM at different SRTs

The fouling potentials of DOM at different SRTs were examined at an equivalent DOC concentration of 5 mg/L to eliminate the concentration effect on experimental results. As shown in Figure 6.10, the fouling potential of DOM considerably increased as SRT shortened. The differences in fouling potential are supposed to originate from the different characteristics of DOM at different SRTs. Although DOM generated at different SRTs had similar AMWD, it was noted that the hydrophobic/hydrophilic and charge properties of DOM varied significantly with SRT. In particular, DOM generated at short SRTs was found to have high proportions of HiN. It is therefore inferred that HiN are most likely the key foulants of DOM responsible for the high fouling potentials of DOM at short SRTs. It should be noted that, in the real case, fouling potentials of DOM at short SRTs would be even higher than those at long SRTs due to its high concentration.

On the other hand, fouling potentials of DOM in the effluent were found to be lower than those in the MBR to a certain extent, especially at short SRTs. This indicates that organic compounds prone to accumulate in the MBR are the major components of DOM responsible for membrane fouling. It is thus inferred that carbohydrates and

proteins may possess relatively high fouling potential. The dominance of carbohydrates and proteins in membrane foulants were also reported in a recent pilot-scale MBR study (Kimura et al., 2005). It is therefore suggested that MBR systems should be operated at long SRTs to minimize the amount of carbohydrates and proteins for DOM fouling control.

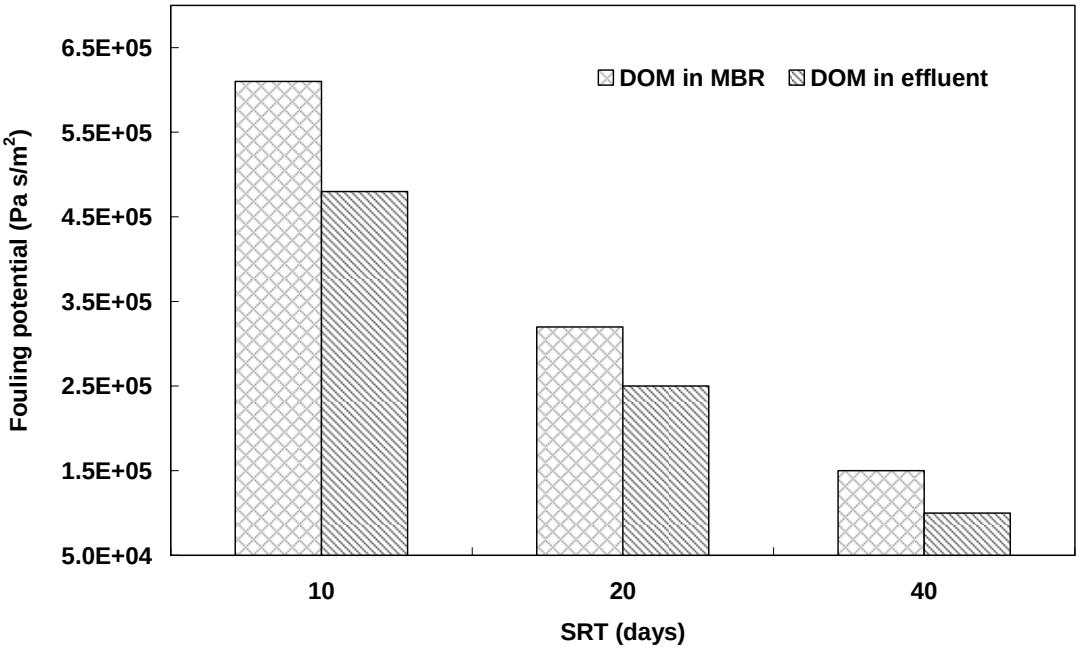

Figure 6.10 Fouling potential of DOM in the MBR and in the effluent at different sludge retention times.

6.7 Concluding Remarks

The research presented here focused on the behaviors, characteristics, and fouling potential of DOM in MBR operation at different SRTs. The following specific conclusions were drawn:

(1) The concentration of DOM in the MBR was always higher than that in the effluent. DOM accumulation in the MBR was more pronounced at short SRTs. Carbohydrates and proteins appeared to be the components of DOM prone to accumulate in the MBR compared with aromatic compounds.

(2) Apparent molecular weight distributions of DOM were similar at different SRTs and almost identical in the MBR and in the effluent. The results indicate that membrane sieving does not work for most DOM and consequently cannot adequately explain DOM accumulation in MBR system.

(3) The majority of DOM was found to be hydrophobic AHS, whose proportion in total DOM gradually increased as SRT lengthened. Moreover, the proportions of AHS in the MBR were found to be always lower than those in the effluent.

(4) The fouling potential of DOM considerably increased as SRT shortened. The hydrophilic neutrals (e.g., carbohydrates) were most likely the main foulants of DOM at short SRTs.

CHAPTER 7

RETARDED TRANSPORT AND ACCUMULATION OF DOM IN MBR SYSTEMS

With the employment of membranes for solid-liquid separation, the behaviors of DOM become more complicated in MBR systems. It has been observed that the membrane in MBR systems act as a barrier for some DOM components, which leads to a higher DOM concentration in the MBR than that in the effluent. This indicates that a certain portion of DOM accumulates within MBR systems. The accumulated DOM would further augment adverse effects of DOM on the MBR performance (Huang et al., 2000). To date, DOM accumulation has mainly been assumed to be a result of membrane sieving (size exclusion) (Huang et al., 2000; Ince et al., 2000; Shin and Kang, 2003). However, the sieving effect alone appears insufficient to explain DOM accumulation in many cases.

The pore sizes of microfiltration (MF) membranes commonly used in MBR systems are in the range of 0.1 — 0.4 μm with the molecular weight cut-off of around 300 kDa for a pore size of 0.1 μm. Sieving of MF membranes may not work for the majority of DOM with molecular weights much lower than 30 kDa (Pribyl et al., 1997; Barker and Stuckey, 1999). It has been assumed that the cut-off performance of MF membranes could be enhanced by the fouling layer developed on the membrane surface (Huang et al., 2000; Shin and Kang, 2003). However, it is questionable that the temporary, loose structured layer can provide a reliable and consistent barrier to the low molecular weight DOM. It is commonly accepted that separation performance is basically determined by the membrane although it can be enhanced within a small range by the accumulated cake layer on the membrane surface. Thus, the DOM generated in the MBR should be able to pass through the MF membrane with the effluent if their sizes are smaller than the pore size of the membrane.

The primary objective of this chapter is to obtain a more fundamental understanding of DOM accumulation in MBR systems. Additional MF experiments were conducted in the membrane reactor with humic acid to delineate the possible controlling mechanisms for the transport of DOM through the porous membrane. Based on the results of transport experiments, a mathematical model was developed for DOM concentrations in the MBR and in the effluent. Model simulations were performed to study the effect of various parameters on system performance and were compared with experimental observations from the lab-scale MBR. The proposed model would provide a new conceptual framework for evaluating the accumulation of DOM and the performance of MBR.

7.1 Transport Experiment with Humic Acid

It has been shown in Figure 6.7 that DOM in the effluent had the same proportion of large components as that in the MBR, which indicates membrane sieving does not work for the majority of DOM. This may be regarded as an important experimental evidence for the inadequacy of size exclusion (sieving) in the explanation of DOM accumulation in MBR systems. To further examine the role membrane sieving plays in DOM accumulation, transport experiments were conducted with commercially available humic acid (H1, 675-2, Sigma-Aldrich, Steinheim, Germany). The humic acid was composed of 39.03% C, 4.43% H, and 0.68% N with molecular weight much smaller than 30 kDa (Liu et al., 2000). The experiments were conducted in the lab-scale membrane reactor having a similar configuration with that shown in Figure 3.3, but an effective volume of 9 L. The hydraulic retention time (HRT) was maintained at 6 hours. Two runs of experiments were carried out with different feed concentrations (DOC = 18 mg/L and DOC = 38 mg/L). Each run was kept within 6 h to avoid the effect of changes in membrane pore size and humic acid properties on the results. Humic acid concentrations were measured using a DR/4000U Spectrophotometer (HACH, Loveland, CO, USA) at the wavelength of 254 nm.

As shown in Figure 7.1, the concentrations of humic acid were higher than the feed concentration in the MBR but lower than the feed concentration in the effluent. The humic acid concentrations both in the MBR and in the effluent increased linearly with time. Apparently, the accumulation of DOM in the MBR cannot be sufficiently explained by the sieving mechanism of the MF membrane because the molecular size (i.e., <10 nm) of the model compounds used here was much smaller than the pore size (i.e., 0.45 μm) of the MF membrane.

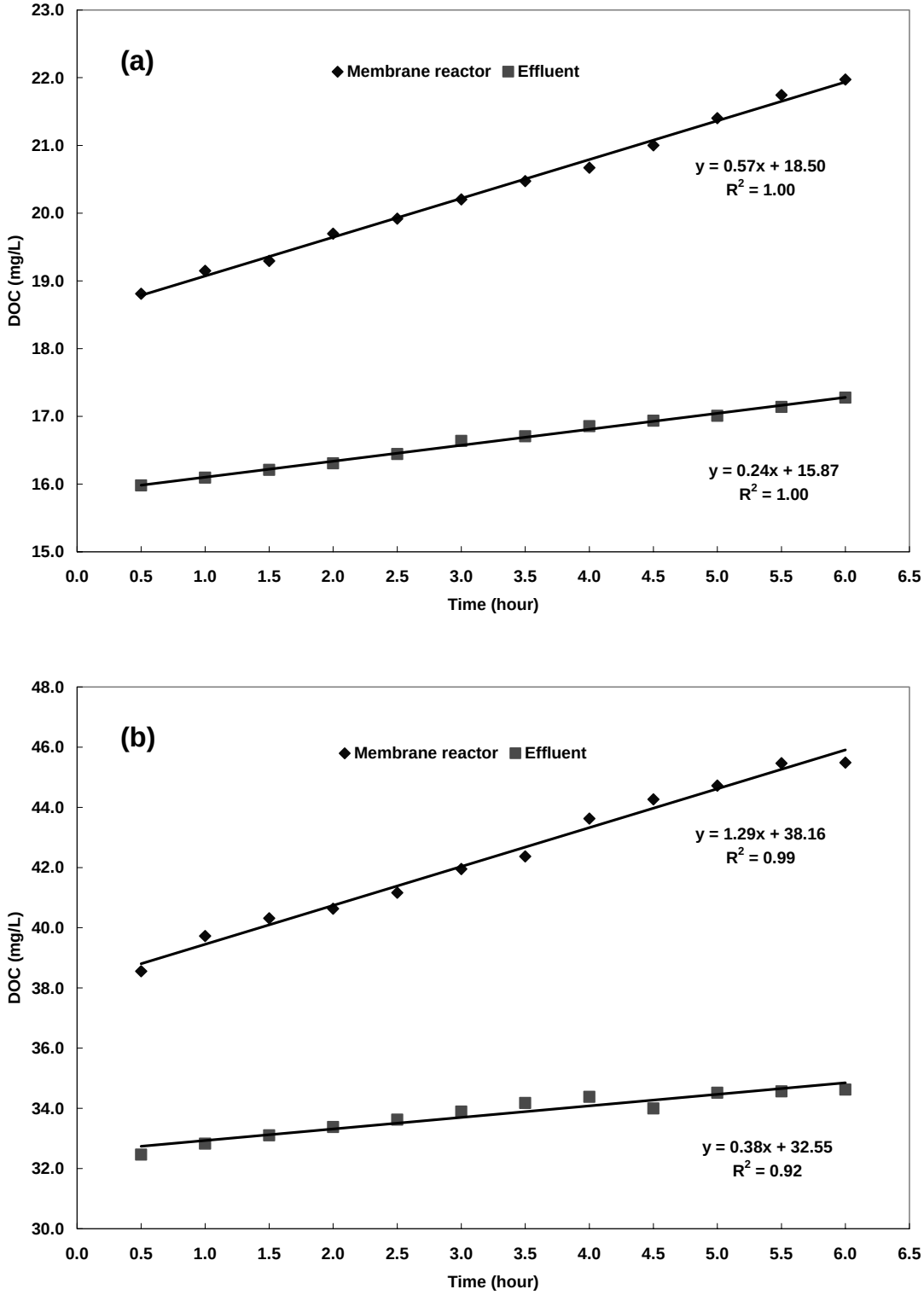

Figure 7.1 Variation of humic acid concentrations in the MBR and in the effluent with operational time (a) DOC = 18 mg/L; and (b) DOC = 38 mg/L.

Since size exclusion of the MF membrane has no significant effect on the transport of DOM through the membrane, there must be other mechanisms rather than sieving that are responsible for the accumulation of DOM in the MBR. In this chapter, the retarded transport of DOM through porous membranes was postulated as a new mechanism for the elevated DOM concentrations in the MBR. Although DOM can pass through the membrane, its velocity is slower than that of water. The slower velocity of DOM leads to lower DOM concentration in the effluent and higher DOM concentration in the MBR.

7.2 DOM Transport Mechanisms through Porous Membranes

Although MF membrane is commonly employed for separating suspended solids from liquid by a sieving mechanism (size exclusion), it can also serve as a barrier to various dissolved species due to their different mobility in the membrane material. The latter can be explained by the retarded transport through a porous medium (Roberts et al., 1986; Deen, 1987). As illustrated in Figure 7.2, water can pass through the membrane easily. However, due to higher affinity of DOM (organic) to membrane material (organic), the convection velocity of DOM can be much slower than that of water. As a result, a greater DOM concentration gradient can be built up across the membrane, which in turn induces dispersion of DOM across the membrane.

7.2.1 Retarded Convection

A viscous flow is generated across the porous membrane under a driving pressure. The convection of DOM in the viscous flow is a major mechanism for DOM transport. However, the velocity of DOM is usually slower than that of water due to the higher affinity of DOM to the membrane material. This phenomenon can be described by

the principle of retarded convection through a porous medium (Krupp et al., 1972; Roberts et al., 1986; Domenico and Schwartz, 1997; Bedient et al., 1999). The retarded convection of DOM through a porous membrane can be related to the water velocity by a retardation coefficient:

$$v_D = \alpha v_w \tag{7.1}$$

where v_D is the velocity of DOM, v_w is the velocity of water, and α is the DOM retardation coefficient. The value of the DOM retardation coefficient α is dependent on the characteristics of DOM and the properties of membrane material.

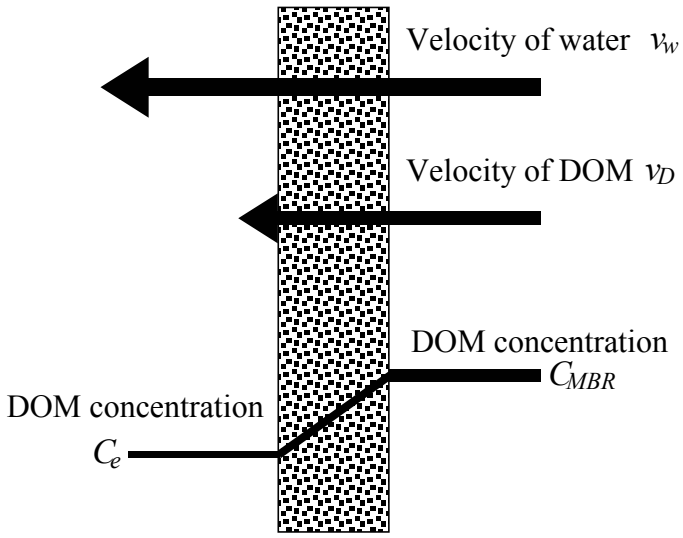

Figure 7.2 Transport of water and DOM through a porous membrane (The arrow length indicates the velocity).

7.2.2 Dispersion

Dispersion is another transport mechanism for DOM through the membrane as long as there is a concentration gradient across the membrane. It is actually a mixing process due to the different paths of DOM passing through a porous membrane. The effect of dispersion on DOM transport is similar to that of diffusion but can be orders stronger

than diffusion and tends to dominate the spreading process when velocities are present (Dagan, 1984; Freyberg, 1986; Domenico and Schwartz, 1997; Bedient et al., 1999). The dispersion of DOM through the membrane can be described (similar to diffusion) with the dispersion coefficient as a function of flow velocity:

$$D = \beta v_w \tag{7.2}$$

where D is the dispersion coefficient, and β is the DOM dispersion factor. The value of DOM dispersion factor β varies with the properties of the membrane matrix.

7.2.3 DOM Transport Modeling

The total flux of DOM across the membrane is given by:

$$J_D = -D\frac{dC}{dx} + v_D C \tag{7.3}$$

where J_D is the DOM flux, and C is the concentration of DOM. The two terms on the right side of Eq. (7.3) are the contributions of dispersion and convection to the total DOM flux, respectively.

Rearranging Eq. (7.3) results in

$$D\frac{dC}{dx} = v_D\left(C - J_D/v_D\right) \tag{7.4}$$

Eq. (7.4) can be integrated over the thickness of the membrane, L, as follows:

$$C_e = J_D/v_D + \left(C_{MBR} - J_D/v_D\right)e^{\frac{v_D}{D}L} \tag{7.5}$$

where C_{MBR} and C_e are the DOM concentrations in the MBR and in the effluent, respectively.

The term J_D in Eq. (7.5) is an unknown that has to be determined. Considering that the DOM concentration in the effluent (C_e) is equal to J_D/v_w, one has

$$J_D = v_w C_e \tag{7.6}$$

Substituting Eq. (7.6) into Eq. (7.5) and rearranging Eq. (7.5) leads to:

$$C_e \frac{v_D}{v_w} = C_e + \left(C_{MBR} \frac{v_D}{v_w} - C_e \right) e^{\frac{v_D}{v_w} \frac{v_w}{D} L} \tag{7.7}$$

It can be seen from Eqs. (7.1) and (7.2) that $\alpha = v_D / v_w$ and $\beta = D / v_w$. Thus, Eq. (7.7) can be rewritten as:

$$C_e = C_{MBR} \frac{\alpha e^{\frac{\alpha}{\beta} L}}{\alpha + e^{\frac{\alpha}{\beta} L} - 1} \quad \left(\text{or} \quad \frac{C_e}{C_{MBR}} = \frac{\alpha e^{\frac{\alpha}{\beta} L}}{\alpha + e^{\frac{\alpha}{\beta} L} - 1} \right) \tag{7.8}$$

Eq. (7.8) clearly shows that the DOM concentration in the effluent or the ratio of DOM concentration in the effluent to that in the MBR is fully determined by the retardation coefficient α and the dispersion factor β, which characterize retardation and dispersion of DOM across the membrane.

7.3 Modeling Study of DOM Transport through Porous Membranes

The effect of dispersion factor on DOM transport through a membrane was studied by model simulations. The MBR is assumed to be operated at the steady-state with constant operating conditions (e.g., feed flow rate, substrate concentration, and composition). The loss of DOM through sludge wasting is assumed to be negligible. The normalized DOM concentration profiles C_e/C_{MBR} for different dispersion factors are presented in Figure 7.3. The retardation coefficient α, water velocity v_w, and membrane thickness L were taken as 0.1, 5.0×10^{-6} m/s, and 0.1 mm, respectively, for all simulation studies.

It can be seen from Figure 7.3 that the two concentration profiles with $\beta \leq 3.0\times10^{-6}$ (labeled as 1 and 2) converged to one line towards the effluent surface of the membrane. In particular, the normalized DOM concentration for curve 1 ($\beta = 1.0\times10^{-6}$) remained constant at 0.1 over a large portion of the membrane thickness. These observations suggest that, for a dispersion factor (β) equal to or less than 3.0×10^{-6} m/s, the DOM transport is predominantly controlled by convection. Dispersion becomes significant for DOM transport when the value of dispersion factor is greater than 3.0×10^{-6}. It is noted from Figure 7.3 that a higher dispersion factor would result in a more moderate decline of DOM concentration across the membrane thickness and a correspondingly higher effluent DOM concentration. For example, the concentration profile corresponds to $\beta = 1.0\times10^{-4}$ (labeled 5) shows a normalized effluent DOM concentration of about 0.54, which is much higher than the convection controlled normalized effluent concentration of 0.1.

The combined effect of both the retardation coefficient and the dispersion factor was simulated. Figure 7.4 shows the relationship between normalized effluent DOM concentration **(**C_e/C_{MBR}) and dispersion factor β for five different retardation coefficients. It can be seen from Figure 7.4 that the normalized effluent DOM concentration increases with increasing value of the retardation coefficient. This phenomenon can be reasonably expected, as a higher retardation coefficient indicates a lower retarded effect of the membrane on the convection of DOM. As a result, DOM can pass through the membrane more readily, which in turn leads to a higher effluent DOM concentration. The straight line (labeled 5) shown in Figure 7.4 represents the case where there is no retardation for the DOM. Under this condition,

the effluent DOM concentration is equal to the DOM concentration in the MBR and there is no DOM accumulation in the MBR.

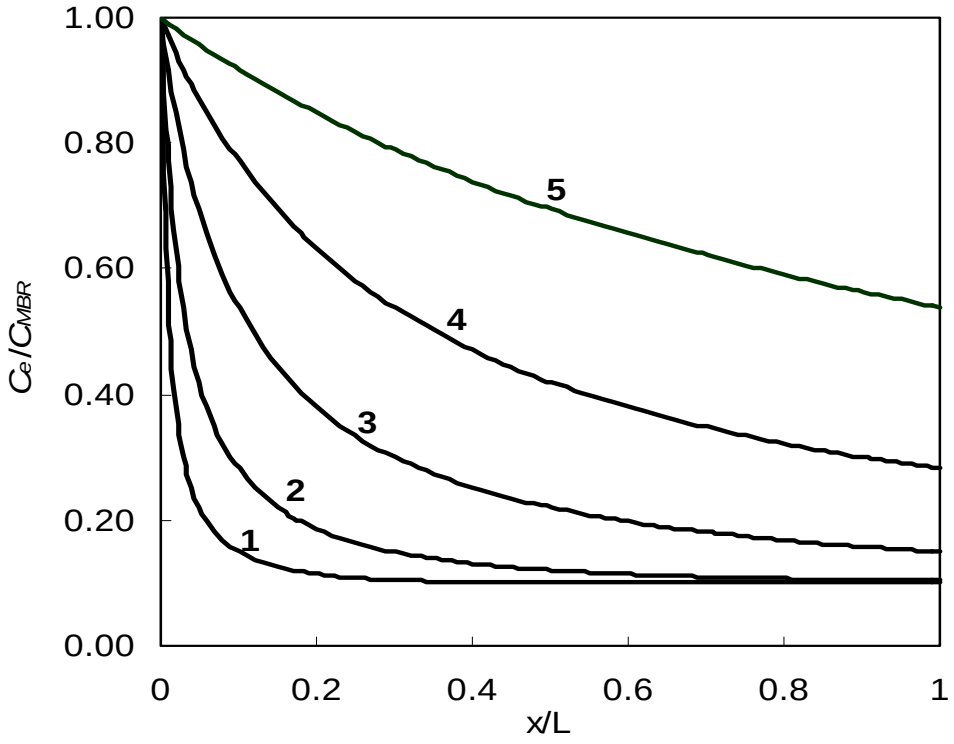

Figure 7.3 Variation of C_e/C_{MBR} along membrane thickness with different dispersion factors. 1. $\beta = 1.0\times10^{-6}$, 2. $\beta = 3.0\times10^{-6}$, 3. $\beta = 1.0\times10^{-5}$, 4. $\beta = 3.0\times10^{-5}$, 5. $\beta = 1.0\times10^{-4}$; $\alpha = 0.1$, $v_w = 5.0\times10^{-6}$ m/s, L = 0.1mm.

The significance of dispersion in DOM transport increases with a decreasing value of retardation coefficient. As shown in Figure 7.4, for a given value of β, the gradient associated with the normalized effluent DOM concentration profile increases with a decreasing value of retardation coefficient. Similarly, over a given range of β values, the normalized effluent DOM concentration increases as the retardation coefficient decreases. For example, when $\alpha = 0.5$, the normalized effluent DOM concentration increases by about 0.38 when β increases from 0 to 3.0×10^{-4}. The corresponding increment is 0.57 when $\alpha = 0.25$.

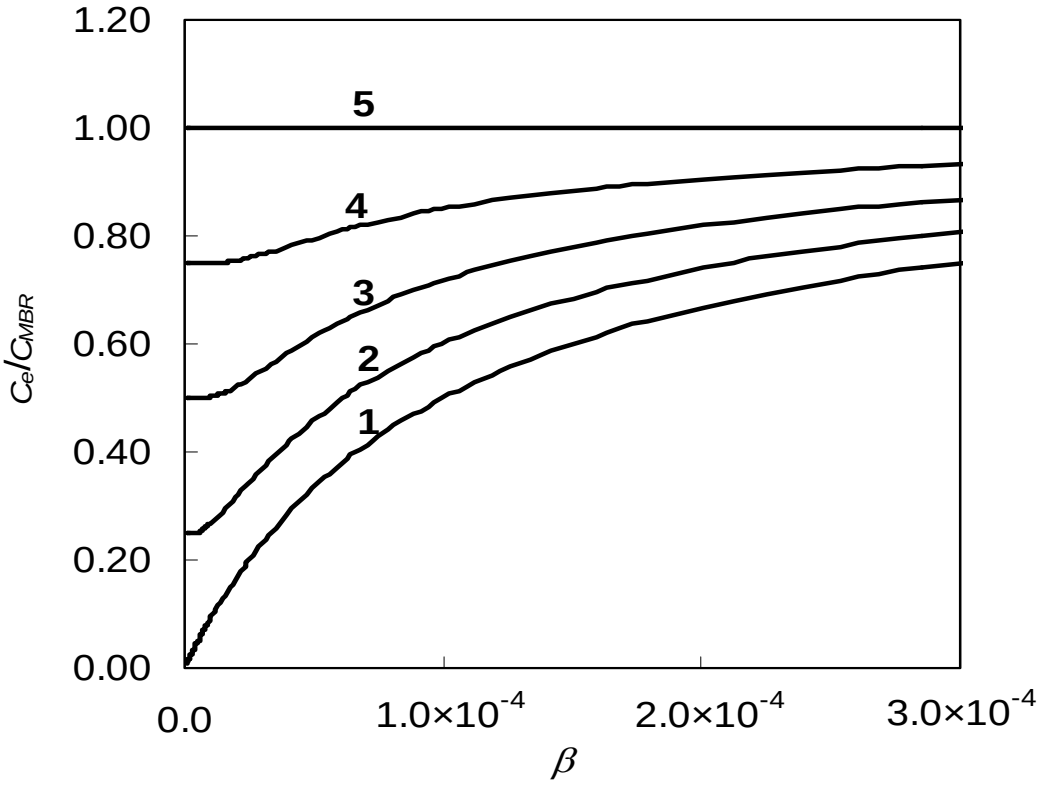

Figure 7.4 C_e/C_{MBR} **as function of** β **with different retardation coefficients. 1.**α **= 0.001; 2.** α **= 0.25; 3.** α **= 0.50; 4.** α **= 0.75; 5.** α **= 1.0;** v_w **=** 5.0×10^{-6} **m/s, L = 0.1mm.**

7.4. DOM Accumulation in MBR Systems

The synthetic wastewater used in this study was readily biodegradable. The average concentration of residual acetate in the MBR was observed to be lower than 2.5 mg/L, indicating that over 99% of the organic carbon in the feedwater was biodegraded. The concentrations of DOM in the MBR and in the effluent, therefore, can be reasonably assumed to be equal to the concentrations of soluble microbial products (SMP). SMP can be defined as the pool of organic compounds produced as a result of microbial activities (Barker and Stuckey 1999). Luedeking and Piret (1959) suggested that SMP can be classified into two categories: (a) utilization associated products that are associated with substrate metabolism and biomass growth and are produced at a rate

proportional to the rate of substrate utilization, and (b) biomass associated products that are associated with biomass decay and are produced at a rate proportional to the concentration of biomass. The rate of SMP formation is usually modeled as follows (Laspidou and Rittmann, 2002):

$$r_{SMP} = \left(k_{UAP} q + k_{BAP}\right) X_T \tag{7.9}$$

where k_{UAP} and k_{BAP} are the formation rate coefficients for utilization associated products and biomass associated products, respectively; q is the specific substrate utilization rate; and X_T is the biomass concentration.

With the knowledge of DOM transport across porous membranes, DOM concentrations in the MBR and in the effluent can be determined with the kinetics of SMP generation in the MBR. By definition, there is no SMP in the influent to an MBR system. The removal of SMP with sludge withdraw is further assumed to be negligible, because MBR systems are generally operated at long SRTs. With the mass balance principle, the governing equation for DOM (i.e., SMP) concentration in the MBR system is given by:

$$\frac{dC_{MBR}}{dt} = \left(k_{UAP} q + k_{BAP}\right) X_T - k_d C_{MBR} - \frac{C_e}{\theta} \tag{7.10}$$

where k_d is the decay rate constant of SMP, and θ (=V/Q with V and Q being the bioreactor volume and flow rate, respectively) is the hydraulic retention time. The effluent concentration of DOM can be related to the DOM concentration in the MBR with a filtration factor $C_e = fC_{MBR}$ and the value of f is given by Eq. (7.8). Eq. (7.10) can be easily solved by integrating the equation with an initial condition of C_{MBR} (0) = 0, i.e.,

$$C_{MBR}(t) = \frac{\left(k_{UAP} q + k_{BAP}\right) X_T \left(1 - e^{-ft/\theta} e^{-k_d t}\right)\theta}{f + k_d \theta} \tag{7.11}$$

Consequently, the effluent DOM concentration can be written as:

$$C_e(t) = fC_{MBR} = \frac{(k_{UAP}q + k_{BAP})X_T\left(1 - e^{-ft/\theta}e^{-k_d t}\right)f\theta}{f + k_d\theta} \tag{7.12}$$

When the system is operated at steady-state and biodegradation of SMP is negligible, DOM (i.e., SMP) concentrations in the MBR and in the effluent can be expressed as follows:

$$C_{MBR} = (k_{UAP}q + k_{BAP})X_T\theta / f \tag{7.13}$$

$$C_e = (k_{UAP}q + k_{BAP})X_T\theta \tag{7.14}$$

It is interesting to see from Eqs. (7.11) — (7.14) that, although the DOM concentration in the MBR is strongly affected by the membrane filtration factor, the steady-state effluent DOM concentration is independent of the filtration factor.

Based on Eqs. (7.13) and (7.14), DOM concentrations both in the MBR and in the effluent were simulated. The kinetic and stoichiometric parameters used in the simulations are listed in Table 7.1. The values of biomass concentration X_T and specific substrate utilization rate q were determined using the equations developed by Lawrence and McCarty (1970) based on Monod relationship as follows:

$$X_T = (\theta_s / \theta)Y(S_i - S)/(1 + b\theta_s) \tag{7.15}$$

$$q = K_{\max}S/(K_s + S) \tag{7.16}$$

$$S = \frac{K_s(1 + b\theta_s)}{\theta_s(YK_{\max} - b) - 1} \tag{7.17}$$

where Y is the true yield coefficient for substrate utilization; θ_s is the sludge retention time; S_i and S are the substrate concentrations in the influent and in the bioreactor, respectively; b is the endogenous decay rate coefficient for biomass; K_{max} is the

maximum specific substrate utilization rate; and K_s is the half-maximum rate concentration for substrate.

The substrate-related parameters K_s, K_{max}, Y, and b shown in Table 7.1 are the typical values associated with aerobic treatment (Huang et al., 2001; Rittmann and McCarty, 2001). The SMP related kinetic constants k_{UAP} and k_{BAP} were selected by the least-square method, which identifies the set of constants that best fits theoretical predictions with experimental observations. Other parameters such as influent concentration (S_i) and hydraulic retention time (θ) were obtained from the experimental data. The values adopted for the filtration factor (f) are based on Eq. (6.1) developed in the previous chapter.

Table 7.1 Values of kinetic and stoichiometric parameters

Parameter	Units	Value
K_s	gCOD/m^3	20
K_{max}	gCOD/gVSS day	16
Y	gVSS/gCOD	0.3
b	day^{-1}	0.1
k_{UAP}	gCOD/gCOD	2.4×10^{-2}
k_{BAP}	gCOD/gVSS day	1×10^{-4}
S_i	mgCOD/L	600
θ	day	0.42
θ_s	day	5-45

The model simulations of DOM concentrations both in the MBR and in the effluent are plotted with experimental measurements as shown in Figure 7.5. The experimental data of C_{MBR} and C_e were represented with triangular symbols and square symbols, respectively. The model simulations for C_{MBR} and C_e were represented with solid line and dash line, respectively. It can be seen from Figure 7.5 that the general trend of

DOM concentrations in the MBR and in the effluent can be well captured by the model. The agreement of the model simulations with the experimentally observed DOM concentrations in the MBR implies that the retarded transport of DOM through membranes can be a possible mechanism for the accumulation of DOM in MBR.

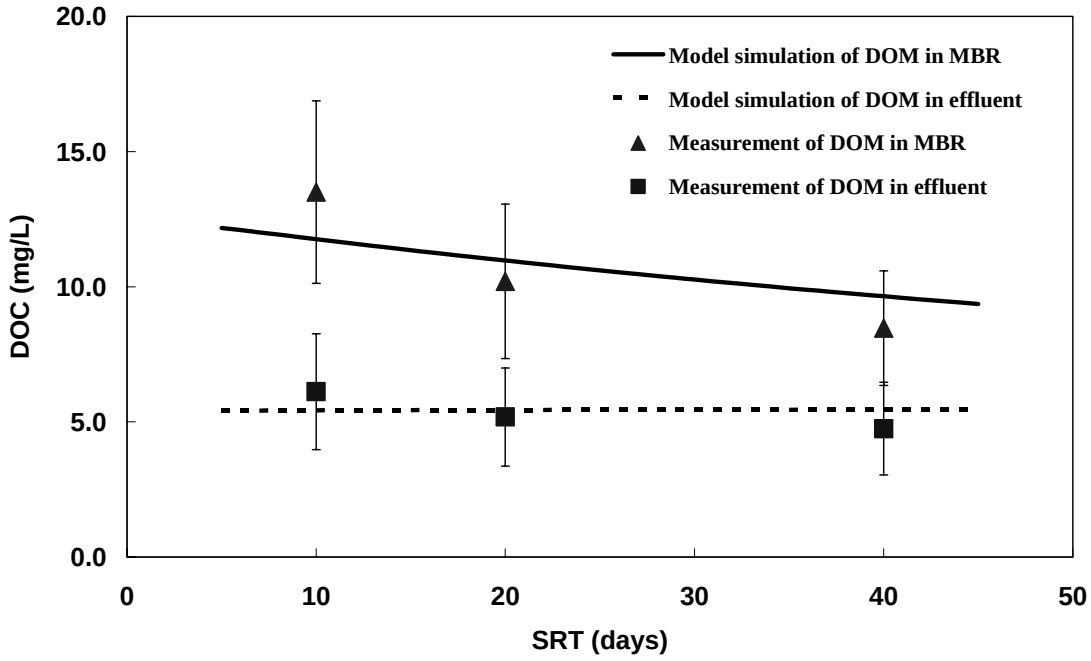

Figure 7.5 Comparison of predicted DOM concentrations in the MBR (C_{MBR}) and in the effluent (C_e) with experimental observations.

The membrane filtration factor f plays an important role with respect to DOM accumulation in MBR systems. To illustrate this phenomenon, DOM concentrations in the MBR system were simulated over a period of 10 days and plotted in Figure 7.6 for different filtration factors. It can be seen that both the DOM concentration at steady-state in the MBR and the time to reach the steady-state increase with decreasing value of membrane filtration factor. It has been demonstrated in this chapter that the filtration factor of a microfiltration membrane is fully determined by the retarded convection and dispersion of DOM in the membrane matrix.

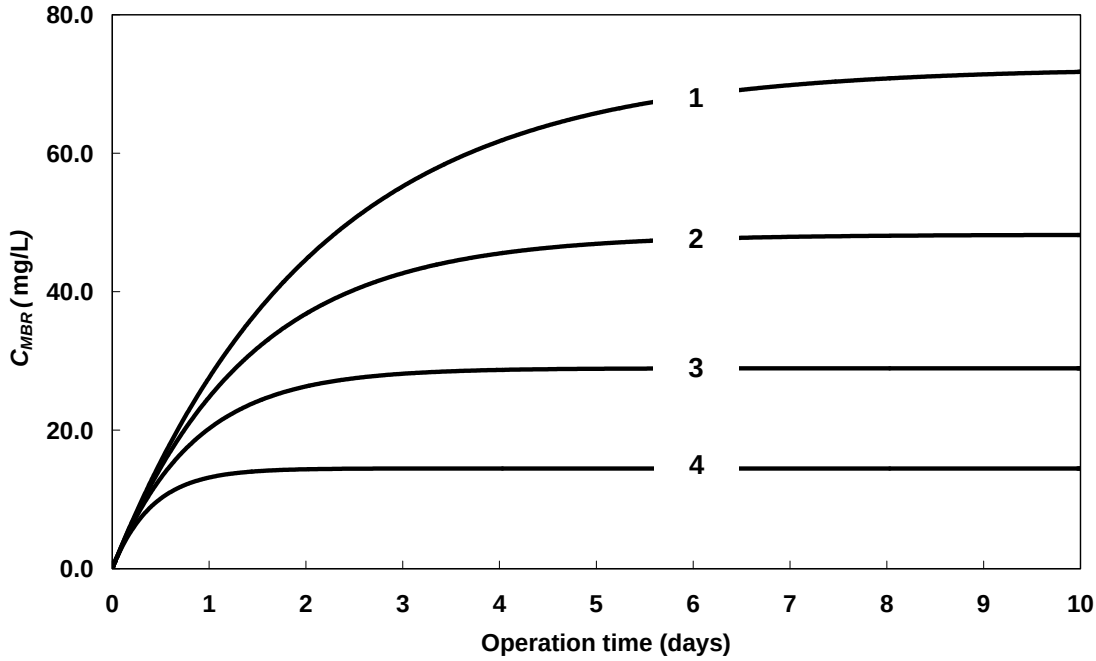

Figure 7.6 Effect of membrane filtration factor on DOM concentration profiles in the MBR at a SRT of 10 days. 1. f = 0.1, 2. f = 0.2, 3. f = 0.3, 4. f = 0.5.

7.5 Concluding Remarks

Size exclusion or sieving of a microfiltration membrane was experimentally demonstrated inadequate to explain the much higher DOM concentration in the MBR than that in the effluent. In this chapter, the transport of DOM through porous membranes was postulated as a combination of retarded convection and dispersion through a porous medium. It is reasonable to believe that the convection velocity of DOM through a porous membrane is slower than that of water because of the high affinity of DOM (organic) to membrane matrix (organic). The retarded convection velocity of the DOM tends to cause DOM accumulation inside the MBR, resulting in a higher DOM concentration in the MBR than that in the effluent. Dispersion can be another mechanism contributing to DOM transport through the porous membrane due

to the built-up of DOM concentration gradient across the membrane. Mathematical models for DOM transport through a porous membrane and DOM concentrations in the MBR and in the effluent have been developed in this study.

The agreement of the experimental observations of DOM concentrations in the MBR and in the effluent with model simulations indicates that the proposed transport mechanisms of retarded convection and dispersion of DOM through a porous membrane can be a better explanation for DOM accumulation in the MBR. The filtration factor, f, is an important parameter charactering the retarded convection and dispersion of DOM through a porous membrane. SRT may have significant effects on the value of f via affecting DOM characteristics. Moreover, it is anticipated that f could be affected by other parameters. Therefore, more experimental and theoretical investigations are needed for a better understanding of the fundamental relationship between the membrane filtration factor and operating conditions.

CHAPTER 8

SUMMARY AND FUTURE PERSPECTIVE

In this thesis, DOM fouling and accumulation in submerged MBR systems have been investigated both experimentally and theoretically. This chapter summarizes the main findings of the research work described in the previous chapters. Several future research avenues are then outlined.

8.1 Summary

Main conclusions obtained from this thesis are summarized as follows:

i) DOM in the MBR systems had a broad spectrum of molecular weight. The majority of DOM had a molecular weight of less than 3 kDa, whereas the components with high molecule weights (> 30 kDa) formed the second largest fraction. The other two fractions with molecular weights in the range of 3-10 kDa and 10-30 kDa, respectively, only represented a very small amount of

DOM. In addition, it was noted that the DOM in the MBR systems treating readily biodegradable synthetic wastewater tends to have a smaller fraction of small molecules but larger fractions of intermediate and large molecules. The apparent molecular weight distributions of DOM were quite similar at different SRTs, even though the concentration of DOM varied significantly.

ii) The fractionation results revealed that hydrophobic AHS were the most abundant component of DOM in the MBR systems. The dominance of AHS became more evident at long SRTs. In contrast, the amount and nature of hydrophilic components were variable and sample source specific. HiN were found to be the major fraction of hydrophilic components at short SRTs, but their proportion in total DOM decreased significantly as SRT lengthened. Moreover, it was noted that, unlike other fractional DOM component, the proportion of HiN significantly decreased after passing through the membrane. This suggests that HiN have relatively low transport rate through membranes and thus are more prone to accumulate in MBR systems.

iii) Microfiltration experiments with DOM in the pilot MBR systems showed that DOM fouling was much more serious with hydrophobic membranes, and was heavily dependent on DOM characteristics. The foulants in DOM were more effectively rejected by hydrophobic membranes. The order of fouling potential of the fractional DOM components, evaluated at the same concentration of Ca^{2+}, was observed to be AHS > HiN > HiB > HiA. In addition, it was noted that membrane fouling caused by HiN and AHS was mainly irreversible. It is thus suggested that DOM having more AHS and HiN

would most likely cause more serious fouling in MBR systems.

iv) The fouling potential of DOM was found to increase as SRT shortened, which may be attributed to the higher proportion of HiN of DOM at short SRTs. It is suggested that MBR systems should be operated at long SRTs to minimize DOM fouling. On the other hand, fouling potentials of DOM in the MBR were consistently higher than those in the effluent. This indicates that organic compounds prone to accumulate in the MBR are the major components of DOM responsible for membrane fouling.

v) Membrane fouling in submerged MBR systems can be well described with a mathematical model that incorporates the concept of reversible and irreversible fouling. The good agreement between theoretical predictions and operational data confirmed our hypothesis that DOM is the key contributor to MBR fouling, mainly responsible for the long-term irreversible fouling of the membrane module. Fouling-related parameters, detachment coefficient (k_r) and fouling strength factor (k_i), which are supposed to be functions of operating conditions, were found to be of key importance in model simulations.

vi) The concentrations of DOM in the MBR were found to be always higher than those in the effluent, indicating that a certain portion of DOM accumulated in the MBR system. DOM accumulation was more pronounced at short SRTs. Carbohydrates and proteins appeared to be the components of DOM prone to accumulate in the MBR compared with aromatic compounds. The apparent

molecular weight distributions of DOM were almost identical in the MBR and in the effluent at all investigated SRTs. The results indicate that membrane sieving does not work for most DOM and consequently cannot adequately explain DOM accumulation in MBR systems. This was further confirmed by the results of the transport experiments with commercial humic acid whose size is much smaller than the membrane pore size.

vii) The retarded transport of DOM through porous membranes was postulated as a new mechanism for DOM accumulation in MBR systems. It is reasonable to believe that the convection velocity of DOM through a porous membrane is slower than that of water because of the high affinity of DOM (organic) to membrane matrix (organic). Dispersion can be another mechanism contributing to DOM transport through the porous membrane due to the built-up of DOM concentration gradient across the membrane. Mathematical models were developed for DOM transport through porous membranes and DOM concentrations in the MBR and in the effluent. The good agreement between experimental data and model simulations indicates that the proposed transport mechanisms of retarded convection and dispersion of DOM through porous membranes can be a better explanation for DOM accumulation in MBR systems.

8.2 Recommendations for Future Study

It is of note that research with respect to DOM fouling and accumulation in submerged MBR systems is far from complete and much work is needed to fully

understand these important issues. Several aspects for future study may arise from the work reported in this thesis. Specifically, the following four aspects are recommended:

1. Apart from membrane hydrophobicity, it is noteworthy that the surface charge of membranes may also affect DOM fouling to some extent by altering the electrostatic interactions between the membrane material and DOM. Since the two microfiltration membranes used in this study (i.e., hydrophilic GVWP and hydrophobic GVHP) have almost identical surface charge in most cases, effect of membrane surface charge on DOM fouling cannot be elucidated. Therefore, research on DOM fouling with membranes having significantly different surface charge remains an interesting area for future work.

2. The mathematic model, incorporating the concept of DOM fouling, offers a new conceptual framework for theoretical investigation of membrane fouling in submerged MBR systems. The two key model parameters, detachment coefficient (k_r) and fouling strength factor (k_i), however, are anticipated to change with altered operating conditions, such as aeration intensity and hydraulic retention time. Thus, another possible avenue of future work is to investigate the possible relationship between k_r, k_i and MBR operational parameters, which would be crucial for further expanding the prediction capacity of the proposed model.

3. DOM fouling and accumulation in MBR systems were found to be significantly affected by SRT. However, it is reasonable to expect that other unexplored MBR operational parameters, such as hydraulic retention time, aeration intensity, and membrane property, can also affect the characteristics

and behaviors of DOM in MBR operation. Future study is therefore needed to look into DOM fouling and accumulation in MBR systems at other operating conditions by employing the methodology developed in this study.

4. It has been shown that DOM accumulation in MBR systems is fundamentally determined by the retardation coefficient α and the dispersion factor β, which characterize the retarded convection and dispersion of DOM through porous membranes. However, at present, the values of α and β for various DOM components have not been experimentally determined due to the complexity of DOM. Therefore, further experimental and theoretical investigations are needed for a more quantitative research on the retarded transport of DOM through porous membranes.

REFERENCE

Ahn, K.H., Song, J.H. and Cha, H.Y. (1998) Application of tubular ceramic membranes for reuse of wastewater from buildings. *Water Sci. Technol.* 38, 373-382.

Aiken, G.R. (1984) Evaluation of ultrafiltration for determining molecular weight of fulvic acid. *Environ. Sci. Technol.* 18, 978-981.

Amy, G. and Cho, J. (1999) Interactions between natural organic matter (NOM) and membranes: Rejection and fouling. *Water Sci. Technol.* 40, 131-139.

Amy, G.L., Bryant, C.W. and Belyani, M. (1987) Molecular weight distributions of soluble organic matter in various secondary and tertiary effluents. *Water Sci. Technol.* 19, 529-538.

Aoustin, E., Schäfer, A.I., Fane, A.G. and Waite T.D. (2001) Ultrafiltration of natural organic matter. *Sep. Purif. Technol.* 22-23, 63-78.

APHA-AWWA-WEF (1998) Standard Methods for Examination of Water and Wastewater, *20th ed. APHA-AWWA-WEF*, Washington DC, USA.

Arceivala, S.J. (1981) Wastewater treatment and disposal: engineering and ecology in pollution control. *M. Dekker*, New York, USA.

Bai, R. and Leow, H.F. (2002) Microfiltration of activated sludge wastewater-the effect of system operation parameters. *Sep. Purif. Technol.* 29, 189-198.

Baker, J., Stephenson, T., Dard, S. and Cote, P. (1995) Characterization of fouling of nanofiltration membranes used to treat surface waters. *Environ. Technol.* 16, 977-985.

Baker, R.J., Fane, A.G., Fell, C.J.D. and Yoo, B.H. (1985) Factors affecting flux in crossflow filtration. *Desalination* 53, 81–93.

Baker, R.W. (2004) Membrane technology and applications. *2nd ed. J. Wiley*, New York, USA.

Barker, D.J. and Stuckey, D.C. (1999) A Review of Soluble Microbial Products (SMP) in Wastewater Treatment Systems. *Water Res.* 33, 3063-3082.

Bedient, P.B., Rifai, H.S. and Newell, C.J. (1999) Ground Water Contamination: Transport and Remediation. *Prentice-Hall*, New Jersey, USA.

Binovi, R. (1983) A replacement for the silt density index: permanganate demand to predict reverse osmosis membrane fouling. *Dissertation, University of Cincinnati,* USA.

Bitton, G. (1999) Wastewater microbiology. *Wiley-Liss*, New York, USA.

Bouhabila, E.H., Aïm, R.B. and Buisson, H. (1998) Microfiltration of activated sludge using submerged membrane with air bubbling (application to wastewater treatment). *Desalination* 118, 315-322.

Bouhabila, E.H., Aïm, R.B. and Buisson, H. (2001) Fouling characterisation in membrane bioreactors. *Sep. Purif. Technol.* 22-3, 123-132.

Bowen, W.R., Calvo, J.I. and Hernandez, A. (1995) Steps of membrane blocking in flux decline during protein microfiltration. *J. Membr. Sci.* 101, 153-165.

Braghetta, A. and DiGiano F.A. (1994) Organic solute association with nanofiltration membrane surface influence of pH and ionic strength on membrane permeability. *AWWA Annual Conference,* Denver, 1009-1029.

Brindle, K. and Stephenson, T. (1996) The application of membrane biological reactors for the treatment of wastewaters. *Biotechnol. Bioeng.* 49, 601-610.

Carroll, T., King, S., Gray, S.R., Bolto[M], B.A. and Booker, N.A. (2000**)** The fouling of microfiltration membranes by NOM after coagulation treatment. *Water Res.* 34, 2861-2868.

Champlin, T.L. and Hendricks, D.W. (1995) Pilot testing NF membranes for direct treatment of low-turbidity surface waters. *Proc. AWWA Membrane Technology Conf.,* Reno, Nevada, 229-249.

Chang, I.S. and Lee, C.H. (1998) Membrane filtration characteristics in membrane coupled activated sludge system—the effect of physiological states of activated sludge on membrane fouling. *Desalination* 120, 221-233.

Chang, I.S., Bag, S.O. and Lee, C.H. (2001) Effects of membrane fouling on solute rejection during membrane filtration of activated sludge. *Process Biochem.* 36, 855-860.

Chang, I.S., Choo, K.H., Lee, C.H., Koh, J.H., Kim, S.W., Paik, U.H. and Koh, U.C. (1994) Application of ceramic membrane as a pretreatment in anaerobic digestion of alcohol-distillery wastes. *J. Membr. Sci.* 90, 131-139.

Chang, I.S., Clech, P.L., Jefferson, B. and Judd, S. (2002) Membrane fouling in membrane bioreactors for wastewater treatment. *J. Environ. Eng.-ASCE* 128, 1018-1029.

Chang, I.S., Lee, C.H. and Ahn, K.H. (1999) Membrane filtration characteristics in membrane coupled activated sludge system: The effect of floc structure of activated sludge on membrane fouling. *Sep. Sci. Technol.* 34, 1743-1758.

Cheremisinoff, P.N. (1994) Biomanagement of wastewater and wastes. *Englewood Cliffs*, New Jersey, USA.

Childress, A.E. and Elimelech, M. (1996) Effect of solution chemistry on the surface charge of polymeric reverse osmosis and nanofiltration membranes. *J. Membr. Sci.* 119, 253-268.

Childress, A.E. and Elimelech, M. (1997) Effects of natural organic matter and surfactants on the surface characteristics of low pressure reverse osmosis and nanofiltration membranes. *Proc. AWWA Membrane Technology Conf.,* New Orleans, 717-725.

Choo, K.H. and Lee, C.H. (1996) Effect of anaerobic digestion broth composition on membrane permeability. *Water Sci. Technol.* 34, 173-179.

Churchouse, S.J. (1998) Kubota Maintains Popular Trend. *Water and Environ. International*, 26-27.

Cicek, N., Franco, P., Suidan, M., Urbain, V. and Manem, J. (1999) Characterization and comparison of a membrane bioreactor and a conventional activated sludge system in the treatment of wastewater containing high molecular weight compounds. *Water Environ. Res.* 71, 64-70.

Clark, M.M. and Heneghan, K.S. (1991) Ultrafiltration of lake water for potable water production. *Desalination* 80, 243-249.

Clark, M.M. and Jucas, P. (1993) Interactions between hydrophobic ultrafiltration membranes and humic substances. *Proc. of AWWA Membrane Technology Conf.,* Baltimore, 259-272.

Clark, M.M. and Lucas, P. (1998) Diffusion and partitioning of humic acid in a porous ultrafiltration membrane. *J. Membr. Sci.* 143, 13-25.

Croué, J.-P., Korshin, G.V. and Benjamin, M. (2000) *Characterization of natural organic matter in drinking water*; AWWA Research Foundation, Denver, Colorado, USA.

Crozes, G., Anselme, C. and Mallevialle, J. (1993) Effect of adsorption of organic-matter on fouling of ultrafiltration membranes. *J. Membr. Sci.* 84, 61-77.

Dagan, G. (1984) Solute transport in heterogeneous porous formations. *J. Fluid Mech.* 145, 151-177.

Daigger, G.T., Rittmann, B.E., Adham, S. and Andreottola, G. (2005) Are membrane bioreactors ready for widespread application? *Environ. Sci. Technol.* 39, 399A-406A.

Deen, W.M. (1987) Hindered transport of large molecules in liquid-filled pores. *AIChE J.* 33, 1409-1425.

Defrance, L. and Jaffrin, M.Y. (1999) Comparison between filtrations at fixed transmembrane pressure and fixed permeate flux: Application to a membrane bioreactor used for wastewater treatment. *J. Membr. Sci.* 152, 203-210.

Defrance, L., Jaffrin, M.Y., Gupta, B., Paullier, P. and Geaugey, V. (2000) Contribution of various constituents of activated sludge to membrane bioreactor fouling. *Bioresour. Technol.* 73, 105-112.

Digiano, F.A., Braghetta, A., Nilson, J. and Utne, B. (1994) Fouling of nanofiltration membranes by natural organic matter. *National Conference on Environmental Engineering American Society of Civil Engineers,* 320-328.

Dignac, M.F., Ginestet, P., Rybacki, D., Bruchet, A., Urbain, V. and Scribe, P. (2000) Fate of wastewater organic pollution during activated sludge treatment: nature of residual organic matter. *Water Res.* 34, 4185-4194.

Domenico, P.A. and Schwartz, F.W. (1997) Physical and Chemical Hydrogeology. *Wiley*, New York, USA.

Dubois, M., Gilles, K.A., Hamilton, J.K., Rebers, P.A. and Smith, F. (1956) Colorimetric method for determination of sugars and related substances. *Anal. Chem.* 28, 350-356.

Dufresne, R., Lavallee, H.C., Lebrun, R.E. and Lo, S.N. (1998) Comparison of performance between membrane bioreactor and activated sludge system for the treatment of pulping process wastewaters. *Tappi J.* 81, 131-135.

Duranceau, S.J. and Taylor, J.S. (1993) Solute charge and molecular weight modeling for prediction of solute mass transfer coefficients. *Proc. of AWWA Membrane Technology Conf.,* Baltimore, 243-249.

Elimelech, M., Chen, W.H. and Waypa, J.J. (1994) Measuring the zeta (electrokinetic) potential of reverse-osmosis membranes by a streaming potential analyzer. *Desalination* 95, 269-286.

Ellis, T.G., Schmit, C.G., Jahan, K., Debik, E. and Eliosov, B. (2004) Activated sludge and other aerobic suspended culture processes. *Water Environ. Res.* 71, 1003-1098.

Fan, L., Harris, J. L., Roddick, F. A. and Booker, N. (2001**)** A. Influence of the characteristics of natural organic matter on the fouling of microfiltration membranes. *Water Res.* 35, 4455-4463.

Fan, X.J., Urvain, V., Qian, Y. and Manem, J. (1999) Ultrafiltration of activated sludge with ceramic membranes in a crossflow membrane bioreactor process. *Proc., Membrane Technology in Environmental Management*, Tokyo, 286-293.

Fane, A.G., Fell, C.J.D. and Nor, M.T. (1981) Ultrafiltration/Activated sludge system–development of a predictive model. *Polym. Sci. Technol.* 13, 631-658.

Fleischer, E.J., Broderick, T.A., Daigger, G.T., Fonseca, A.D, Holbrook, R.D.,Murthy, S.N. (2005) Evaluation of membrane bioreactor process capabilities to meet stringent effluent nutrient discharge requirements. *Water Environ. Res.* 77, 162-178.

Forster, C.F. (2003) Wastewater treatment and technology. *Thomas Telford*, London, UK.

Freyberg, D.L. (1986) A natural gradient experiment on solute transport in a sand aquifer. 2. Spatial moments and the advection and dispersion of nonreactive tracers. *Water Resour. Res.* 22, 2031-2046.

Futamura, O., Masuo, K. and Koyosi, T. (1994) Organic waste water treatment by activated sludge process using integrated type membrane separation. *Desalination* 98, 17-25.

Gander, M., Jefferson, B. and Judd, S. (2000) Aerobic MBRs for domestic wastewater treatment: A review with cost considerations. *Sep. Purif. Technol.* 18, 119-130.

Ghyoot, W., Beeckman, M., Van den Hende, P. and Verstraete, W. (1997) Treatment of low and high strength wastewater with a membrane bioreactor. *Proc., 94th Event of the European Federation of Biotechnology Part I*, Oostende, Belgium.

Gill, W.N., Wiley, D.E., Fell, C.J.D. and Fane, A.G. (1988) Effect of viscosity on concentration polarization in ultrafiltration. *Aiche J.* 34, 1563-1567.

Gourley, L., Britten, M., Gauthier, S.F. and Pouliot, Y. (1994) Characterization of adsorptive fouling on ultrafiltration membranes by peptides mixtures using contact-angle measurements. *J. Membr. Sci.* 97, 283-289.

Gunder, B. (2001) The membrane-coupled activated sludge process in municipal wastewater treatment. *Technomic*, Lancaster, PA, USA.

Hartree, E.F. (1972). Determination of protein: a modification of the Lowry method that gives a linear photometric response. *Anal. Biochem.* 48, 422-427.

Her, N., Amy, G., Foss, D., Cho, J., Yoon, Y. and Kosenka, P. (2002) Optimization of method for detecting and characterizing NOM by HPLC-size exclusion chromatography with UV and on-line DOC detection. *Environ. Sci. Technol.* 36, 1069-1076.

Hiemstra, P., Van Paassen, J., Rietman, B., Nederlof, M. and Verdouw, J. (1997) Reduction of color and hardness of groundwater with nanofiltration –Is pilot plant investigation really important? *Proc. AWWA Membrane Technology Conf.,* New Orleans, 857-881.

Hillis, P. (2000) Membrane technology in water and wastewater treatment. *Royal Society of Chemistry*, Cambridge, UK.

Hong, S.K. and Elimelech, M. (1997) Chemical and physical aspects of natural organic matter (NOM) fouling of nanofiltration membranes. *J. Membr. Sci.* 132, 159-181.

Howe, K.J. and Clark, M.M. (2002) Fouling of Microfiltration and Ultrafiltration Membranes by Natural Waters. *Environ. Sci. Technol.* 36, 3571-3576.

Howell, J.A., Chua, H.C. and Arnot, T.C. (2004) In situ manipulation of critical flux in a submerged membrane bioreactor using variable aeration rates, and effects of membrane history. *J. Membr. Sci.* 242, 13-19.

Hu, J.Y., Ong S.L., Shan J.H., Kang J.B. and Ng W.J. (2003) Treatability of organic fractions derived from secondary effluent by reverse osmosis membrane. *Water Res.* 37, 4801-4809.

Huang, X., Gui, P. and Qian, Y. (2001) Effect of sludge retention time on microbial behaviour in a submerged membrane bioreactor. *Process Biochem.* 36, 1001-1006.

Huang, X., Liu, R. and Qian, Y. (2000) Behaviour of soluble microbial products in a membrane bioreactor. *Process Biochem.* 36, 401-406.

Imai, A., Fukushima, T., Matsushige, K. and Kim, Y.H. (2001) Fractionation and characterization of dissolved organic matter in a shallow eutrophic lake, its inflowing rivers, and other organic matter sources. *Water Res.* 35, 4019-4028.

Imai, A., Fukushima, T., Matsushige, K., Kim, Y.H. and Choi, K. (2002) Characterization of dissolved organic matter in effluents from wastewater treatment plants. *Water Res.* 36, 859-870.

Imai, A., Matsushige, K. and Nagai, T. (2003) Trihalomethane formation potential of dissolved organic matter in a shallow eutrophic lake. *Water Res.* 37, 4284-4294.

Ince, B.K., Ince, O., Sallis, P.J. and Anderson, G.K. (2000) Inert COD production in a membrane anaerobic reactor treating brewery wastewater. *Water Res.* 34, 3943-3948.

Ishiguro, K., Imai, K. and Sawada, S. (1994) Effects of biological treatment conditions on permeate flux of UF membrane in a membrane/activated sludge wastewater treatment system. *Desalination* 98, 119-126.

IUPAC (1996) Terminology for membranes and membrane processes. *J. Membr. Sci.* 120, 149-159.

Jacangelo, J.G., Aieta, E.M., Carns, K.E., Cummings, E.W. and Mallevialle, J. (1989) Assessing hollow-fiber ultrafiltration for particulate removal. *J. AWWA* 81, 68-75.

Jackson, B.P., Ranville, J.F., Bertsch, P.M. and Sowder, A.G. (2005) Characterization of colloidal and humic-bound Ni and U in the "dissolved" fraction of contaminated sediment extracts. *Environ. Sci. Technol.* 39, 2478-2485.

Jorand, F., Zartarian, F., Thomas, F., Block, J.C., Bottero, J. Y., Villemin, G., Urbain, V. and Manem, J. (1995) Chemical and structural (2D) linkage between bacteria within activated sludge flocs. *Water Res.* 29, 1639-1647.

Jucker, C. and Clark, M.M. (1994) Adsorption of aquatic humic substances on hydrophobic ultrafiltration membranes. *J. Membr. Sci.* 97, 37-52.

Kaiya, Y., Itoh, Y., Takizawa, S. and Fujita, K. (1996) Fouling analysis and control in membrane treatment process for potable purpose. *World Filtration Congress,* Budapest, Hungary, 526-530.

Kim, J.S., Lee, C.H. and Chang, I.S. (2001) Effect of pump shear on the performance of a crossflow membrane bioreactor. *Water Res.* 35, 2137-2144.

Kim, K.J., Chen, V. and Fane, A.G. (1993) Ultrafiltration of colloidal silver particles - flux, rejection, and fouling. *J. Colloid Interface Sci.* 155, 347-359.

Kim, K.J., Fane, A.G., Fell, C.J.D. and Joy, D.C. (1992) Fouling mechanisms of membranes during protein ultrafiltration. *J. Membr. Sci.* 68, 79-91.

Kimura, K., Yamato, N., Yamamura, H. and Watanabe, Y. (2005) Membrane Fouling in Pilot-Scale Membrane Bioreactors (MBR systems) Treating Municipal Wastewater. *Environ. Sci. Technol.* 39, 6293-6299.

Knoell, T., Safarik, J., Cormack, T., Riley, R., Lin, S.W. and Ridgway, H. (1999) Biofouling potentials of microporous polysulfone membranes containing polyether-ethersulfone/polyethersulfone block copolymer: Correlation of membrane surface properties with bacterial attachment. *J. Membr. Sci.* 157, 117-138.

Krupp HK, Biggar SW, Nielsen DR. (1972) Relative flow rates of salt in water in soil. *Soil Sci. Soc. Am. J.* 36, 412-417.

Kwon, B., Lee, S., Cho, J., Ahn, H., Lee, D. and Shin, H.S. (2005) Biodegradability, DBP Formation, and Membrane Fouling Potential of Natural Organic Matter: Characterization and Controllability. *Environ. Sci. Technol.* 39, 732-739.

Laspidou, C.S. and Rittmann, B.E. (2002) A unified theory for extracellular polymeric substances, soluble microbial products, and active and inert biomass. *Water Res.* 36, 2711-2720.

Lawrence, A.W. and McCarty, P.L. (1970) A unified basis for biological treatment design and operation. *J. Environ. Eng. Div. ASCE* 102, 55-70.

Lee, J., Ahn, W.-Y. and Lee, C.-H. (2001) Comparison of the filtration characteristics between attached and suspended growth microorganisms in submerged membrane bioreactor. *Water Res.* 35, 2435-2445.

Lee, W., Kang, S. and Shin, H. (2003) Sludge characteristics and their contribution to microfiltration in submerged membrane bioreactors. *J. Membr. Sci.* 216, 217-227.

Leenheer, J.A. (1981) Comprehensive approach to preparative isolation and fractionation of dissolved organic carbon from natural waters and wastewaters. *Environ. Sci. Technol.* 15, 578-587.

Leenheer, J.A. and Croué, J.P. (2003) Characterizing dissolved aquatic organic matter. *Environ. Sci. Technol.* 37, 18A-26A.

Leenheer, J.A., Croué, J.P., Benjamin, M., Korshin, G.V., Hwang, C.J., Bruchet, A. and Aiken, G., (2000) Natural organic matter and disinfection by-products. *American Chemical Society*, Washington DC, USA.

Leenheer, J.A., Rostad, C.E., Gates, P.M., Furlong, E.T. and Ferrer, I. (2001) Molecular resolution and fragmentation of fulvic acid by electrospray ionization/multistage tandem mass spectrometry. *Anal. Chem.* 73, 1461-1471.

Lin, C.F., Lin T.Y. and Hao, O.J. (2000) Effects of humic substance characteristics on UF performance. *Water Res.* 34, 1097-1106.

Liu, R., Huang, X., Wang, C., Chen, L. and Qian, Y. (2000) Study on hydraulic characteristics in a submerged membrane bioreactor process. *Process Biochem.* 36, 249-254.

Logan, B.E. and Jiang, Q. (1990) Molecular size distributions of dissolved organic matter. *J. Environ. Eng.-ASCE* 116, 1046-1062.

Lowry, O.H., Rosebrough, N.J., Farr, A.L. and Randall, R.J. (1951) Protein measurement with the Folin phenol reagent. *J. Biol. Chem.* 193, 265-275.

Lubbecke, S., Vogelpohl, A. and Dewjanin, W. (1995) Wastewater treatment in a biological high-performance system with high biomass concentration. *Water Res.* 29, 793-802.

Luedeking, R. and Piret, E.C. (1959) A kinetic study of lactic acid fermentation batch process at controlled pH. *J. Biochem. Microbiol. Tech. Eng.* 1, 393-412.

Maartens, A., Swart, P. and Jacobs, E.P. (1998) Humic membrane foulants in natural brown water: characterization and removal. *Desalination* 115, 215-227.

MacCarthy, P. (2001) The principles of humic substances: an introduction to the first principle. In *Humic substances, structures, models, and functions.* 273, 19-30.

Mackey, E.D. (1999) Fouling of ultrafiltration and nanofiltration membranes by dissolved organic matter. *Dissertation,* Rice University, USA.

Madaeni, S.S., Fane, A.G. and Wiley, D. (1999) Factors influencing critical flux in membrane filtration of activated sludge. *J. Chem. Technol. Biotechnol.* 74, 539-543.

Mallevialle, J., Anselme, C. and Marsigny, O. (1989) Effects of humic substances on membrane processes. *ACS Symp. Ser.* 219, 749-767.

Metcalf and Eddy, Inc. (2003) Wastewater Engineering: Treatment and Reuse. *4th ed. McGraw-Hill*, New York, USA.

Mulder, M. (1996) Basic principles of membrane technology. *2nd ed. Kluwer Academic*, Boston, USA.

Nagaoka, H., Yamanishi, S. and Miya, A. (1998) Modeling of biofouling by extracelluar polymers in a membrane separation activated sludge. *Water Sci. Technol.* 38, 497-504.

Namour, P. and Müller M.C. (1998) Fractionation of organic matter from wastewater treatment plants before and after a 21-day biodegradability test: physical-chemical method for measurement of the refractory part of effluents. *Water Res.* 32, 2224-2231.

Nilson, J.A. and DiGiano, F.A. (1996) Influence of NOM composition on nanofiltration. *J.—Am.Water Works Assoc.* 88, 53-66.

Norwood, D.L. and Christman, R.F. (1987) Structural characterization of aquatic humic material. 2. Phenolic content and its relationship to chlorination mechanism in an isolated aquatic fulvic acid. *Environ. Sci. Technol.* 21, 791-798.

Nyström, M., Kaipia, L. and Luque, S. (1995) Fouling and retention of nanofiltration membranes. *J. Membr. Sci.* 98, 249-262.

Nyström, M., Ruohomäki, K. and Kaipia, L. (1994) Humic acid as a fouling agent in filtration. *International Specialist Conference on Desalination and Water Reuse, Perth,* 119-128.

Nyström, M., Ruohomäki, K. and Kaipia, L. (1996) Humic acid as a fouling agent in filtration. *Desalination* 106, 79-87.

Odegaard, H. and Thorsen, T. (1989) Removal of humic substances by membrane processes. *ACS Symp. Ser.* 219, 769-782.

Ognier, S., Wisniewski, C. and Grasmick, A. (2002) Characterisation and modelling of fouling in membrane bioreactors. *Desalination* 146, 141-147.

Piccolo, A., Conte, P., Trivellone, E., Van Lagen, B. and Buurman, P. (2002) Reduced Heterogeneity of a Lignite Humic Acid by Preparative HPSEC Following Interaction with an Organic Acid. Characterization of Size-Separates by Pyr-GC-MS And 1H-NMR Spectroscopy. *Environ. Sci. Technol.* 36, 76-84.

Pieracci, J., Crivello, J.V. and Belfort, G. (1999) Photochemical modi-fication of 10 kDa polyethersulfone ultrafiltration membranes for reductionof biofouling. *J. Membr. Sci.* 156, 223-240.

Pribyl, M., Tucek, F., Wilderer, P.A. and Wanner, J. (1997) Amount and nature of soluble refractory organics produced by activated sludge micro-organisms in sequencing batch and continuous flow reactors. *Water Sci. Technol.* 35, 27-34.

Ray, B.T. (1995) Environmental engineering. *PWS*, New York, USA.

Reckhow, D.A., Singer, P.C. and Malcolm, R.L. (1990) Chlorination of humic materials. Byproduct formation and chemical interpretation. *Environ. Sci. Technol.* 24, 1655-1664.

Rittmann, B.E. (1987). Aerobic biological treatment. *Environ. Sci. Technol.* 21, 128-136.

Rittmann, B.E. and McCarty, P.L. (2001) Environmental biotechnology: principles and applications. *McGraw-Hill*, New York, USA.

Roberts, P.V., Goltz, M.N. and Mackay, D.M. (1986) A natural gradient experiment on solute transport in a sand aquifer. 3. Retardation estimates and mass balances for organic solutes. *Water Resour. Res.* 22, 2047-2058.

Schäfer, A.I., Mauch, R., Waite, T.D. and Fane, A.G. (2002) Charge Effects in the Fractionation of Natural Organics Using Ultrafiltration. *Environ. Sci. Technol.* 36, 2572-2580.

Schäfer, A.I., Schwicker, U., Fischer, M.M., Fane, A.G. and Waite T.D. (2000) Microfiltration of colloids and natural organic matter. *J. Membr. Sci.* 171, 151-172.

Schäfer. A.I. (2001) Natural organics removal using membranes: principles, performance and cost. *Technomic*, Lancaster, PA, USA.

Schultz, S.G. (1980) Basic principles of membrane transport. *Cambridge University Press*, New York, USA.

Scott, J.A., Neilson, D.J., Liu, W. and Boon, P.N. (1998) A dual function membrane bioreactor system for enhanced aerobic remediation of high strength industrial waste. *Water Sci. Technol.* 38, 413-420.

Shimizu, Y., Rokudai, M., Thoya, S., Kayawake, T., Yazawa, T., Tanaka, H. and Eghchi, K. (1989) Filtration characteristics of charged membranes for methanogenic wastes. *J. Chem. Eng. Jpn*. 22, 635-641.

Shimizu, Y., Rokudai, M., Thoya, S., Tanaka, H. and Eghchi, K. (1990) Effect of membrane resistance on filtration characteristics for methanogenic wastes. Kakaku Kogaku Ronbunshu 16, 145-151.

Shimizu, Y., Shimodera, K.I. and Watanabe, A. (1993) Cross flow microfiltration of bacterial cells. *J. Ferment. Bioeng.* 76, 493-500.

Shin, H.-S. and Kang, S.-T. (2003) Characteristics and fates of soluble microbial products in ceramic membrane bioreactor at various sludge retention times. *Water Res.* 37, 121-127.

Singh, G. and Song, L. (2005) Quantifying the effect of ionic strength on colloidal fouling potential in membrane filtration. *J. Colloid Interface Sci.* 284, 630-638.

Song, L. (1998) Flux decline in crossflow microfiltration and ultrafiltration: mechanisms and modeling of membrane fouling. *J. Membr. Sci.* 139, 183-200.

Song, L. and Elimelech, M. (1995) Theory of concentration polarization in crossflow filtration, *J. Chem. Soc. Faraday Trans.* 91, 3389-3398.

Song, L., Chen, K.L., Ong, S.L. and Ng, W.J. (2004) A new normalization method for determination of colloidal fouling potential in membrane processes. *J. Colloid Interface Sci.* 271, 426-433.

Speth, T.F. and Summers, R.S. (1996) Evaluating membrane foulants from conventionally-treated drinking waters. *American Chemical Society*, Part 1.

Tardieu, E., Grasmick, A., Geaugey, V. and Manem, J. (1999) Influence of hydrodynamics on fouling velocity in a recirculated MBR for wastewater treatment. *J. Membr. Sci.* 156, 131-140.

Thorsen, T., Harz, A. and Odegaard, H. (1997) Influence of raw water characteristics and membrane pore size on the performance of ultra-filters for NOM (humic substances) removal. *IWSA World Congress*, Madrid.

Thorsen, T., Krogh, T. and Bergan, E. (1993) Removal of humic substances with membranes with membranes system, use and experiences. *Proc. of AWWA Membrane Technology Conf*., Baltimore, 131-143.

Thurman, E.M. and Malcolm, R.L. (1981) Preparative isolation of aquatic humic substances. *Environ. Sci. Technol.* 15, 463-466.

Thurman E.M. (1985) Organic Geochemistry of Natural Waters. *M. Nijhoff and W. Junk Publishers*, Dordrecht, the Netherlands.

Tu, S.-C., Ravindran, V., Badriyha, B.N. and Pirbazari, M. (1997) A membrane transport model for predicting permeate flux in nanofiltration processes. *Proc. AWWA Membrane Technology Conf.,* New Orleans*,* 487-498.

Ueda, T., Hata, K. and Kikuoka, Y. (1996) Treatment of domestic sewage from rural settlements by a membrane bioreactor. *Water Sci. Technol.* 34, 189-196.

Urbain, V., Mobarry, B., De Silva, V., Stahl, D.A., Rittmann, B.E. and Manem, J. (1998) Integration of performance, molecular biology and modeling to describe the activated sludge process. *Water Sci. Technol.* 37, 223-229.

Visvanathan, C., Aim, R. B. and Parameshwaran, K. (2000) Membrane separation bioreactors for wastewater treatment. *Crit. Rev. Environ. Sci. Technol.* 30, 1-48.

Visvanathan, C., Yang, B.S., Muttamara, S. and Maythanukhraw, R. (1997) Application of air backflushing technique in membrane bioreactor. *Water Sci. Technol.* 36, 259-266.

Wang, Y., Kim, J.H., Choo, K.H., Lee, Y.S. and Lee, C.H. (2000) Hydrophilic modification of polypropylene microfiltration membrane by ozone-induced graft polymerization. *J. Membr. Sci.* 169, 269-276.

Weishaar, J.L., Aiken, G.R., Bergamaschi, B.A., Fram, M.S., Fujii, R. and Mopper, K. (2003) Evaluation of specific ultraviolet absorbance as an indicator of the chemical composition and reactivity of dissolved organic carbon. *Environ. Sci. Technol.* 37, 4702-4708.

Wen, C., Huang, X. and Qian, Y. (1999a) Domestic wastewater treatment using an anaerobic bioreactor coupled with membrane filtration. *Process Biochem.* 35, 335-340.

Wen, X.H., Xing, C.H. and Qian, Y. (1999b) A kinetic model for the prediction of sludge formation in a membrane bioreactor. *Process Biochem.* 35, 249-254.

Wiesner, M.R., Clark, M.M., Jacangelo, J.G., Lykins, B.W., Marinas, B.J., Omelia, C.R., Rittmann, B.E., Semmens, M.J., Brittan, J., Fiessinger, F., Gemin, J., Summers,

R.S., Thompson, M.A. and Tobiason, J.E. (1992) Committee report - membrane processes in potable water-treatment. *J.-Am. Water Works Assoc.* 84, 59-67.

Wijmans, J.G., Nakao, S. and Smolders, C.A. (1984) Flux limitation in ultrafiltration-osmotic-pressure model and gel layer model. *J. Membr. Sci.* 20, 115-124.

Wisniewski, C. and Grasmick, A. (1998) Floc size distribution in a membrane bioreactor and consequences for membrane fouling. *Colloid Surf. A-Physicochem. Eng. Asp.* 138, 403-411.

Wisniewski, C., Grasmick, A. and Cruz, A.L. (2000) Critical particle size in membrane bioreactors case of a denitirifying bacterial suspension. *J. Membr. Sci.* 178, 141-150.

Wong, S., Hanna, J.V., King, S., Carroll, T.J., Eldridge, R.J., Dixon, D.R., Bolto, B.A., Hesse, S., Abbt-Braun, G. and Frimmel, F.H. (2002) Fractionation of natural organic matter in drinking water and characterization by C-13 cross-polarization magic-angle spinning NMR spectroscopy and size exclusion chromatography. *Environ. Sci. Technol.* 36, 3497-3503.

Xing, C.H., Tardieu, E., Qian, Y. and Wen, X.H. (2000) Ultrafiltration membrane bioreactor for urban wastewater reclamation. *J. Membr. Sci.* 177, 73-82.

Xing, C.H., Wen, X.H., Qian, Y. and Tardieu, E. (2001) Microfiltration- membrane-coupled bioreactor for urban wastewater reclamation. *Desalination* 141, 63-73.

Yamamoto, K., Hissa, M., Mahmood, T. and Matsuo, T. (1989) Direct solid liquid separation using hollow fiber membrane in an activated sludge aeration tank. *Water Sci. Technol.* 21, 43-54.

Yuan, W. and Zydney, A.L. (1999) Humic acid fouling during microfiltration. *J. Membr. Sci.* 157, 1-12.

Yuan, W. and Zydney, A.L. (2000) Humic Acid Fouling during Ultrafiltration. *Environ. Sci. Technol.* 34, 5043-5050.

Zhang, B., Yamamoto, K., Ohgaki, S. and Kamiko, N. (1997) Floc size distribution and bacterial activities in membrane separation activated sludge processes for small scale wastewater treatment/reclamation. *Water Sci. Technol.* 35, 37-44.

Zhang, M. and Song, L. (2000) Pressure-dependent permeate flux in ultra- and microfiltration. *J. Environ. Eng.-ASCE* 126, 667-674.

APPENDIX

Appendix A: Photographs of the pilot MBR systems

Figure A.1 Photographs of the three pilot MBR systems.

Appendix B: Schematic Diagrams of the pilot MBR systems

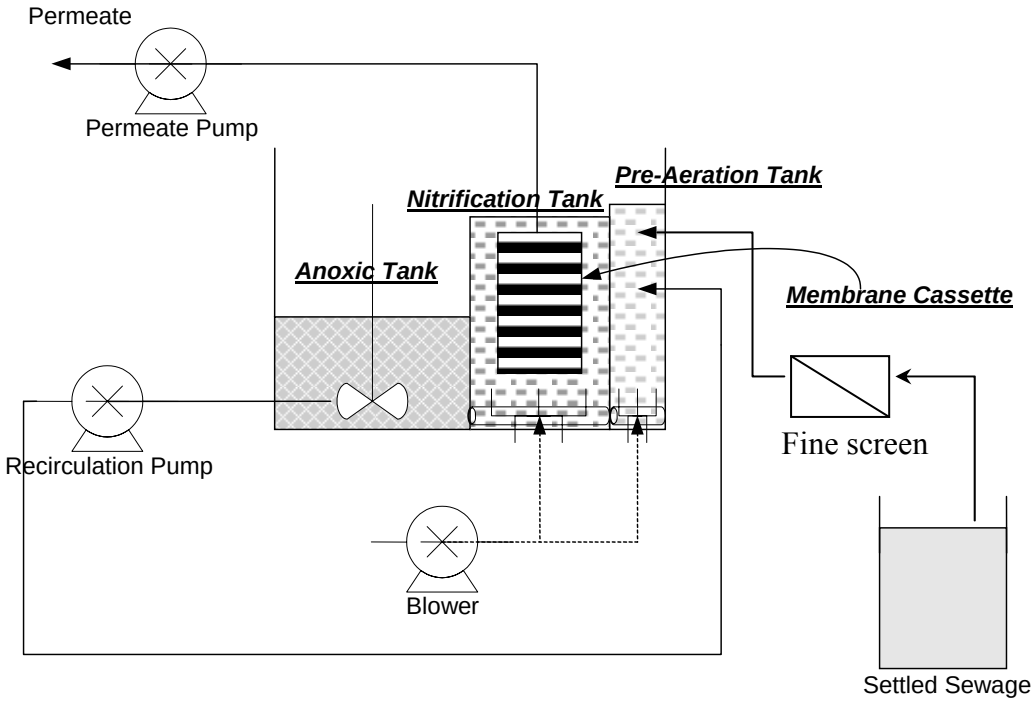

Figure B.1 Schematic diagram of MBR 1.

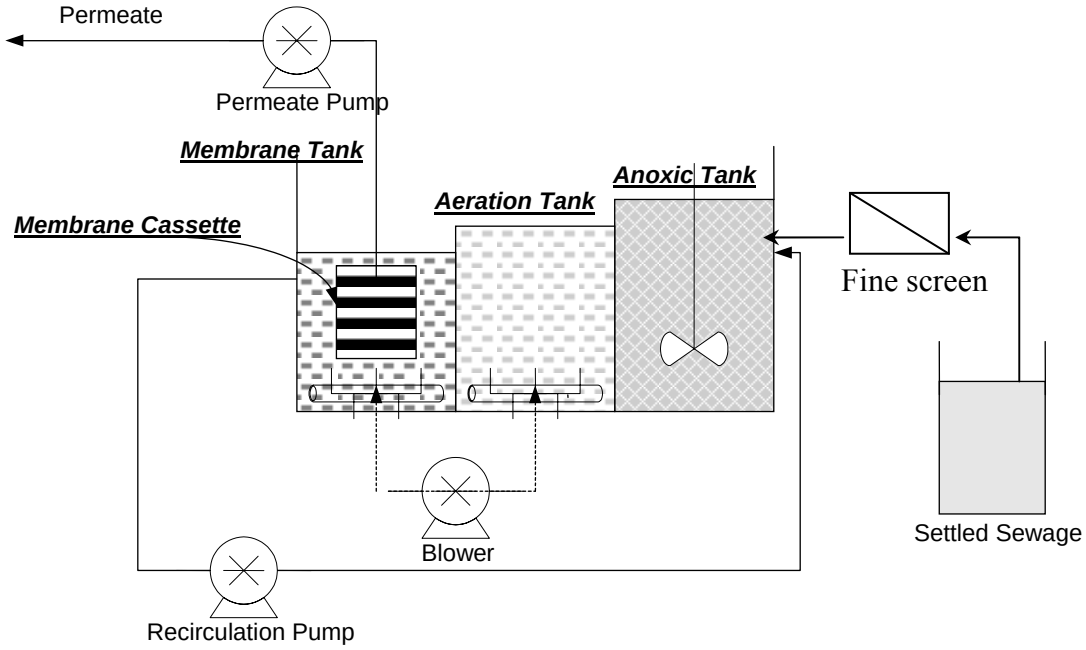

Figure B.2 Schematic diagram of MBR 2.

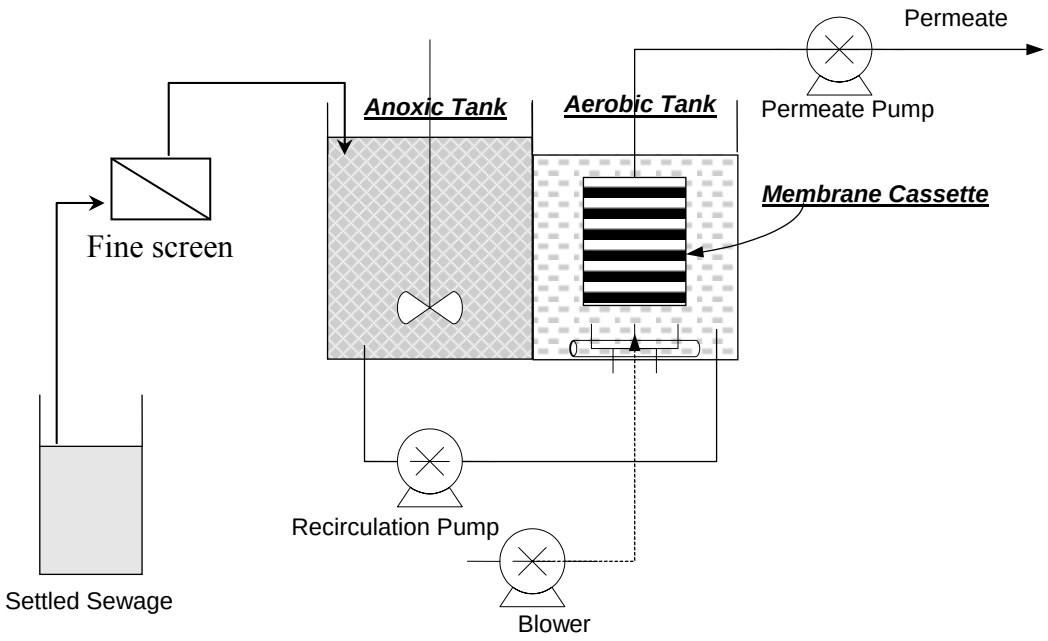

Figure B.3 Schematic diagram of MBR 3.

Appendix C: Publications from This Research Work

C.1 Journal Paper:

1. Liang, S., Song, L., Tao, G., Kekre, K. A. and Seah, H. (2006) "A modeling study of fouling development in membrane bioreactors for wastewater treatment." *Water Environ. Res.*, 78, 857-864.
2. Liang, S., Liu, C. and Song, L. (2007) "Soluble microbial products in membrane bioreactor operation: behaviors, characteristics, and fouling potential." *Water Res.*, 41, 95-101.
3. Song, L., Liang, S. and Yuan, L. (2007) "Retarded transport and accumulation of soluble microbial products in a membrane bioreactor." *J. Environ. Eng.-ASCE*, 133, 36-43.

4. Liang, S. and Song, L. (2007) "Characteristics and fouling behaviors of dissolved organic matter in submerged membrane bioreactor systems." *Environ. Eng. Sci.*, 24, 652-662.

C.2 Conference Paper:

1. Liang, S., Song, L., Ong S. L. and Ng W. J. (2004) "Characteristics and fouling property of dissolved organic matter in membrane bioreactors." Presented at North American Membrane Society (NAMS) 15th Annual Meeting, June 26-30, Honolulu, HI, USA.

2. Liang, S. and Song, L. (2005) "Simulations of fouling development in a submerged membrane bioreactor for domestic wastewater treatment." Presented at North American Membrane Society (NAMS) 16th Annual Meeting, June 11-15, Providence, RI, USA.